estec

European Space Research
and Technology Centre
Keplerlaan 1
2201 AZ Noordwijk
The Netherlands
T +31 (0)71 565 6565
F +31 (0)71 565 6040
www.esa.int

I-SOC Scientific Requirements

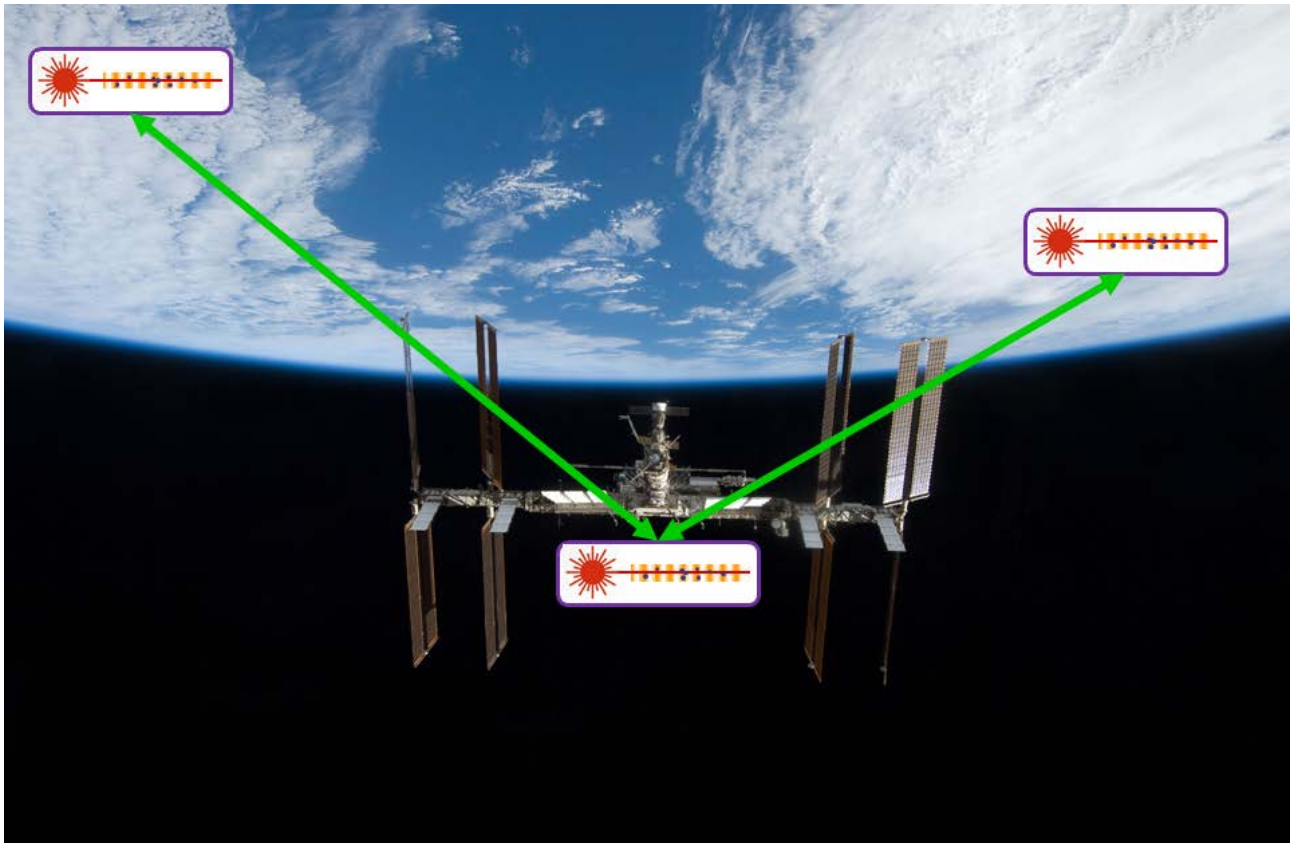

Prepared by Luigi Cacciapuoti (SCI-S) and Stephan Schiller (HHU Düsseldorf)
European Space Agency

Reference SCI-ESA-HRE-ESR-ISOC
Issue/Revision 1.1
Date of Issue 09/06/2017
Status Approved

APPROVAL

Title I-SOC Scientific Requirements	
Issue Number 1	**Revision Number** 1
Author Luigi Cacciapuoti (SCI-S) and Stephan Schiller (HHU Düsseldorf)	**Date** 09/06/2017
Approved By	**Date of Approval**
I-SOC Science Team:	
S. Schiller (UDUS)	See Annex 4
U. Sterr (PTB)	See Annex 4
C. Lisdat (PTB)	See Annex 4
N. Poli (LENS)	See Annex 4
G. Tino (LENS)	See Annex 4
I. Prochazka (CTU)	See Annex 4
R. Le Targat (OBSPARIS)	See Annex 4
J. Lodewyck (OBSPARIS)	See Annex 4
C. Salomon (ENS)	See Annex 4
Y. Singh (UOB)	See Annex 4
K. Bongs (UOB)	See Annex 4
F. Levi (INRIM)	See Annex 4
ESA Project Scientist: L. Cacciapuoti (SCI-S)	31/07/2017
UIB Board: L. De Parolis (acting HRE-UP)	1/08/17
UIB Board: L. De Parolis (HRE-PI)	
UIB Board: A. Schoen (HRE-PI)	2.8.17

CHANGE LOG

Reason for change	Issue Nr.	Revision Number	Date
SPOT review	1	1	09/06/2017

CHANGE RECORD

Issue Number 1	Revision Number 1		
Reason for change	**Date**	**Pages**	**Paragraph(s)**
Role of Science Team in in the configuration control of the document clarified.	09/06/2017	Page 7	Sec. 1.1
Applicability of design guidelines provided in Annex 1 clarified.	09/06/2017	Page 65	Annex1
List of TBRs updated following comments received by CADMOS	09/06/2017	Page 107	Annex 5
Following CADMOS recommendation, #SR-PL-38 is now including reference to requirements #SR-PL-43 to #SR-PL-48	09/06/2017	Page 58	#SR-PL-38
Removed unnecessary items from the I-SOC mission overview.	09/06/2017	Page 19-20	Sec. 2.4
New requirement covering the role of the Mission Control Center (USOC).	09/06/2017	Page 64	#SR-OP-07

DISTRIBUTION

Name/Organisational Unit

Table of contents:

1 INTRODUCTION

1.1 Purpose

This document presents the scientific objectives of the ESA mission I-SOC and provides the top level science requirements.
I-SOC is a mission in the Fundamental Physics domain conceived to test to high accuracy a fundamental principle of metric theories of gravitation, the dilation of time by gravity. It is related to the Einstein Equivalence Principle (EEP).
The scientific case described in this document was initially submitted as response to a call for scientific use of the ISS, in 2005. A first study ("SOC") was performed under ESA funding in 2006-2009, followed by an EU-FP7 project "SOC2", in 2010-2015, a EU-H2020 Initial Training Network "FACT" contributed with parts of its activity in 2013-17. The I-SOC mission was recommended by the ESA-appointed "Fundamental Physics Roadmap Advisory Team" (FPR-AT) as a result of an extensive consultation process conducted in the fundamental physics community [RD01].
This Experiment Scientific Requirements document (ESR) will be the basis for the I-SOC mission design during the assessment study phase, which is planned to start at the in 2017 and will be concluded with the presentation of the study results to the ESA advisory structure in 2019.
During the assessment phase, it is expected that the requirements may be adjusted driven by technical feasibility within the programmatic boundaries or by the progress of ongoing research programs on optical clocks. The I-SOC Science Team will evaluate eventual changes and submit them to ESA for approval.. Any changes will be logged in this document to provide a record of the evolution.
This document also aims at showing the links between science requirements and mission performance requirements, in order to help to understand, trace, and support the analysis of the relation between mission specifications and scientific objectives.

1.2 Document Overview

The document is organized as follows. Section 2 discusses the I-SOC science case, addressing the fundamental physics tests that will be conducted and providing the mission overview. The scientific objectives are detailed in Section 3 where, for each of the primary mission objectives, the measurement principle is also discussed.
The requirements breakdown is presented in Section 4, which is directly derived from the I-SOC scientific objectives.
In Annex 1, the working principle of the I-SOC clock, its main subsystems, functions and interfaces are detailed. This appendix is intended to provide a set of recommendation/guidelines for the design of the main instrument and of the links.

1.3 Acronyms

ACES	Atomic clock ensemble in space
CDMA	Code Division Multiple Access
DDS	Direct Digital Synthesizer
DLR	Deutsches Zentrum für Luft und Raumfahrt
EEP	Einstein Equivalence Principle

ELT+	European Laser Link
ESR	Experiment Scientific Requirements
FCOL	Frequency Comb Optical Link
FDP	Frequency Distribution Package
FPGA	Field Programmable Gate Array
FPR-AT	Fundamental Physics Roadmap Advisory Team
GPS	Global Positioning System
GR	General Relativity
GTD	Gravitational Time Dilation
IF	Intermediate Frequency
I-SOC	Space Optical Clock on ISS
LCT	Laser Communication Terminal
LLI	Local Lorentz Invariance
LPI	Local Position Invariance
MOC	Mission Operations Centre
MWL	MicroWave Link
PHARAO	Projet d'Horologe Atomique par Refroidissement d'Atomes en Orbite
PN	Pseudo Noise
PPS	Pulses Per Second
PSO	Primary Science Objective
PSD	Power Spectral Density
PVT	Position, Velocity, Time
QM	Quantum Mechanics
RDS	Relativistic Doppler shift
RMS	Robertson-Mansouri-Sexl
SAW	Surface Acoustic Wave
SFC	Space Frequency Comb
SME	Standard Model Extension
SLOC	Space Lattice Optical Clock
SLR	Satellite Laser Ranging
SR	Special Relativity
SSO	Secondary Science Objective
TC	Telecommanding
TEC	Total Electron Content
TWSTFT	Two-Way Satellite Time and Frequency Transfer
USO	Ultra Stable Oscillator (quartz)
USOC	User Support and Operation Center
UTC	Universal Time Coordinated
WEP	Weak Equivalence Principle

1.4 References

RD01 FPR-AT, *A Roadmap for Fundamental Physics in Space*, http://sci.esa.int/fprat (2010)
RD02 C.W. Misner, K.S. Thorne, and J.A. Wheeler, *Gravitation* (Freeman, San Francisco, 1973)
RD03 C. M. Will, *Living Rev. Relativity* **9**, 3 (2006)
RD04 V.V. Flambaum and M.G. Kozlov, *Phys. Rev. Lett.* **98**, 240801(2007)
RD05 E. Reinold et al., *Phys. Rev. Lett.* **96**, 151101(2006);
RD06 T.Tzanavaris et al., *Phys. Rev.Lett.* **95**,041301(2005)
RD07 N.Kanekar et al., *Phys. Rev. Lett.* **95**, 261301(2005)

RD08 V.V. Flambaum, *Int. Jounr. Mod. Phys. A* **22**, 4937 (2007)
RD09 T. Dent et al., *Phys. Rev. D* **76**, 063513 (2007)
RD10 V.F. Dmitriev et al., *Phys. Rev D* **69**, 063506 (2004)
RD11 J.C. LoPresto et al., *Astrophys. J.* **376**, 757 (1991)
RD12 T.P. Krisher et al., *Phys. Rev. Lett.* **70**, 2213 (1993)
RD13 A. Papapetrou, *Proc. Roy. Soc. London* **A209**, 248 (1951)
RD14 W.G. Dixon, *Nuovo Cimento* **XXXIV No.2**, 317 (1964)
RD15 J. E. Moody and F. Wilczek, *Phys. Rev. D* **30**, 130 (1984)
RD16 T. Damour, et al., *Phys. Rev. D* **66**, 046007 (2002)
RD17 D. B. Kaplan and M. B. Wise, *JHEP* **08**, 037 (2000)
RD18 E. Göklü and C. Lämmerzahl *Class. Quantum Grav.* **25** 10501 (2008)
RD19 R.F.C. Vessot et al., *Phys. Rev. Lett.* **45**, 2081 (1980)
RD20 L. Cacciapuoti and C. Salomon, *Eur. Phys. J. Special Topics* **172**, 57 (2009)
RD21 J.G. Williams et al., *Phys. Rev. Lett.* **93**, 261101 (2004)
RD22 S. Schlamminger et al., *Phys. Rev. Lett.* **100**, 041101 (2008)
RD23 http://smsc.cnes.fr/MICROSCOPE/index.htm
RD24 H. Müller et al., *Nature* **463**, 926 (2010)
RD25 P. Wolf et al., *Nature* **467**, 7311 E1 (2010)
RD26 M.A. Hohensee et al., *Phys. Rev. Lett.* **106**, 151102 (2011)
RD27 P. Wolf et al., to be published in *Class. Quantum Grav.*
RD28 K.C. Littrell et al., *Phys. Rev. A* **56**, 1767 (1997)
RD29 S. Fray et al., *Phys. Rev. Lett.* **93**, 240404 (2004)
RD30 H.P. Robertson, *Rev. Mod. Phys.* **21**, 378 (1949)
RD31 R. Mansouri and R.U. Sexl, *Gen. Rel. Grav.* **8**, 479 (1977)
RD32 R. Mansouri and R.U. Sexl, *Gen. Rel. Grav.* **8**, 515 (1977)
RD33 R. Mansouri and R.U. Sexl, *Gen. Rel. Grav.* **8**, 809 (1977)
RD34 D. Colladay, V.A. Kostelecký, *Phys. Rev. D* **55**, 6790 (1997)
RD35 D. Colladay, V.A. Kostelecký, *Phys. Rev. D* **58**, 116002 (1998)
RD36 V.A. Kostelecký, *Phys. Rev. D* **69**, 105009 (2004)
RD37 Ch. Eisele et al., *Phys. Rev. Lett.* **103**, 090401 (2009)
RD38 S. Hermann yet al., *Phys. Rev. D* **80**, 105011 (2009)
RD39 P. Wolf at al., *Phys. Rev. D* **70**, 051902 (2004)
RD40 P. Wolf et al., *Phys. Rev. Lett.* **96**, 060801 (2006)
RD41 L. Duchayne et al., *A&A* **504**, 653 (2009)
RD42 N.K. Pavlis and M.A. Weiss, *Metrologia* **40**, 66 (2003)
RD43 B. Hoffman, *Phys. Rev. Lett.* **121**, 337 (1961)
RD44 P. Wolf and G. Petit, *A&A* **304**, 653 (1995)
RD45 A. Peters, K.Y. Chung and S. Chu, *Nature* **400**, 849 (1999)
RD46 T. Lévèque et al., *Phys. Rev. Lett.* **103**, 080405 (2009)
RD47 S. Vitale et al., "*Recommendation for an algorithm for Power Spectral Density estimation for LISA Phathfinder*", **S2-UTN-TN-3040**, Issue 1 – Rev. 0 (2006)
RD48 Stable32 Frequency Stability Analysis: http://www.wriley.com
RD49 A. Derevianko and M. Pospelov, *Hunting for topological dark matter with atomic clocks*, Nature Physics **10**, 933-936 (2014)
RD50 A. Derevianko, *Atomic clocks and dark-matter signatures*, J. Phys.: Conf. Ser. **723**, 012043 (2016)
RD51 C. Voigt and H. Denker, Validation of GOCE Gravity Field Models in Germany, *Newton's Bulletin* **5,** 37-48 (2015)
RD52 H. Denker, Regional Gravity Field Modelling: Theory and Practical Results, in: Sciences of Geodesy II, ed. G. Xu (Berlin Heidelberg: Springer) 185-291 (2013)
RD53 C. Voigt, H. Denker and L. Timmen, "Time-variable gravity potential components for optical clocks and the definition of international time scales", to appear in Metrologia (2016)
RD54 S. B. Koller, J. Grotti, St. Vogt, A. Al-Masoudi, S. Dörscher, S. Häfner, U. Sterr, Ch. Lisdat, "A transportable optical lattice clock with $7{\cdot}10^{-17}$ uncertainty", Phys. Rev. Lett. 118, 073601 (2017)
RD55 Hobinger T. et al., Radio Science, 48, 1 (2013)
RD56 Kaplan E., *Understanding GPS: Principles and Applications*, ArtechHouse, 1996
RD57 Hejc G. et al., *Proceeding of the 41st Precise Time and Time Interval (PTTI) Conference*, 2009

RD58 Van Dierendonck A.J. et al., *Navigation* **39**, 265 (1992)

RD59 Ascarrunz F.G. et al., *Proceedings of the 30th Precise Time and Time Interval (PTTI) Conference*, 1998

RD60 Audoin C. and Guinot B., *The Measurement of Time*, Cambridge University Press, 2001

RD61 A. D. Ludlow, Boyd, M. M. , Ye, J. , Peik, E. , and Schmidt, P.O. , "Optical atomic clocks", Reviews of Modern Physics, vol. 87, no. 2, pp. 637 - 701, 2015

RD62 B. J. Bloom, Nicholson, T. L. , Williams, J. R. , Campbell, S. L. , Bishof, M. , Zhang, X. , Zhang, W. , Bromley, S. L. , and Ye, J. , "An optical lattice clock with accuracy and stability at the 10-18 level", Nature, vol. 506, pp. 71-75, 2014.

RD63 N. Poli et al. "Optical atomic clocks", Riv. Nuovo Cim. 36, 555 (2013)

RD64 N. Hinkley, J. A. Sherman, N. B. Phillips, M. Schioppo, N. D. Lemke, K. Beloy, M. Pizzocaro, C. W. Oates, and A. D. Ludlow "*An atomic clock with 10^{-18} instability*", Science 341, 1215-1218, 2013

RD65 I. Ushijima, M. Takamoto, M. Das, T. Ohkubo & H. Katori, "*Cryogenic optical lattice clocks*", Nature Photonics 9, 185-189 (2015)

RD66 P. Panek, I. Prochazka and J. Kodet, "*Time measurement device with four femtosecond stability*", Metrologia 47, L13-L16 (2010)

RD67 I. Prochazka, J. Kodet and J. Blazej, "*Solid state photon counters with sub-picosecond timing stability*", Rev. Sci. Instrum. 84, 046107 (2013); doi: 10.1063/1.4802950, ISSN 0273-1177.

RD68 V.D. Shargorodsky, V.P. Vasiliev, M.S. Belov, I.S. Gashkin, N.N. Parkhomenko , "Spherical Glass Target Microsatellite", in Proceedings of the 15th International Workshop on Laser Ranging (editors J. Luck, C. Moore and P. Wilson), pp. 566-570, (2006), Canberra, Australia. Oakley, J. P., *Whole-angle spherical retroreflector using concentric layers of homogeneous optical media*. Applied Optics 46, 1026-1031 (2007)

RD69 Grebing et al., Optica 3, 563-569 (2015)

RD70 B. Argence, E. Prevost, T. Lévèque, R. L. Goff, S. Bize, P. Lemonde and G. Santarelli, *Prototype of an ultra-stable optical cavity for space applications*, Opt. Express **20**, 25409-25420 (2012)

RD71 K. Bongs et al. (SOC2 consortium), "*Development of a strontium optical lattice clock for the SOC mission on the ISS*", C. R. Physique 16, 553–564 (2015); http://dx.doi.org/10.1016/j.crhy.2015.03.009

RD72 G. D. Cole, W. Zhang, M. J. Martin, J. Ye and M. Aspelmeyer, "*Tenfold reduction of Brownian noise in optical interferometry*", Nature Photonics **7**, 644-650 (2013)

RD73 S. Falke, M. Misera, U. Sterr, and C. Lisdat, *Delivering pulsed and phase stable light to atoms of an optical clock*, Appl. Phys. B **107**, 301-311 (2012)

RD74 R. Le Targat, L. Lorini, Y. Le Coq, M. Zawada, J. Guéna, M. Abgrall, M. Gurov, P. Rosenbusch, D. G. Rovera, B. Nagórny, R. Gartman, P. G. Westergaard, M. E. Tobar, M. Lours, G. Santarelli, A. Clairon, S. Bize, P. Laurent, P. Lemonde and J. Lodewyck, *Experimental realization of an optical second with strontium lattice clocks*, Nature Com. **4**, 2109 (2013)

RD75 J. Lodewyck, S. Bilicki, E. Bookjans, J.-L. Robyr, C. Shi, G. Vallet, R. Le Targat, D. Nicolodi, Y. Le Coq, J. Guéna, M. Abgrall, P. Rosenbusch and S. Bize, *Optical to microwave clock frequency ratios with a nearly continuous strontium optical lattice clock*, Metrologia **53**, 1123 (2016)

RD76 A. Nevsky, S. Alighanbari, Q.-F. Chen, I. Ernsting, S. Vasilyev, S. Schiller, G. Barwood, P. Gill, N. Poli and G. M. Tino, *Robust frequency stabilization of multiple spectroscopy lasers with large and tunable offset frequencies*, Opt. Lett. **38**, 4903-4906 (2013)

RD77 D. Nicolodi, B. Argence, W. Zhang, R. Le Targat, G. Santarelli and Y. Le Coq, *Spectral purity transfer between optical wavelengths at the 10^{-18} level*, Nature Photonics **8**, 219-223 (2014)

RD78 S. Origlia, S. Schiller, M. S. Pramod, L. Smith, Y. Singh, W. He, S. Viswam, D. Świerad, J. Hughes, K. Bongs, U. Sterr, C. Lisdat, S. Vogt, S. Bize, J. Lodewyck, R. Le Targat, D. Holleville, B. Venon, P. Gill, G. Barwood, I. R. Hill, Y. Ovchinnikov, A. Kulosa, W. Ertmer, E.-M. Rasel, J. Stuhler, and W. Kaenders, *Development of a strontium optical lattice clock for the SOC mission on the ISS*, Proc. SPIE **9900**, 990003-990003-12 (2016) doi: 10.1117/12.2229473; http://arxiv.org/abs/1603.06062

RD79 G. Santarelli, P. Laurent, P. Lemonde, A. Clairon, A. G. Mann, S. Chang, A. N. Luiten and C. Salomon, *Quantum projection noise in an atomic fountain: A high stability cesium frequency standard*, Phys. Rev. Lett. **82**, 4619-4622 (1999)

RD80 M. Schioppo, N. Poli, M. Prevedelli, S. Falke, C. Lisdat, U. Sterr, and G. M. Tino, *A compact and efficient strontium oven for laser-cooling experiments*, Rev. Sci. Instrum. **83**, 103101 (2012)

RD81 C. Shi, J.-L. Robyr, U. Eismann, M. Zawada, L. Lorini, R. Le Targat and J. Lodewyck, *Polarizabilities of the ^{87}Sr clock transition*, Phys. Rev. A **92**, 012516 (2015)

RD82 D. Świerad, S. Häfner, S. Vogt, B. Venon, D. Holleville, S. Bize, A. Kulosa, S. Bode, Y. Singh, K. Bongs, E. M. Rasel, J. Lodewyck, R. Le Targat, C. Lisdat and U. Sterr, *Ultra-stable clock laser system development towards space applications*, Scientific Reports **6**, 33973 (2016)

RD83 P. G. Westergaard, J. Lodewyck, L. Lorini, A. Lecallier, E. A. Burt, M. Zawada, J. Millo and P. Lemonde, *Lattice-induced frequency shifts in Sr optical lattice clocks at the 10^{-17} level*, Phys. Rev. Lett. **106**, 210801 (2011)

RD84 P. A. Williams, W. C. Swann and N. R. Newbury, *High-stability transfer of an optical frequency over long fiber-optic links*, J. Opt. Soc. Am. B **25**, 1284-1293 (2008)

RD85 R.A. Williams, S. Donnellan, T.I. Ferreiro, G.P. Barwood, I.R. Hill, P. Gill, *Optical Cavity Acceleration Sensitivity Reduction via Feed-forward Correction*, poster, EFTF 2014.

RD86 T. Akatsuka, M. Takamoto, and H. Katori, 2010, Phys. Rev. A 81, 023402

RD87 J. Deschenes et al., Phys. Rev. X, 6, 021016 (2016)

2 TESTING THE EINSTEIN EQUIVALENCE PRINCIPLE WITH I-SOC

2.1 Fundamental Physics Experiments and Space

One of the most exciting challenges that physics is facing in the present days is represented by the harmonization of gravitation and quantum theory and, more generally, by the unification of the four fundamental interactions of Nature (strong, electromagnetic, weak, and gravitational). General Relativity (GR) and Quantum Mechanics (QM) are the frameworks from which the developments of all the grand unification theories start.
GR explains the behaviour of space-time and matter on cosmologically large scales and of very dense compact astrophysical objects. GR is based on the Einstein's Equivalence Principle (EPP) which in its purest form states that:

I. *Weak Equivalence Principle (WEP)*: The trajectories of freely falling test bodies are independent of their structure and composition;
II. *Local Lorentz Invariance (LLI)*: In local freely falling frames, the outcome of any non-gravitational test experiment is independent of the velocity of the frame;
III. *Local Position Invariance (LPI)*: In local freely falling frames, the outcome of any non-gravitational test experiment is independent of where and when in the universe it is performed.

For at least half a century after its first formulation, Einstein's theory of general relativity has been considered as "a theorist's paradise, but an experimentalist's hell" [RD02]. No theory was in fact more beautiful and at the same time more difficult to test. A century later the technology and the scientific progress became mature to challenge general relativity with tests based not only on astronomical observations, but also on laboratory experiments. Recently, the spectacular first direct detection of gravitational waves from black holes has added one more jewel to the scientific crown of GR.
QM on its hand, accounts for the behaviour of matter at small scales (nanometers and below), and ultimately leads, together with special relativity, to the so-called Standard Model of strong and electroweak interactions accounting for all the observable known forms of matter.
Clocks exhibiting high stability and high accuracy can be used to perform precision tests of LLI and LPI. WEP experiments based on matter-wave interferometry can be seen as a first and non-trivial attempt in interpreting the free fall of microscopic quantum objects and more generally Einstein's general relativity in the framework of quantum theory.
Clocks and matter-wave interferometers based on cold-atom samples have already demonstrated excellent performances for the accurate measurement of time, of tiny rotations and accelerations, and for the detection of faint forces. So far, their use has been limited to ground, the Earth's surface. These instruments have opened new fascinating perspectives for testing general relativity as well as alternative theories of gravitation, for studying quantum mechanics, and exploring the boundaries of quantum gravity.
Space can be an ideal environment for improving the performance of precision instruments and for pushing measurement accuracy to the limits. With a suitable spacecraft and orbit, Space can ensure:

- Infinitely long and unperturbed "free fall" conditions;
- Long interaction times;

- Quiet environmental conditions and absence of seismic noise;
- Huge free-propagation distances and variations in altitude;
- Large velocities and velocity variations;
- Large variations of the gravitational potential.
- Access to a large part of the surface of Earth

Therefore, a space-based laboratory is in principle able to provide unique experimental conditions, necessary to exploit the ultimate limits of quantum sensors. It can provide measurement accuracy levels not accessible on ground.
On the ISS, due to its intrinsic characteristics, only some of the above features are available in unrestricted from. For example, vibrational noise is present, variations in altitude and gravitational potential are very limited. Nevertheless, the ISS also provides advantages to researchers, such as the possibility to have a massive payload installed, which is the case for the proposed mission.

2.2 I-SOC Science Case

Einstein's theory of general relativity is a cornerstone of our current description of the physical world. It is used to describe the flow of time in presence of gravity, the motion of bodies from satellites to galaxy clusters, the propagation of electromagnetic waves in the presence of massive bodies, and the dynamics of the universe as a whole. Indeed, the measurement of general relativistic effects is very challenging, due to their small size [RD03].
Although very successful so far, general relativity, as well as numerous other alternative or more general theories of gravitation, are classical theories. As such, they are fundamentally incomplete, because they do not include quantum effects. A theory solving this problem would represent a crucial step towards the unification of all fundamental forces of Nature. Several approaches have been proposed and are currently under investigation (e.g. string theory, quantum gravity, extra spatial dimensions) and all of them tend to lead to tiny violations of basic principles. Therefore, a full understanding of gravity will require experiments able to determine its connection with the quantum world. This topic is a prominent field of activity and includes the current studies of dark energy.
Precision experiments for testing the assumptions and predictions of general relativity can be performed on scales ranging from the laboratory to the solar system, in the latter case using satellites, spacecraft, or the orbiting Earth. The implementation of tests with significantly improved sensitivity obviously requires the use of state-of-the-art sensors, at least as far as it is compatible with the boundary condition of the experiment, e.g. space-compatible systems in case of satellite-based experiments.
I-SOC is designed to test aspects of the Einstein Equivalence Principle related to the flow of time using a quantum sensor, namely an atomic clock. Its results can be interpreted as tests of general relativity and other metric theories of gravity and as tests for the existence of new fields associated to matter.
The outcome of the I-SOC mission will be either a confirmation of one of the foundations of general relativity within the accuracy provided by the instruments, or the discovery of a deviation. In the latter case, the mission would provide a first indication of the breakdown of current (classical) gravitational physics theories and could pave the way towards a unified theory of all forces.

I-SOC can perform three main experiments with significantly improved accuracy.

Gravitational Time dilation Tests

One of the most fascinating effects predicted by general relativity and other metric theories of gravity is the Einstein's gravitational red-shift or gravitational time dilation effect.
As direct consequence of Einstein's Equivalence Principle, time runs (or clocks tick) more slowly near a massive body. This effect can be detected when comparing identical time intervals, but measured by clocks placed at different positions in a gravitational field. The measurements consist of counting the number of the ticks of the respective clocks. The effect results in a different number of ticks measured by two clocks located at different gravitational potentials. Equivalently, one can describe the effect by stating that the frequencies of the ticks, as observed at an arbitrary location, differ.
In general, time and frequency can be transferred between locations by using electromagnetic waves directly generated from the local clock and transmitted to an arbitrary detection position x'.
Consider two identical clocks (i=1, 2), therefore having an identical oscillation frequency when operating side-by-side. When they are operated at different locations x_1 and x_2, the measurement of their frequencies at an arbitrary detection position x' yields a frequency ratio:

$$\frac{\nu_2(x')}{\nu_1(x')} = 1 + \frac{U(x_2) - U(x_1)}{c^2}. \qquad (1)$$

Here, $\nu_i(x')$ is the frequency of clock i located at x_i, as observed (measured) at the particular location x' where the comparison between the two clocks takes place (see Figure 2-1). U is the gravitational potential, which in case of a spherically symmetric body of mass M is given by $U(x) = -GM/|x|$, if GR is valid. Equation 1 is a simplification, valid for stationary clocks and observers and for weak gravitational fields. According to Einstein's theory of general relativity, this frequency ratio is universal, i.e. it is independent of the nature of the clocks and of the type (composition) of the mass M. In addition, it is independent of x'.

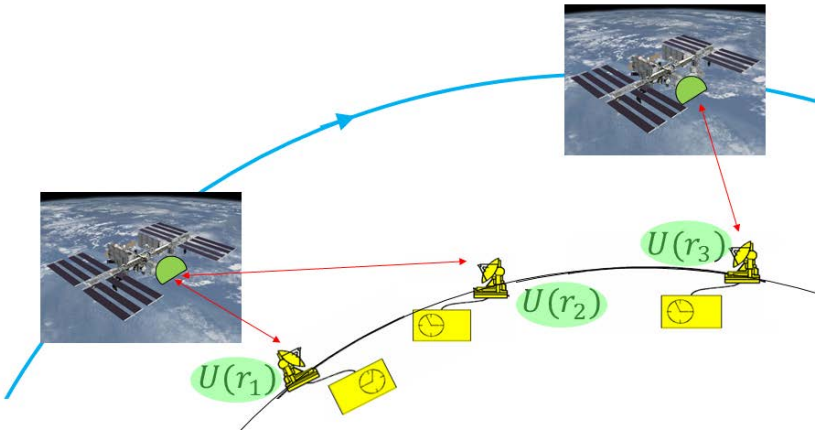

Figure 2-1: The two-way link of I-SOC (red double arrows) will be used to compare the space clocks to clocks on the ground located in r_1 , r_2 and r_3. In addition, it will allow to compare two clocks on the ground in common-view (at locations r_1 and r_2), and also in non-common-view (the ISS sequentially and individually links to clocks at locations r_1 and r_3). In the latter case the I-SOC on-board clock serves as a local oscillator.

I-SOC searches for a possible violation of the gravitational red-shift formula, equation 1. Such a violation may be described phenomenologically by a dependence on the gravitational potential of one or more of the fundamental constants X that determine the clock frequency: $X = X(U/c^2)$, where X is a generic dimensionless fundamental constant or a dimensionless combination of fundamental constants. Such dependence would correspond to a violation of the principle of Local Position Invariance.

In the Standard Model there are three fundamental dimensionless parameters determining the structure and energy levels of stable matter (atoms, molecules): the electromagnetic fine-structure constant α and the ratios of the electron mass m_e and the light quark mass m_q to the QCD (Quantum ChromoDynamics) energy scale Λ_{QCD}, $X_{e,q}=m_{e,q}/\Lambda_{QCD}$. The fundamental masses m_e and m_q are proportional to the vacuum Higgs field which determines the electroweak unification scale. Therefore, the constants $m_{e,q}/\Lambda_{QCD}$ can also be seen as the ratio of the weak energy scale to the strong energy scale.

Extensive studies of atomic and molecular spectra of gas clouds in the distant universe are currently undertaken to search for a difference of these constants compared to today's values (see RD04, RD05, RD06, RD07, RD08 and references therein). Also, some differences between Big Bang nucleosynthesis data and calculations can be naturally explained by a variation of fundamental constants (see RD09, RD10 and references therein).

How can a space-time variation of the fundamental constants and a dependence on the gravitational potential may occur? Light scalar fields very naturally appear in modern cosmological models, affecting the Standard Model parameters α and $m_{e,q}/\Lambda_{QCD}$. One of these scalar fields is dark energy, which causes the accelerated expansion of the Universe. Another hypothetical scalar field is the dilaton, which appears in string theories together with the graviton [RD16]. Cosmological variation of these scalar fields could occur because of drastic changes of matter composition of the Universe. During the Big Bang nucleosynthesis the Universe was dominated by radiation, then by cold dark matter, and now by dark energy. Changes of the cosmic scalar field $\varphi_0(t)$ lead to the variation of the fundamental constants $X(\varphi_0)$. Massive bodies (galaxies, stars, planets) can also affect physical constants. They have large scalar charge S proportional to the number of particles $S=s_p \cdot Z+s_e \cdot Z+s_n \cdot N$, where Z is the number of protons and of electrons and N is the number of neutrons; s_p, s_e, s_n are the scalar charges of protons, electrons, and neutrons respectively. In addition, there is also a contribution of the nuclear binding energy (scalar charge of virtual mesons mediating nuclear forces). The scalar charge produces a Coulomb-like scalar field $\varphi_s=S/R$, where R is the distance from the massive body.

The total scalar field $\varphi=\varphi_0+\varphi_s$ can therefore induce variation of the fundamental constants inversely proportional to the distance R from massive bodies,

$$X(\varphi) = X(\varphi_0 + \varphi_s) = X(\varphi_0) + \delta X(R),$$

$$\delta X(R) = dX/d\varphi \cdot S/R.$$

A nonzero δX would correspond to a violation of the Local Position Invariance principle.

The gravitational potential $U(R)=-GM/R$ is proportional to the number of baryons $Z+N$ and inversely proportional to the distance. Therefore, the change of fundamental constants near massive bodies can be written as

$$dX/X = K_{X,i} \cdot \delta\left(U_i / c^2\right),$$

where the index i refers to a particular composition of the mass M. The coefficients $K_{X,i}$=-($dX/d\varphi$)·S_i/GM_i are not universal. Indeed, as the Sun mostly consists of hydrogen, its scalar charge is S_{Sun}~Z·(s_p+s_e). On the contrary, the Earth contains heavier elements where the number of neutrons exceeds the number of protons (N~1.1·Z). Therefore, the scalar charge of the Earth, S_{Earth}~Z·(1.1·s_n+s_p+s_e), is sensitive also to the neutron scalar charge and to the contribution of the nuclear binding.

When the frequencies of two identical clocks (of nominal frequency ν_0) at different locations are compared, Eq. 1 becomes

$$\frac{\nu_2(x')}{\nu_1(x')} = 1 + \left[1 + \sum_X A_X K_{X,i}\right] \cdot \frac{U(x_2) - U(x_1)}{c^2},$$

where the factor A_X = X·($d\ln\nu_0/dX$) provides the sensitivity of the clock frequency to a particular constant X and can be calculated by using atomic and nuclear theory [RD08].

In this way, the results of space-to-ground comparisons of clocks can be given as a limit for (or nonzero values of) $K_{X,\mathrm{Earth}}$, with X being a known combination of the three fundamental constants $m_e/\Lambda_{\mathrm{QCD}}$, $m_q/\Lambda_{\mathrm{QCD}}$, and α. The comparison of clocks on ground (null solar gravitational red-shift experiment) will give limits to $K_{X,\mathrm{Sun}}$.

The Earth gravitational red-shift was measured with $1.4 \cdot 10^{-4}$ inaccuracy in the 1976 Gravity Probe-A experiment [RD19] by comparing a ground clock with a clock on a rocket as the height changed. The best-performing clocks available at the time, hydrogen masers, were used for this experiment. The ACES mission, planned to fly on the ISS in the 2018-2020 timeframe, seeks to improve this test by a factor of approximately 70, by using the PHARAO cold atom clock [RD20].

I-SOC will use an atomic clock of the newest generation, an optical clock, thus achieving a test with a factor 10 improvement compared to ACES.

Today (2016), three ground clocks (Europe, Japan, USA) have already reached an inaccuracy of $(3\text{-}4) \cdot 10^{-18}$ and two similar clocks have been shown to be in agreement at the 10^{-18} level. By the time of the I-SOC mission in 2024, it is likely that they will have further improved to the level of few times 10^{-19}. These clocks in combination with ISOC will enable a test of the gravitational red-shift in the Sun and Moon fields, which is complementary to the test in the Earth field. Such tests will reach fractional inaccuracies down to $1 \cdot 10^{-6}$ and $2 \cdot 10^{-4}$, respectively. In comparison, the best current results for the Sun field time dilation shift are at the few % level [RD11,RD12]. To our knowledge, the gravitational time dilation caused by the Moon has so far not been measured.

Lorentz Invariance and Standard Model Extension Tests

The foundation of Special Relativity (SR) is the Lorentz Invariance hypothesis. According to this principle, the outcome of any local test experiment in a free-falling apparatus is independent of the velocity and orientation of the apparatus. Over the last century a numerous tests have provided demonstration of the validity of SR at different accuracy levels.

One of the most intriguing aspects of Einstein's theory of special relativity is directly embedded in the transformation laws between various inertial reference systems. In fact, although Lorentz transformations are kinematical equations, they depend on the speed of light c, which is a dynamical parameter derived from Maxwell's field equations.

At present, numerous alternative test theories predict violations of the basic principles of special relativity. Kinematical theories [RD30,RD31,RD32,RD33] postulate the existence of a preferred reference system, often identified with the frame in which the cosmic microwave background (CMB) is isotropic. In this frame, light is assumed to propagate isotropically and with constant speed c_0. Any deviation from the Equivalence Principle is then introduced in terms of a parameterisation of the transformation laws between the preferred frame and inertial reference systems.
A different and more fundamental approach is offered by dynamical test theories in which couplings between gravitational and non-gravitational fields can be introduced in a modified Lagrangian allowing for violations of the Einstein's Equivalence Principle [RD34,RD35,RD36]. In particular, modified Maxwell's equations and a modified Dirac's equation will respectively result in a modification of the properties of electromagnetic fields (photon sector) and of atomic spectra (matter sector). Dynamical test theories became important because modified Maxwell and Dirac equations were derived in the low energy limit from string theory and loop gravity.
Lorentz Invariance and Standard Model extension (SME) tests can be improved in space due to the higher velocity variation of an orbiting laboratory with respect to Earth-based experiments. The measurements can be performed by using different kinds of instruments, both frequency references based on ultra-stable high-finesse resonators and atomic clocks, and by comparing them during the orbital motion of the spacecraft. Depending on the particular scheme, the set-up will be sensitive to violations of special relativity induced by variations of the speed of light with the orientation or the velocity of the local reference frame. In addition, operating the I-SOC atomic clock on transitions involving Zeeman sublevels with opposite spin orientation with respect a static magnetic field, it is possible to perform specific SME tests in the "matter sector", i.e. related to the properties of subatomic particles.

Dark matter

Correlations between frequency fluctuations of atomic clocks can indicate the interaction of dark matter topological defects with the conventional matter that clocks are made of [RD49,RD50]. In order to detect topological defects as they cross the Earth (with putative velocity $v_g \approx 230$ km/s), ground clocks should be intercompared continuously. If the defect overlaps with a first clock but not a second, a frequency difference between the two occurs. If the two clocks are in common-view with I-SOC at that particular moment, I-SOC can in principle measure this effect. But because this situation is relatively improbable and because the duration of such intercomparisons is short, this is not very useful. Therefore, the comparison of "nearby" clocks is better performed by other means, e.g. long-distance fiber links. I-SOC in non-common-view mode is also not useful because v_g is much larger than the ISS orbital velocity (approx. 8 km/s) and so the defect is gone before the ISS performs the comparison. However, one scenario in which I-SOC can play a role is the following. Consider a dark matter defect of size *smaller* than the Earth. After it has passed through the Earth, it will have produced a permanent phase shift (i.e. a time offset) in some clocks and no phase shift in others, depending on their overlap with the defect. This residual shift can be measured by I-SOC, after the defect is gone. Thus, the I-SOC mission can contribute to the search for dark matter.

2.3 Additional Science with I-SOC

I-SOC has important applications in domains other than fundamental physics. In this section, we provide a list of topics that will be investigated by I-SOC bringing a major scientific contribution in the field. With the present payload and platform capabilities, the following topics will be addressed:

Clock Comparisons and International Atomic Time Scales

Depending on application, several time scales are used which are routinely maintained by metrology institutes and international organizations. Universal Time (UT), derived from the observation of the Earth's rotation period, standardizes the biological time based on the day and night life cycle. On the other side, time scales can be built out of atomic clocks. As an example, we can mention the time scale disseminated by GPS satellites or the International Atomic Time scale (TAI). TAI is maintained by the Bureau International des Poids et Mesures (BIPM). It plays a major role as base of UTC (Universal Time Coordinated), recognized worldwide as the official international time, which differs from TAI by an integer number of leap seconds.
I-SOC provides the means for connecting atomic clocks on the ground in a global network, enabling comparisons of ground clocks down to the $3{\cdot}10^{-19}$ fractional frequency uncertainty level. Clock comparisons via I-SOC will contribute to the realization of international atomic time scales and to improvement of their stability and accuracy. Synchronization of clocks, space-to-ground and ground-to-ground, to the 20 ps level using ELT+ will allow the distribution of such time scales to unprecedented performance levels[1].

Geodesy

The mission also provides a new tool for mapping the gravitational potential on the Earth's surface with high spatial resolution and at a high level of accuracy (down to 0.15 cm of differential height over the geoid). This is achieved through the measurement of the differential gravitational shift between two ground clocks with up to $3{\cdot}10^{-19}$ fractional frequency uncertainty. Common-view and non-common-view comparisons of ground clocks, transported to all continents and to several locations per continent, provide direct information on the geopotential differences at the locations covered by the ground clocks. I-SOC will therefore contribute to establishing a global reference frame for the Earth gravitational potential. Such a network is key for accurate long-term tracking of height- and gravity-related quantities like sea level rise or groundwater loss. Due to its unique high spatial and temporal resolution, this method is complementary to current and future gravity space geodetic missions such as CHAMP, GRACE and GOCE as well as to altimetry

[1] We note that with optical links based on transmission of frequency comb radiation, the synchronization error should be reduced further to the few-ps level. Due to the low technological maturity of that link type in Europe, this option is not further considered at present.

missions like JASON and Envisat in defining the Global Geodetic Observing System (GGOS).

Optical and Microwave Ranging

The simultaneous operation of two links in two different frequency domains (microwave and optical) allows the cross-comparison of different ranging techniques, including one-way optical ranging, two-way optical ranging, and microwave ranging. The I-SOC microwave link MWL is capable of a high ranging stability, while its accuracy would need to be calibrated against optical measurements. Such studies will be important for future missions operating both around the Earth and in deep space.
At the same time, atmospheric propagation delays due to both troposphere and ionosphere, which affect ranging at both microwave and optical frequencies, can be measured. Investigations can include the tracking of the differences of mapping functions at optical and microwave frequencies.

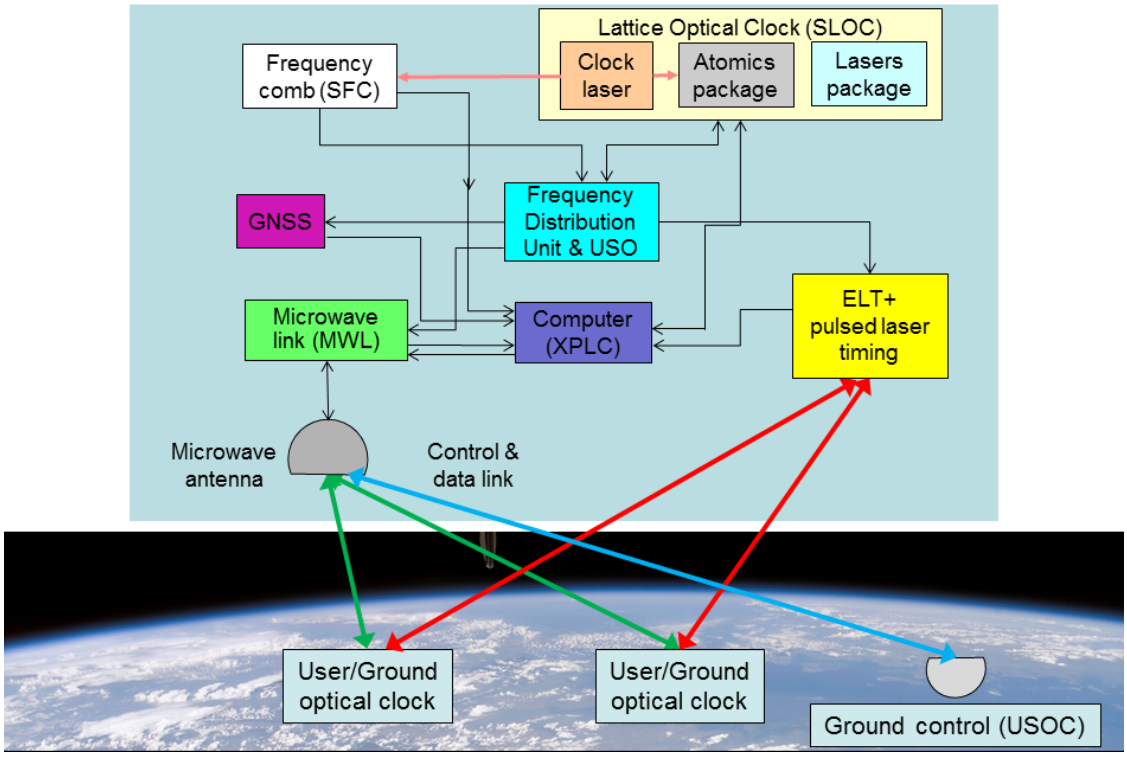

Figure 2-2: The I-SOC payload and its links to ground. Some elements (e.g. Power distribution unit (PDU)) are not shown).

2.4 I-SOC mission overview

I-SOC is an ESA mission in fundamental physics based on the newest generation of atomic clocks, operated in the microgravity environment of the International Space Station (ISS).
The I-SOC payload will be accommodated on-board the ISS at the External Payload Facility of the Columbus module (CEPF).
The I-SOC instrument package consists of an optical atomic clock, a frequency comb, and an ensemble of three time/frequency links of highest performance (red and green arrows in Figure 2-2).
I-SOC provides four measurement functions:

1. The I-SOC clock mean frequency can be compared with the mean frequency of clocks on ground.
2. The I-SOC clock frequency is distributed to ground by the links.
3. The I-SOC clock can be synchronized with a particular ground clock, enabling the latter's time/frequency to be distributed to ground, anywhere in the ISS visibility domain, via the links, providing the opportunity to compare distant terrestrial clocks (i.e. not in common-view of the ISS).
4. When two or more clocks are in common-view of the ISS, they can be compared/synchronized directly, since the uncertainties due to the space clock are in common mode in this synchronous measurement, and therefore are rejected.

These comparisons will allow I-SOC to perform tests of Einstein's theory of general relativity, by providing the most accurate measurement of the gravitational red-shift (time dilation), a search for time variations of fundamental constants (by supporting comparisons of ground clocks), tests of the Standard Model Extension, and search for dark matter. Furthermore, I-SOC will also develop high-performance applications in different areas of research including geodesy and Earth observation.
I-SOC consists of the following elements:

- The I-SOC Payload including
  - The I-SOC Instrument:
    - Space lattice optical clock (SLOC), a frequency standard based on laser- cooled Sr atoms
  - The PL support subsystems:
    - SFC, the space frequency comb
    - MicroWave Link (MWL)
    - European Laser Timing (ELT+) optical link
    - Frequency Distribution Package (FDP), including backup USO
    - GNSS receiver
    - eXternal PayLoad Computer (XPLC)
    - Power Distribution Unit (PDU)
    - Dedicated operation software, mechanical, thermal, and harness
  - The Columbus External Payload Adapter (CEPA), developed by NASA/Boeing

- The Launcher/Carrier, the ISS on-orbit transportation elements.

- The ESA Columbus laboratory with the selected payload location and the corresponding Columbus Payload Integration (CPI) activities.

- The end-to-end mission operations and ground segment consisting of:
  - NASA operations and ground segment
  - Columbus ground segment, represented by the Columbus Control Centre (CCC)
  - I-SOC ground segment, including
    - The I-SOC User Support and Operation Center (USOC), installed at TBR-01
    - The distributed User Ground Stations (UGS)
    - The I-SOC data analysis center installed at TBR-02

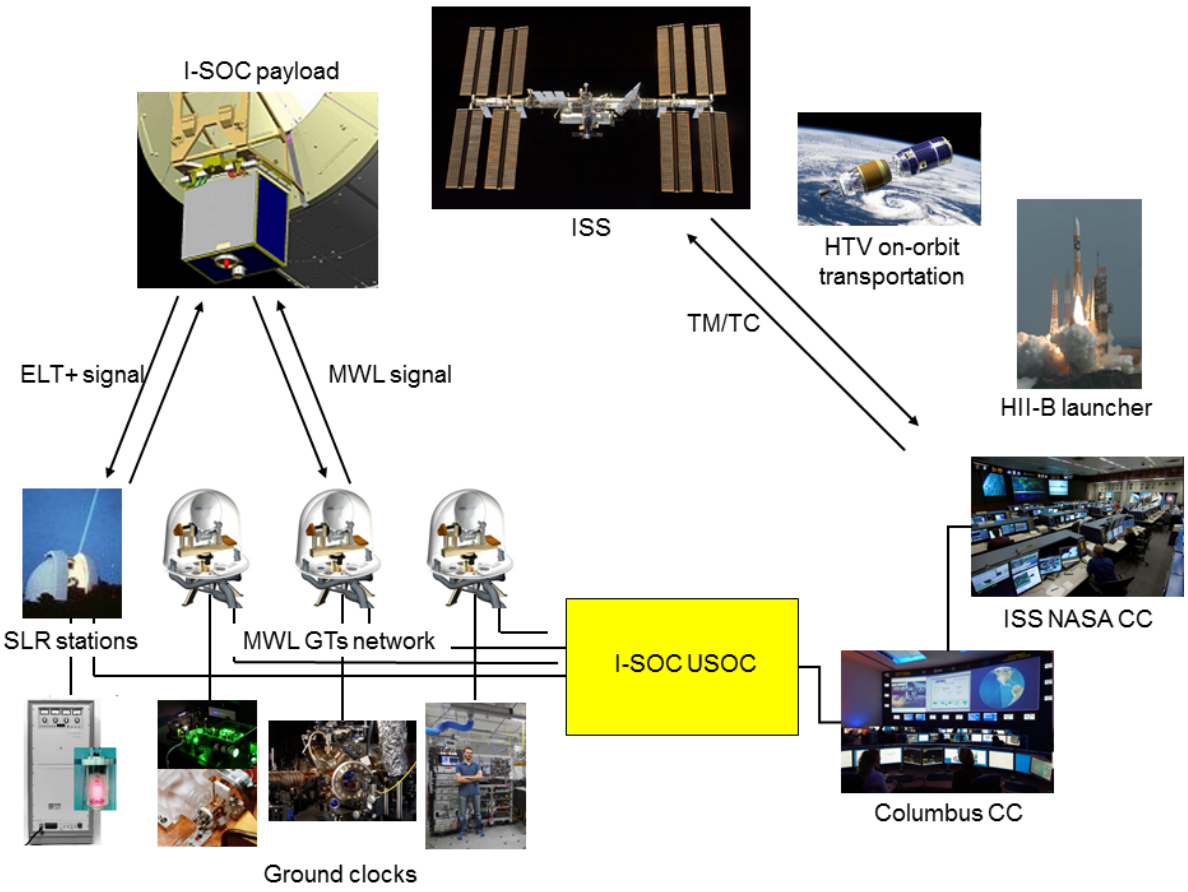

Figure 2-3: The I-SOC mission elements.

2.4.1 *Key On-board Instruments*

The atomic clock is an optical lattice clock, based on ultracold atoms trapped in a standing-wave of laser light. It is based on the strong European developments in this field, including the dedicated studies in the ELIPS-3 programme “Space optical clock” (SOC) and

subsequent EU-funded projects “SOC2” and ITN “FACT”. Goal performance is a fractional frequency instability $5 \cdot 10^{-16}/\tau^{1/2}$, and inaccuracy $1 \cdot 10^{-17}$.
The clock signal is converted by SFC, a femtosecond frequency comb, into a form suitable for optical and microwave transfer to/from Earth. The FDP distributes the I-SOC clock signal to two (plus one optional) time & frequency transfer systems.
All data handling processes are controlled by the eXternal PayLoad Computer (XPLC): it receives data and status information from the subsystems, controls the subsystems by sending high-level commands, transmits data and information to ground, and receives commands from ground.
The mission will connect approximately 10 stationary optical atomic clocks (in national metrology laboratories and on additional reference sites) on ground and 3 – 4 transportable optical clocks (Figure 2-4) in a worldwide network and nearly continuously compare them with each other using the precise time/frequency transfer links.
The links are similar to those already developed for the ACES mission: the microwave link MWL, and the pulsed optical link ELT+ [2].
The comparisons can be carried out in common-view, without the need for a high performance on-board clock (the on-board back-up quartz oscillator (USO) is sufficient).
In the non-common-view comparisons, a low instability of the atomic clock is particularly important; the performance of such comparisons will be limited by the on-board clock.

[2] In this document we also describe the performance of an optional link, the frequency comb optical link FCOL. Its ultralow instability is particularly advantageous for common-view comparisons, strongly reducing the integration time needed to reach the specified frequency uncertainty in the comparison of ground clocks. This has two advantages, a more precise test of the Sun’s and Moon’s time dilation and a more extensive geodetic campaign.

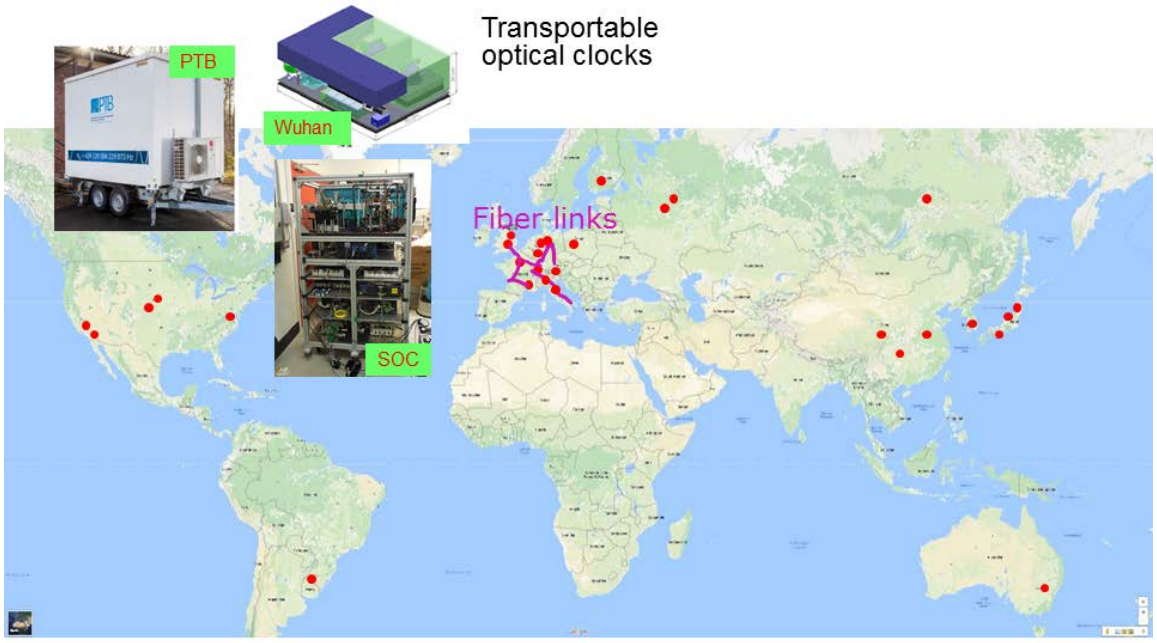

Ca: NRC
USA: NIST, JILA, USNO, JPL, AOSense
Bra: U. Sao Carlos

I: INRIM, LENS
F: Obs. Paris, U. Marseille
CH: METAS
D: PTB, U. Düsseldorf, U. Hannover
UK: U. Birmingham, NPL
PL: FAMO
FIN: MIKES
A: Innsbruck

Rus: VNIFTRII, FIAN, ILP
J: NIMJ, RIKEN, U. Tokyo, NICT
K: KRISS
Ch: Wuhan IPM, NTSC, NIM....
Aus: U.West.Aust.

Figure 2-4 (Top) Locations with stationary high-accuracy clocks and examples of transportable optical clocks, as of 2016. (Bottom) The present and future status of fiber-optical links in Europe (from Fritz Riehle, Nature Photonics **11**, 25 (2017)): Frequency links (green), frequency links commissioned (yellow) and time links (blue). AOS, Astrogeodynamic Observatory in Borowiec near Poznan, Poland; BEV, Bundesamt für Eich- und Vermessungswesen, Vienna, Austria; GUM, Główny Urząd Miar — Central Office of Measures,

Warsaw, Poland; INRIM, Istituto Nazionale di Ricerca Metrologica, Turin, Italy; LNE-SYRTE, Laboratoire National de Métrologie et d'Essais — Système de Références Temps-Espace, Paris, France; MPQ, Max Planck Institute for Quantum Optics Garching/Munich, Germany; NPL, National Physical Laboratory, Teddington, UK; Nikhef, National Institute for Nuclear and High-Energy Physics, Amsterdam, the Netherlands; PTB, Physikalisch-Technische Bundesanstalt, Braunschweig, Germany; SP, Technical Research Institute of Sweden, Boras, Sweden; UFE, Institute of Photonics and Electronics of the Czech Academy of Science, Prague, Czech Republic; VSL, Dutch National Metrology Institute, Delft, the Netherlands; VTT, VTT-MIKES Metrology, Espoo, Finland. Image from Google Earth, US Dept of State Geographer, © 2016 Google, Image Landsat, Data SIO, NOAA, US Navy, NGA, GEBCO.

2.4.2 *Orbit*

I-SOC will be operated on the ISS. The ISS mean altitude is approximately 400 km, with approximate 90 min period and an inclination angle of 51.6 degree. The altitude is not constant, decreasing with a rate in the range 0.5 - 2 km/month due to atmospheric drag, which is compensated with repeated orbit lift maneuvers. The altitude variation must be taken into account, in order to correctly determine the gravitational time dilation. The altitude uncertainty (averaged over the measurement duration) must be less than approximately 1 m. Note that this is larger than the value 10 cm calculated from a simple consideration of the gravitational time dilation (GTD) effect assuming an I-SOC clock with $1{\cdot}10^{-17}$ uncertainty. This is because the relativistic Doppler shift (RDS) also depends on altitude and the two effects compensate each other to a large extent: lower altitude leads to smaller GTD, but also higher speed and thus larger RDS.

2.4.3 *Mission duration*

The planned mission duration is 24 months with the possibility of extending it to 36 months. During the first 6 months, the performance of the SLOC clock in space will be established.
In the second part of the mission (7 to 24 months), the on-board clock will be run in an optimal configuration and perform a large number of comparisons of ground-based clocks operating both in the microwave and the optical domain.
During the whole mission duration, common view and non-common view comparisons of ground clocks will be performed. The longer the mission duration, the larger the number of such comparisons is and the larger the science output will be. For the geodesy measurements and the dark matter search the science gain is roughly proportional to mission duration. For the measurement of the Sun and Moon GTD effect the gain is at most proportional to the square root of mission duration. For the Earth GTD measurement a long duration is not relevant. Finally for the goal of technology demonstration (long-term effects on the clock), a long mission is obviously favorable.

3 I-SOC SCIENTIFIC OBJECTIVES

In this section, the I-SOC scientific objectives are enunciated.
For each scientific objective, the performance evaluation by simulations and numerical models is described in order to demonstrate compliance of the mission performance to the scientific objectives.
The state-of-the-art is also discussed, reporting present techniques and performance levels, the proposed measurement strategy adopted in the frame of the I-SOC project, and the improvements expected with respect to available experimental results.

3.1 Primary Scientific Objectives

The top level scientific objectives of the I-SOC mission are in the fundamental physics domain. As discussed in Sec. 2.2, they address precision tests of the Einstein's Equivalence Principle. They are:

#PSO-01 Measurement of the Earth gravitational red-shift effect to a fractional uncertainty of $2 \cdot 10^{-7}$.
Improvement compared to ACES mission: factor 10 (from more accurate space clock).

#PSO-02 Measurement of the Sun gravitational red-shift effect to a fractional uncertainty of $1 \cdot 10^{-6}$.
Improvement compared to ACES mission: factor 100 (this factor is estimated and arises from a combination of improvements in all aspects: link, space clock instability, ground clock stability, modelling improvements).

#PSO-03 Measurement of the Moon gravitational red-shift effect to a fractional uncertainty of $2 \cdot 10^{-4}$.
Improvement compared to ACES mission: factor 100 (this factor is estimated and arises from a combination of improvements in all aspects: link, space clock instability, ground clock stability, modelling improvements).

Clock Comparisons and International Atomic Time Scales

#PSO-04 Contribution to the realization of atomic time scales to fractional frequency inaccuracy lower than $1 \cdot 10^{-18}$ and synchronized to the few ps level.
Improvement compared to ACES mission: factor 100 to 1000 (better links plus factor 10 from better ground clocks and factor 10 from larger number of measurements).

Geodesy

#PSO-05 Enable mapping of the geopotential on the land masses of North America, South America, Africa, Europe, Asia, Australia, with approximately 300 km · 300 km grid size using transportable $1 \cdot 10^{-18}$ clocks, with a resolution of 0.15 m^2/s^2 (1.5 cm on the differential geoid height).

Improvement compared to ACES mission: factor 10 000 (factor 1000 from larger number of measurement points and factor 10 from higher resolution).

#PSO-06 Inter- and intracontinental differential geopotential measurements with resolution in the gravitational potential U at the level down to 0.05 m^2/s^2 (0.5 cm on the differential geoid height).
Improvement compared to ACES mission: factor 100 (factor 10 from larger number of measurement and factor 10 from higher resolution).

I-SOC can also perform Local Lorentz Invariance and Standard Model Extension (SME) tests, for example by comparing the frequency of the on-board-reference cavity with the on-board atomic clock as the ISS moves along its orbit. These experiments are presently not considered as part of the primary mission objectives. They will be reassessed at a later stage when detailed simulations are available.

3.2 Additional Scientific Objectives

Clock Comparisons and International Atomic Time Scales

#SSO-01 Space-to-ground time transfer with inaccuracy lower than 50 ps via MWL and 30 ps (target: 20 ps) via ELT+.

#SSO-02 Synchronization of clocks on ground to better than 50 ps via MWL and 30 ps via ELT+ (target: 20 ps).

Optical and Microwave Ranging

#SSO-03 Cross-comparisons of different ranging techniques: one-way optical ranging, two-way optical ranging, microwave ranging.

#SSO-04 Measurement of the differential atmospheric propagation delays in the optical and microwave.

3.3 Scientific Performance

For the purpose of analysing the feasibility of the mission against its primary scientific objectives, a measurement concept based on the reference payload design has been identified. Text [in blue] refers to the scientific requirements listed in Sec. 3, derived from and relative to this reference payload.

3.3.1 *Clock Measurements*

The gravitational potential U for both ground and space clocks is a sum of three major contributions coming from Earth, Sun, and Moon:

$$U(\boldsymbol{r}) = U_{\mathrm{Earth}}(\boldsymbol{r}) + U_{\mathrm{Sun}}(\boldsymbol{r}) + U_{\mathrm{Moon}}(\boldsymbol{r}). \quad (2)$$

For simplicity, here and hereafter, we omit a relativistic Doppler shift term that occurs for Earth-bound clocks (related to the spin of the Earth) and for the I-SOC clock (related to ISS motion. Since the variations of the individual contributions with the position $\boldsymbol{r}$ of the

satellite or of the ground stations have different signature, it is possible to independently determine them and therefore measure each of the three time dilation effects. The Earth time dilation measurement relies on space-to-ground clock comparisons while the Moon and Sun measurements rely on ground-to-ground comparisons.

(I) The concept of the gravitational time dilation measurement in the Earth field is shown in Figure 3-1. The clock on the I-SOC spacecraft is compared with a particular clock on ground. The typical duration of a ISS pass above a ground station in Europe is about 300 s. However, comparisons are repeated in order to obtain a good statistic. The measurement yields the frequency ratio ν_{gc}/ν_{ISOC}. This value arises from a complex procedure involving corrections stemming from the velocities of the ground and satellite clocks (leading to second-order Doppler effects) that need to be evaluated.

(II) I-SOC also allows the comparisons of distant ground clocks via non-common-view comparisons (Figure 2-1). Here, the ISS and the I-SOC instruments are in contact with only one ground clock at a time.
Such comparisons allow a measurement of the time dilation in the gravitational field of the Sun and the Moon (
Figure 3-2). Here, the frequency ratio ν_{gc1}/ν_{gc2} of two ground clocks is measured repeatedly. The two clocks are as far apart as possible in East-West direction, i.e. on different continents. With frequent comparisons, ideally one comparison per orbit (92 min), an extended time series of frequency ratios can be obtained that will allow identifying any ~12 h modulation due to the effects of Sun and Moon (the period of the effect differs slightly for the two bodies and so the two effects can be disentangled given a sufficiently long time series).
The comparison is expected to yield zero modulation amplitude, due to the fact that the Earth is in free fall in the field of the Sun and the Moon. However, after subtracting from the data the second-order Doppler effect due to Earth motion (which can be measured independently and/or modelled), the GTD modulations due to the Sun and to the Moon field can be extracted. Sun and Moon contributions can be distinguished due to their different time signatures.
The same measurement data can also be applied to relativistic geodesy and synchronization of ground clocks.

(III) The I-SOC time and frequency transfer links also allow for the common-view comparison of terrestrial clocks (Figure 2-1). In the common-view technique, two ground clocks are simultaneously compared to the space clock. The difference of simultaneous measurements then provides a direct comparison of the two clocks on the ground. This measurement does not require a high-performance frequency reference on-board the I-SOC payload. Indeed, the frequency noise of the space clock, which appears as common mode in the two simultaneous link measurements, is rejected to high degree when the difference of the two space-to-ground comparisons is evaluated.
This measurement mode is also used for geodesy and synchronization of ground clocks.

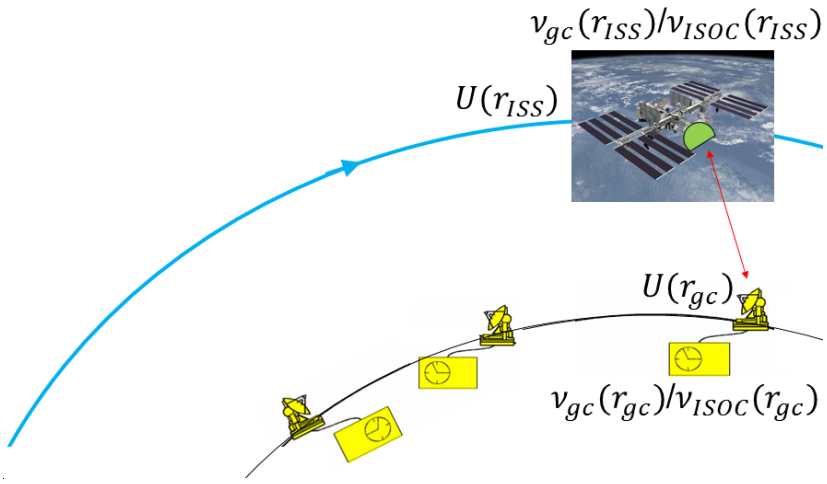

Figure 3-1: Measurement principle of the gravitational time dilation effect in the field of the Earth. Both at the ground clock location $\boldsymbol{r}_{gc}$ and at the ISS location $\boldsymbol{r}_{ISS}$ a measurement of the ratio of the frequencies of the ground clock and space clock is obtained. The two ratios will be the inverse of each other, differing from unity due to the GTD and the relativistic Doppler shift (ground and ISS velocities are not indicated in the figure).

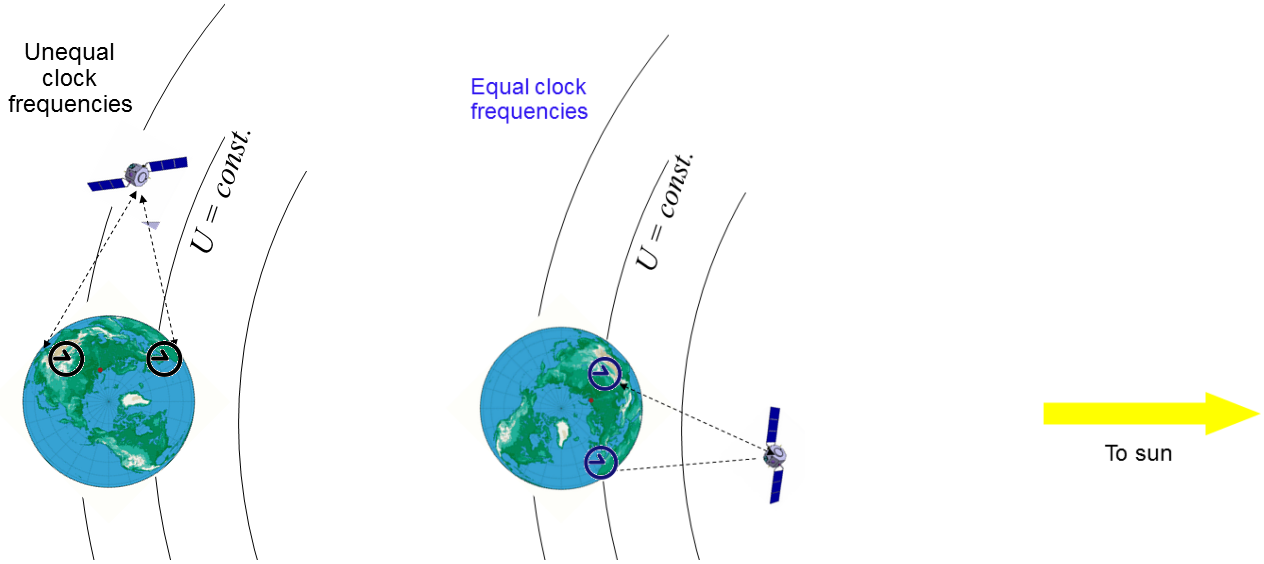

Figure 3-2: Measurement principle of the gravitational time dilation effect in the field of the Sun. Two snapshots of the orientation of a pair of clocks w.r.t. the Sun are shown. **Left**: the two clocks experience different solar gravitational potential. **Right**: the clocks experience the same gravitational potential. If the Earth center would be fixed in space, still allowing rotation around its axis, the clock frequency ratio would differ between the two orientations. Because the Earth is in free-fall in the Sun's field, the effect is nulled because of the additional effect of the relative RDS, thus satisfying the Equivalence principle. The location of the ISS is only schematic. In reality, the clocks are compared in non-common-view-mode. Due to the rotation of the Earth, the differential Sun GTD varies in time and is sampled by the non-common-view comparisons.

3.3.2 *Measurement Modeling and Assumptions*

The accuracy levels that can be achieved in gravitational time dilation tests and ground clock comparisons depend on the combination of several effects:

1. I-SOC orbit and ground terminals positions:
   - ISS orbit;
   - Location of the microwave and optical link ground terminals;
   - Link visibility constraints;
2. I-SOC operational constraints:
   - Mission lifetime;
   - Orbital manoeuvres;
3. Clocks and links performance:
   - Instability and inaccuracy of the ground and space clocks;
   - Instability and inaccuracy of the links;
4. Relativistic effects:
   - Knowledge of ground and space clock positions and velocities;
   - Knowledge of the gravitational potential at the ground and space clock positions;

The constraints imposed by 1 to 4 are discussed in the following sections and included in the numerical simulations developed to verify the mission performance against the I-SOC scientific objectives.

I-SOC Ground Terminals Position

Ground stations, both fixed and mobile ones, can be chosen to serve the mission.
The fixed ground stations are to be chosen to serve the mission goals.

(I) For the tests of the gravitational time dilation, the major metrology institutes having already today clocks with high accuracy are a suitable choice: Torino, Braunschweig, Paris, Teddington (Europe), Boulder (USA), and Tokyo (Japan). In these centres, high-performance optical and microwave atomic clocks are operational today and will certainly be operational at the time of the I-SOC mission.

(II) These institutes also require a regular comparison of their optical frequency standards for the purpose of generating an accurate time scale and for the search for a time variation of the fundamental constants.

(III) The ELT+ optical link requires a SLR station. By the time of the I-SOC mission, at least one European SLR station will be linked to an optical clock by stabilized optical fiber link. Alternatively, a transportable optical clock could be deployed at the SLR station location and used for a measurement campaign.
The mobile ground stations are chosen to perform a geodesy survey campaign with the aim of covering an area as large as possible.
The I-SOC mission is open to additional groups joining as users. Indeed, there are research activities on high-performance optical clocks in progress in more countries than the above, including Korea and China.
A parameter to be taken into account is the visibility of the ground stations from the ISS. For the microwave link, 100% visibility is assumed, since microwave frequencies show only small sensitivity to weather conditions. For the optical links, we assume 50% average probability that a given ground clock can be

compared with the space clock when flies by and 25% average probability that a pair of ground clocks can perform a common-view comparison; these figures are compatible with historical weather data on clouds coverage at the baseline ground station locations.
In addition, both optical links are considered to be in full tracking mode at elevations higher than 30 degrees and lower than 85 degrees. Both the minimum and maximum elevations of optical links are limited by a number of factors: ELT+ optical receiver design, atmospheric transmission at lower elevations, available accurate atmospheric models for low elevations, backscattered background signal for zenith and very high tracking speed for elevations > 85 degrees. Therefore, the ground-ISS contact time is assumed to be 300 s at most for the microwave link and ~ 200 s for the optical link.

I-SOC Operational Constraints

The duration of the I-SOC routine science phase is at least 2 years [#SR-OP-01, #SR-OP-02]. During this phase, mission operations shall ensure the minimum measurement time needed for averaging the uncertainties in the clock GTD tests down to level stated as goals.

Clock Performances

The performance of the I-SOC clock is specified in #SR-PL-03 and #SR-PL-04 to a fractional frequency instability of $8 \cdot 10^{-16}/\tau^{1/2}$, and a fractional frequency inaccuracy of $1 \cdot 10^{-17}$.
Future ground clocks are here specified to have projected fractional frequency instability of $1 \cdot 10^{-16}/\tau^{1/2}$ [#SR-GS-01] and a fractional frequency inaccuracy of $3 \cdot 10^{-19}$ [#SR-GS-02].
Future mobile ground clocks are here specified to have projected fractional frequency instability of $2 \cdot 10^{-16}/\tau^{1/2}$ [#SR-GS-01] and a fractional frequency inaccuracy of $1 \cdot 10^{-18}$ [#SR-GS-02]. These values are Allan deviations. The modified Allan deviations shown in the figures (where the integration time τ is large) have values $\sqrt{2}$ times smaller.
Figure 3-3 shows the clocks' performances.

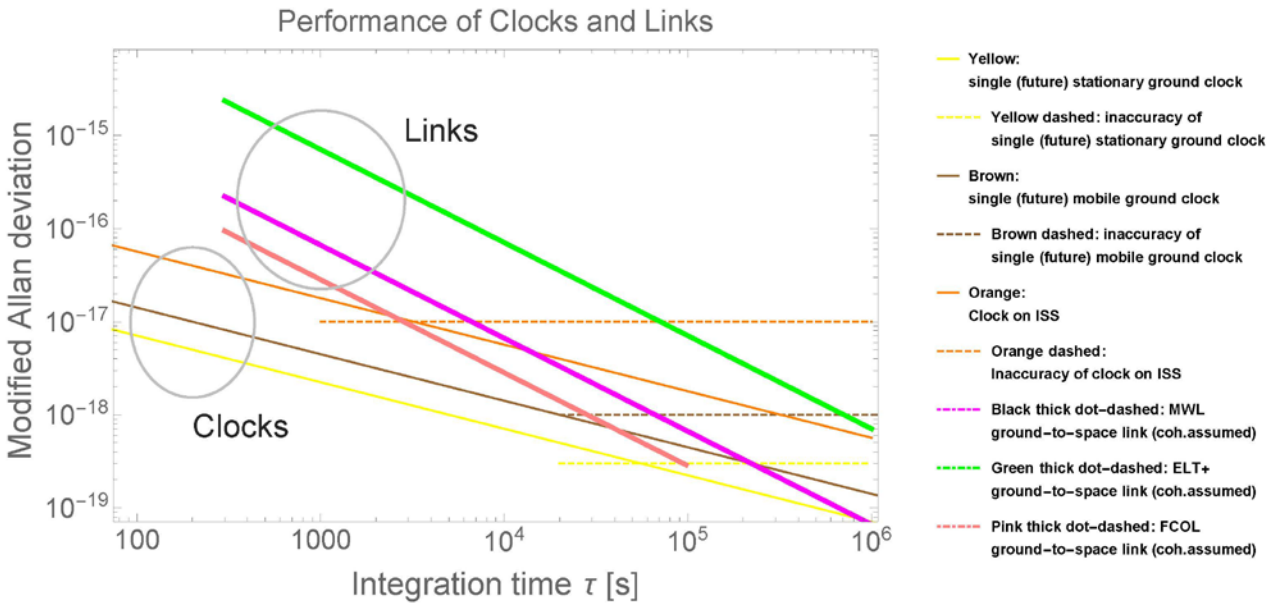

Figure 3-3: Performance of clocks and links, for the case of measurement of the Earth's gravitational time dilation. The thick dot-dashed lines show the contribution of the three types of links (excluding the space clock) to this measurement. They were computed using Eq. (3) below. The minimum required integration time occurs when these contributions drop well below the space clock uncertainty (orange dashed line). Here, clear weather conditions have been assumed for all ISS passes.

Link Performances

Requirements #SR-PL-09 and #SR-PL-16 define the fractional frequency instability of the I-SOC microwave and optical links.

The MWL performances are being established in ongoing ESA industrial studies tailored on the STE-QUEST mission proposal. For ground-to-ground clock comparisons [a], the specified fractional frequency instability of the I-SOC microwave link σ_{MWLgg} accounts for the following noise terms:

- White phase noise averaging down to $1.6 \cdot 10^{-14}$ after 10 s of integration time;
- Flicker phase noise with modified Allan deviation of $1.6 \cdot 10^{-13}/\tau$;
- Long-term performance $6 \cdot 10^{-17}/\tau^{1/2}$;
- Flicker floor at the $5.0 \cdot 10^{-19}$ level [#SR-PL-09];
- Inaccuracy is $5 \cdot 10^{-19}$ [#SR-PL-10].

For ELT+, TDEV is specified at 0.5 ps at 100 s, and <1 ps for longer times up to $1 \cdot 10^6$ s. These values should result in frequency comparison inaccuracy of $1 \cdot 10^{-18}$ [#SR-PL-16]. At 300 s, the ISS contact time, we assume 0.5 ps.

Combining the ground and space segments, one can conclude that the precision obtainable within one pass of I-SOC / ISS could be below 0.5 ps @ 100 s. The value of overall timing

stability ≈ 1 ps is expected for time intervals of up to 10^6 s. Thus, the best fractional accuracy possible with this method will be 1 ps/10^6 s = $1{\cdot}10^{-18}$.
The space-to-ground instability [b] is equal to $\sigma_{link}(\tau) = \sigma_{MWLgg}(\tau)/\sqrt{2}$. Figure 3-3 shows the I-SOC links performance relevant for space-to-ground comparisons[3].

Orbitography

Orbitography requirements are defined in #SR-PL-43, #SR-PL-44, #SR-PL-45, #SR-GS-09, #SR-GS-10, #SR-GS-11 and further discussed below. Those requirements have been derived to contribute negligible noise to the links and in modelling the gravitational frequency shift and the second-order Doppler shift and therefore they will not be considered in the modelling of the clock comparison measurements.
The uncertainty in the evaluation of the relativistic correction due to the uncertainty of the orbit determination of space and ground clocks can be made smaller than that due to the space clock frequency uncertainty if the orbit height uncertainty is less than 1 m. This may be deduced from the analysis of the ACES mission (clock at $1{\cdot}10^{-16}$, 10 m height uncertainty), by a simple scaling argument.

Ground geopotential modelling

The uncertainty of the geopotential model has two contributions: from the static part and from the time-dependent part. In well-studied locations, such as Germany, the uncertainty of the static part is today approximately 0.1 to 0.3 m^2/s^2 (*0.1 m^2/s^2 is equivalent to 1 cm or $1{\cdot}10^{-18}$ clock inaccuracy*) [RD51]. The time-dependent contribution is dominated by the solid earth tides, approximately 5 m^2/s^2, but can be modelled at the level of 0.1 m^2/s^2 [RD53].
Thus, for the absolute measurement of the GTD (ground vs. space), with the "worse" (space) clock at $1{\cdot}10^{-17}$ uncertainty level (equivalent to 1 m^2/s^2 uncertainty of the potential), already today the total uncertainty of the potential at ground clock locations such as in Germany is sufficiently small.
The uncertainty of the geopotential on the continental scale is e.g. 0.2 to 0.5 m^2/s^2 in Europe [RD52]. On the intercontinental scale the uncertainty is similar [RD53]. Thus, if the ratio of frequencies of two clocks on different continents is to be determined, the combined (factor $\sqrt{2}$) geopotential uncertainty of 0.3 to 0.7 m^2/s^2 will limit the inaccuracy to approximately $7{\cdot}10^{-18}$.
This limitation is where I-SOC provides a major science opportunity. Employing ground clocks whose (natural, intrinsic) frequency ratio is known (e.g. equal to 1 if they are

[3] For comparison, the Figure 3-3 also shows FCOL. It is specified at 20 fs instability for integration between 1 s and $1{\cdot}10^5$ s. The value 20 fs, significantly higher than results achieved on the ground for 10 km long links, arises because of the long integration time, high velocity and look-ahead requirement. Inaccuracy is $1{\cdot}10^{-19}$ [**Error! Reference source not found.**]. FCOL is highly advantageous for all scientific goals, except for #PSO-01, allowing highest science performance.

identical clocks), their comparison via I-SOC allows a geopotential difference measurement with significantly better accuracy than today, namely to the 0.1 m^2/s^2 level.

3.3.2.1 Modeling of the link performance

The comparison of distant clocks is based on the transmission of time-tagged signals, coherently generated from the local clocks, from ground to space.
A ground clock and the space clock can be compared via a single leg of the link.
A ground clock can be compared with another ground clock using the common-view and the non-common view technique, depending on their distance.

The Common-View Technique

In this scheme, the two ground clocks, geographically close enough to be in common view with the ISS, are simultaneously compared to the same on-board time signal using two different link channels. The difference between the two space-to-ground comparisons provides the comparison of the two ground clocks.
Although a space clock is needed in the common-view comparison technique, *its frequency stability does not play a role as its noise contribution is in principle rejected in the differential measurement*. The level of rejection will however depend on the symmetry between the two channels of the link flight segment electronics.
Due to the low orbit of the ISS and the limited duration of each pass, the common-view technique will only be suitable for comparing ground clocks over relatively short distances. This has important applications for geodesy, in particular between transportable clocks. This method is not applicable for intercontinental comparisons.
The total noise in the common-view comparison has been introduced above as σ_{MWLgg} . It is equal to the quadratic sum of the noise contribution of the two space-to-ground links.
For the ground-clock-to-space-clock comparison, the noise of the link enters only once.
By repeating a common-view measurement of the frequency ratio of two clocks during N subsequent passes of the ISS, the statistical uncertainty of the mean frequency ratio can be reduced by a factor $N^{1/2}$ compared to that of a single measurement.
However, if the clocks run continuously during that time (meaning that effectively the each clock has means to track the number of oscillations occurring during the whole measurement interval of N ISS passes), even a reduction by N can be achieved. A necessary condition for this is that the clocks' oscillations must be *uninterrupted*.
The common-view technique requires that signals from two ground clocks can be received simultaneously on-board I-SOC. In case of MWL, several channels can be implemented with modest extra cost. In case of ELT+, multiple ground systems may be operated simultaneously without any extra costs. The photon counting principle of ELT+ detection enables this mode of operation[4].

[4] However, in case of FCOL, two space optical terminals (telescopes with pointing mechanisms) are required, which represents a non-negligible cost and mass.

The Non-common-View Technique

A non-common view comparison between two ground clocks C_1 and C_2 takes place in two steps: C_1 is first compared to the I-SOC time scale when in visibility with the space clock; the ISS travels to the visibility cone of C_2 . This is represented by the dead time Δt. Then a comparison between C_2 and the space clock follows. In a non-common view comparison, the space clock acts as a flywheel transferring the time scale from C_1 to C_2 over the dead time Δt. In this way, it is possible to compare clocks over intercontinental distances to a time resolution that will then depend on the link stability and on the time error accumulated by the space clock over the dead time.
A more sophisticated approach is described further below in the section on #PSO-02, p. 37.
The expected inaccuracy of comparisons of ground clocks in non-common view is therefore limited by the quadratic sum of the following uncertainties:

- The link noise (including signals distribution and link contribution) in the comparison between the I-SOC clock and each ground clock. Over one ISS pass (~ 300 s) this term is[5]:
    - MWL: 83 fs
    - ELT+: 0.5 ps (ground stations currently perform at 1 ps, and 500 fs is a realistic expectation for the near future)

For each link type, this noise is multiplied by $\sqrt{2}$ in case of a ground-to-ground comparison.

- The time error $\sigma_x(\tau)$ (TDEV) accumulated by the space clock over the dead time τ. It is calculated from the frequency instability $\sigma_y(\tau)$ as $\sigma_x(\tau) = (\tau/3^{1/2})$ Mod $\sigma_y(\tau)$; in the case of white frequency noise, Mod $\sigma_y(\tau) = 2^{-1/2}\ \sigma_y(\tau)$.

- The time error due to the I-SOC signal distribution and link noise over the duration Δt between the two space-to-ground comparisons.

- The uncertainty in the evaluation of relativistic correction stemming from the errors in the orbit determination of space and ground clocks and in the geopotential model.

The total time uncertainty can be converted into a fractional frequency uncertainty by dividing by τ. This is further elaborated on below in the section on #PSO-02.

3.3.2.2 Evaluations

An approximate computation of the expected inaccuracy of the various clock comparisons proceeds in two steps.

[5] FCOL: 20 fs

First, the clock and link inaccuracies are computed in the way as described above, without including the relativistic corrections. Thus, the values obtained represent the best possible case.
Second, from the values, we derive the requirements concerning the uncertainty of the relativistic corrections, i.e. of orbit determination and of geopotential values on ground and in space. We then discuss the feasibility of achieving these requirements.

3.3.2.3 Results

#PSO-01: *Measurement of the Earth gravitational red-shift effect to a fractional frequency uncertainty of $2 \cdot 10^{-7}$*

1. Measurement of the Gravitational Time Dilation Effect in the Earth field

This measurement approach relies on the absolute comparison between the space clock and one clock on ground. The difference in the two clocks' frequencies is compared with the Einstein prediction.
The target accuracy is derived from the SLOC fractional frequency inaccuracy of $1 \cdot 10^{-17}$ [#SR-PL-04]. For an ISS orbit of 400 km altitude, the gravitational red-shift term is about $+4.6 \cdot 10^{-11}$, thus the expected measurement inaccuracy is $(1 \cdot 10^{-17} / 4.6 \cdot 10^{-11}) = 2 \cdot 10^{-7}$.
To achieve this value, three issues need to be addressed.

(I) The ground clock must have an inaccuracy below $0.5 \cdot 10^{-17}$. Such clocks already exist today (2017) and will likely be widespread, including mobile ones.

(II) The link must have a sufficient accuracy and stability. The minimum integration time to reach the above inaccuracy results from the condition that the SLOC instability and the link instability are both less than the SLOC inaccuracy. Refer to Figure 3-3.
Since the ground-to-ISS contact time is limited to approximately 300 s, a duration over which the space clock's instability averages down to approximately $3 \cdot 10^{-17}$, i.e. higher than its specified inaccuracy of $1 \cdot 10^{-17}$, the goal inaccuracy in the measurement of the Earth's time dilation cannot be reached during a single ISS contact.
Two modalities will be implemented to extend the measurement duration:

A. Simple statistical averaging.
MWL allows reaching a statistical uncertainty in the space clock's frequency determination of approximately $2 \cdot 10^{-16}$ during a single ISS pass.
Independent measurements of the space clock's frequency on different ISS passes can be averaged, reducing the statistical uncertainty by a factor (number of passes)$^{1/2}$. Thus, after approximately 1600 ISS passes (spanning 1 year[6]) the statistical uncertainty will be lower by a factor 2 than the specified space clock systematic uncertainty.

[6] This number is not affected if the space clock instability is reduced since it is dominated by MWL instability

For the ELT+ link, given its 20-fold higher noise than MWL, this modality would lead to an impractically long overall measurement duration[7].

B. Oscillation tracking.

The measurement consists in measuring the ratio of the number of oscillations of the space clock and of the ground clock that have occurred during the interval τ, where τ is a multiple of the ISS period. Thus, both space and ground clocks must be oscillating uninterruptedly during this interval τ, and all oscillations must be counted, i.e. coherence must be maintained.

This comparison yields the difference of oscillation periods of the ground and space clocks. Thus, the gravitational time dilation (averaged over the interval τ) can be extracted.

The statistical uncertainty of the frequency comparison due to the link only is calculated by:

$$\sigma_y(\tau) = \frac{\sqrt{2\sigma_{x,\mathrm{link}}(\tau_{\mathrm{contact}})^2}}{\tau} \qquad (3)$$

τ_{contact}= 300 s is the ISS contact time and τ is the total time. Figure 3-3 shows this modality.

We use the expression above and determine the integration time necessary to reach $0.5 \cdot 10^{-17}$ statistical uncertainty for the three link types[8]:

MWL: $\tau \approx$ 4 hours → 3 orbits

ELT+: $\tau \approx 21/2(0.5\text{ ps})/(0.5 \cdot 10^{-17}) \rightarrow$ 1.6 days

In practice, this measurement will be repeated during the whole mission, in order to characterize the long-term drift of the space clock.

(III) In order to be able to take advantage of the space clock inaccuracy of $1 \cdot 10^{-17}$, and reach a fractional inaccuracy of $2 \cdot 10^{-7}$ in the time dilation, a knowledge of the ground-space gravitational potential difference ΔU with fractional inaccuracy of approximately $1 \cdot 10^{-7}$ (an equivalent height inaccuracy of $(1 \cdot 10^{-7}) \cdot (400\text{ km}) = 4$ cm) is required. Of course, ΔU must be determined not from clock frequency difference measurements, but from geodetic (mechanical) measurements, including satellite gravimetry.

As discussed above, the gravitational potential on the ground is known with an uncertainty of approximately 4 cm. We believe that based on current models also the gravitational potential difference ΔU between ground and an altitude h ≈ 400 km above ground can be modelled with similar uncertainty. Thus, the science goal #PSO-01 for the Earth GTD is achievable.

[7] FCOL allows reaching a statistical uncertainty in the space clock's frequency determination of approximately $1 \cdot 10^{-16}$ during a single ISS pass, dominated by the space clock's instability. Then, approximately 400 ISS passes (spanning 3 months, under clear weather conditions) are needed.

[8] FCOL: $\tau = 2^{1/2}(20\text{ fs})/(0.5 \cdot 10^{-17}) \approx 6000$ s → 1 orbits

Alternatively, we propose the following hybrid approach. ΔU is related to the gravitational acceleration as (for simplicity, we omit the discussion of the influence of Earth rotation):

$$\Delta U = \int_{\text{groundclocklocation}}^{\text{ISS}} \vec{g}(\vec{r}) \cdot d\vec{r} \tag{4}$$

Here, the integration path from the ground clock location to the ISS location is arbitrary, and can be chosen conveniently. In practical terms, the measurement must be split into two steps, $\Delta U = \Delta U_{\text{ground-}h\text{max}} + \Delta U_{h\text{max-ISS}}$.

Close to the Earth surface, g varies less predictably than up high in the atmosphere. Therefore, precise measurements are done close to ground. A gravimeter is transported from the location of the laboratory clock to a suitably chosen altitude h_{max} (e.g. 1 km) above ground, performing measurements of g along the way. This transport could be implemented using first a crane and then an unmanned or manned aerial vehicle. Accurate, transportable gravimeters, mechanical or atomic, are COTS instruments already available today. The fractional uncertainty of a high-quality, rugged gravimeter for field use (model A10 of MicrogLacoste) is 10 µGal, or $1{\cdot}10^{-8}$ fractionally and therefore sufficient for keeping its contribution to the fractional error of $\Delta U_{\text{ground-}h\text{max}}$ below $1{\cdot}10^{-6}$, and the fractional error of ΔU below $1{\cdot}10^{-7}$. The measurement precision of the gravimeter is $2{\cdot}10^{-9}$ after 2 minutes. If needed, a more precise gravimeter can be used.

Then, starting at the altitude h_{max}, models of the gravitational potential, obtained from satellite gravimetry, are expected to be sufficiently precise and can be used to derive the potential difference between h_{max} and the ISS altitude. Measurements of this type can be performed by geodesy research groups.

The ISS altitude h_{ISS} varies substantially as a function of time (with a rate of 0.5 – 2 km/month or 1 - 4 mm/min). Clearly, accurate data of the ISS altitude with time resolution at the minute level must be available over the time span of the measurement and used in the data analysis.

However, the altitude of the ISS does not actually need to be measured at the 4 cm level, because the space clock frequency also depends on the ISS velocity (due to the relativistic, i.e. 2nd -order Doppler shift), which is itself a function of ISS altitude. The correlation between the two quantities relaxes the need for the accuracy of the ISS altitude by a factor of approximately 10, i.e. to the 40 cm level. This accuracy can be achieved by combining data from laser ranging (including to the corner-cube reflector of the I-SOC payload), from the GNSS receiver of the I-SOC payload, and from the standard ISS-GNSS receivers.

The measurement of $\Delta U_{\text{ground-hmax}}$ is in principle needed only for a single ground clock. However, it is very important to perform independent measurements with a second and even third ground clock station. This will greatly enhance the reliability of the I-SOC results. The capability of I-SOC to do so is an important strength.

Finally, for measurement modality (A), the above requirements refer to the ISS velocity and altitude during (i.e. averaged over) the actual contact intervals of a few 100 s. The statistical contribution to ISS orbital parameters uncertainty will average down with the number of passes, but not any systematic contribution.

For modality (B) the requirements refer to the time average over 1 (FCOL) to few (MWL) orbits. This concerns both statistical uncertainty and systematic uncertainty. Because of the difference in the orbit parameter uncertainty for modality (A) and (B), it is clearly valuable to implement both modalities, thus allowing for a consistency check.

2. Time-resolved measurement of the Earth-field Time Dilation

The ISS orbit altitude h_{ISS} varies in time. The variations are a few km over a few weeks, followed by altitude raising manoeuvres that occur within approximately one day. This corresponds to a fractional frequency shift of the space clock compared to a ground clock of a few 10^{-13}. This variation can be measured without requiring that the space clock has absolute accuracy, it suffices that it has a long-term stability over a time scale T. If we consider the time interval T of continued altitude decrease, then T ≈ 1 month. If instead we consider performing one measurement before a raising manoeuvre and one measurement afterwards, the time scale T ≈ 1 day. If the total systematic shift is stable to the level $\sigma_y(T)$, the time dilation can be measured with uncertainty $\sigma_y(T)/(2{\cdot}10^{-13})$. Technically, the second case is more advantageous, since it will be easier to achieve a low $\sigma_y(T)$ if T is 1 day instead of 1 month.
The space clock instability specification is $\sigma_y(1\ \text{day}) < 1.5{\cdot}10^{-18}$. Thus, a measurement along these lines can in principle allow a fractional uncertainty on the time dilation of $<1{\cdot}10^{-5}$. A corresponding orbitographic accuracy is required (better than, e.g. $1{\cdot}10^{-5} \cdot 2$ km = 2 cm, or approximately 10 cm if correlation with the Doppler effect is taken into account), which is more stringent than in the case described under 1. above. Note that the 10 cm value is a requirement on the orbit parameters averaged over a few orbits.
A gravimetric survey near the ground clock is not required for this modality. Time variations of the gravitational potential at the ground clock location can be neglected.
While the uncertainty of this measurement is a factor 50 higher than that of the goal #PSO-01, the different measurement modality provides a useful consistency check of the understanding of error sources.

#PSO-02: ***Measurement of the Sun gravitational time dilation effect to a fractional uncertainty of $1{\cdot}10^{-6}$, with a goal of $5{\cdot}10^{-7}$***

This measurement tests for a source-mass dependence of the time dilation effect, which could arise from an anomalous coupling of matter to the Standard Model quantum fields. It may also be interpreted as a search for the neutron's scalar charge.
The gravitational red-shift effect induced by the Sun is measured by comparing ground clocks in non-common-view. The Sun field contribution varies according to the orientation of the ground clock pair with respect to the Earth-Sun direction. Figure 3-2 shows the two examples of orientations of a clock pair with respect to this direction. This effect has a 24-h period and a **peak-to-peak amplitude of about $1{\cdot}10^{-12}$ between two clocks located on opposite sides of the Earth**.
As the ground clocks are in free fall with respect to the Sun, the dilation effect is actually cancelled [RD43]. Indeed, according to the Equivalence principle, "free fall" means that gravitational effects of the source mass are not discernible in the free-falling frame of reference, here the Earth. The cancellation occurs between the GTD effect and the second-order Doppler shift due to the motion of the ground clocks relative to each other [RD43]. Nevertheless, the measurement of this null effect allows achieving the primary scientific objective #PSO-02 because the second-order Doppler shift responsible for this cancellation can be calculated from the measured clock velocity (and relying on independent experimental confirmation of the validity of Lorentz transformations and thus the formula for the second-order Doppler shift) with at least the same accuracy and so the actual Sun GTD deduced from the (a priori) null result.

During the time of the I-SOC mission, ground clocks in the participating national metrology laboratories may have reached instabilities of $1{\cdot}10^{-19}$. Such a level would in principle enable a measurement of the Sun GTD with fractional uncertainty of $1{\cdot}10^{-7}$. In the following, we discuss whether such a level can indeed be reached.
The analysis of the Sun redshift test presented here is simplified and therefore assumes only two clocks on the ground [#SR-GS-04] with instability given by #SR-GS-01, connected to the space clock via two links with performance as specified in #SR-PL-09.
The statistical uncertainty of the frequency comparison in non-common-view mode is calculated by (following the approach used in the analysis of the ACES mission):

$$\sigma_y(\tau) = \frac{\sqrt{2\sigma_{x,link}(\tau_{contact})^2+\sigma_{x,SLOC}(\tau)^2}}{\tau}. \quad (5)$$

$\tau_{contact}$= 300 s is the ISS contact time. As opposed to the common-view case, here, the instability of the space clock (acting as a local oscillator), $\sigma_{x,SLOC}(\tau)$, does contribute to the link instability, albeit to a more or less significant amount, depending on the type of link considered.

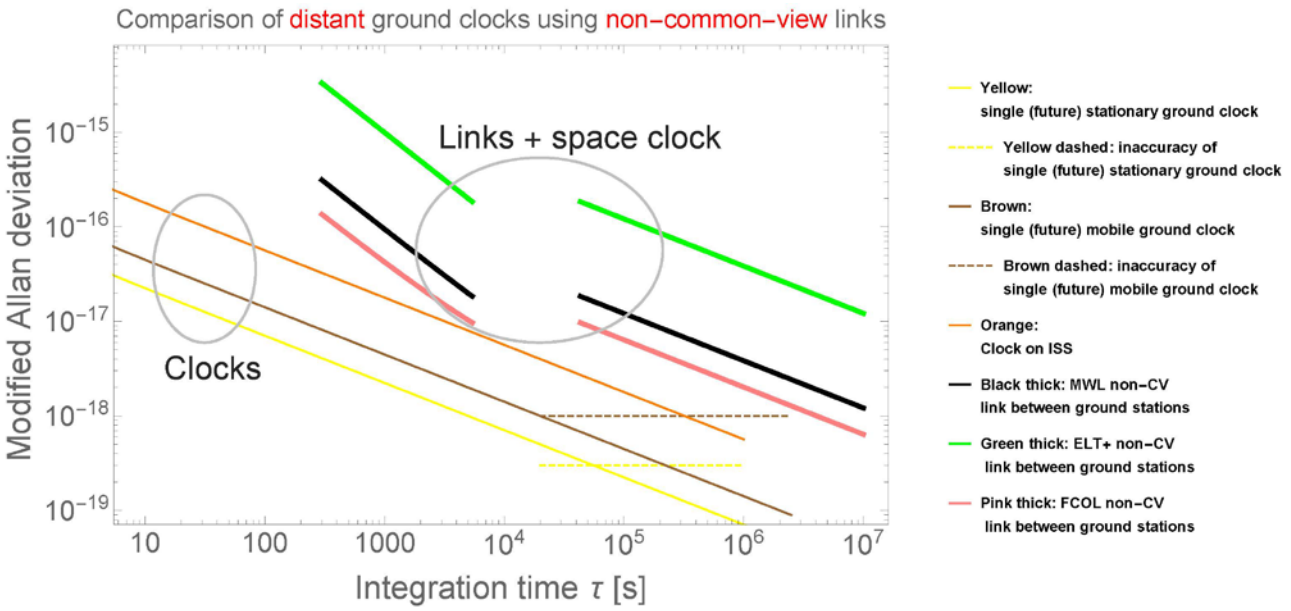

Figure 3-4: Performance of links, incl. space clock contribution, and of clocks, for the case of comparison of distant clocks in **non-common view**. This performance applies to the following science goals: Sun's and Moon's gravitational time dilation, world-wide time scale, and relativistic geodesy. The thick lines show the contribution of the three types of links to such a measurement, where the instability of the space clock is also *included*. Here, clear weather conditions have been assumed for all ISS passes, so that ELT+ and FCOL are not affected. The changes in slope are explained in the text. It is to be noted that the orange line (SLOC) and the black line (SLOC+MWL) do not get close, indicating that the SLOC instability is not a limiting effect.

Figure 3-4 shows $\sqrt{2}\sigma_y(\tau)$ of Eq.(5) for the three links plus space clock, for integration times between $\tau_{contact}$ and T_{ISS} (first parts of the thick lines). This case is meant to represent relativistic geodesy with clocks that are located at distances not permitting a common-view comparison any more. The maximum flight time of the ISS in-between two

such clocks would be $T_{ISS}/2$. However, we have extended the lines up to $\tau = T_{ISS}$. This is case is where the ground clock is compared with the space clock over a full orbit (measurement of Earth GTD). In this set of lines, phase continuity was assumed.
We now give the expected performance of the GTD measurement, before actually describing the measurement in detail. The statistical uncertainty contributed by *the link + SLOC* results from an integration time equal to the ISS period. We must consider the combined uncertainty of *two* time interval measurements (explanation below), which results in $\sqrt{2}\sigma_y(T_{ISS})$. The values are[9,10]:

SLOC+MWL: $2{\cdot}10^{-17}$
SLOC+ELT+: $2{\cdot}10^{-16}$

These values are much larger than the instability performance of today's and future ground clocks for the given integration time. Thus, their available performance is not made full use of – the links limit the potential performance.
In the figure, we also show how these uncertainties are further reduced by *statistical* averaging. *We assume statistical averaging for times longer than 12 h because we conservatively assume phase coherence to be able to be kept* ***only*** *over 12 h*. Statistical averaging is described by $\sqrt{2}\sigma(T_{ISS})/\sqrt{\tau/(1\,\mathrm{day}/2)}$ for $\tau >$ day/2, where we assume that there are 2 ground-ground comparisons per day. This is a reasonable assumption since on average, there are 5 passes of the ISS over a given ground station each day, and 2 are needed to accomplish one ground-ground comparison (see below).
For MWL, the integration time to reach $1{\cdot}10^{-18}$ statistical uncertainty is approximately 160 days. For ELT, this level cannot be reached[11].
We now proceed to the analysis of the measurement procedure. The concept is shown in Figure 3-5.

[9] SLOC+FCOL: $1{\cdot}10^{-17}$. The value decreases to $0.8{\cdot}10^{-17}$ if the SLOC instability is reduced from 8 to $5{\cdot}10^{-16}/\tau^{1/2}$.
[10] These two values do not change if the SLOC instability is reduced from 8 to $5{\cdot}10^{-16}/\tau^{1/2}$ since they are dominated by link noise.
[11] The FCOL is the only link that can capitalize on the specified space clock instability. The $1{\cdot}10^{-18}$ level is reached after approximately 35 days.

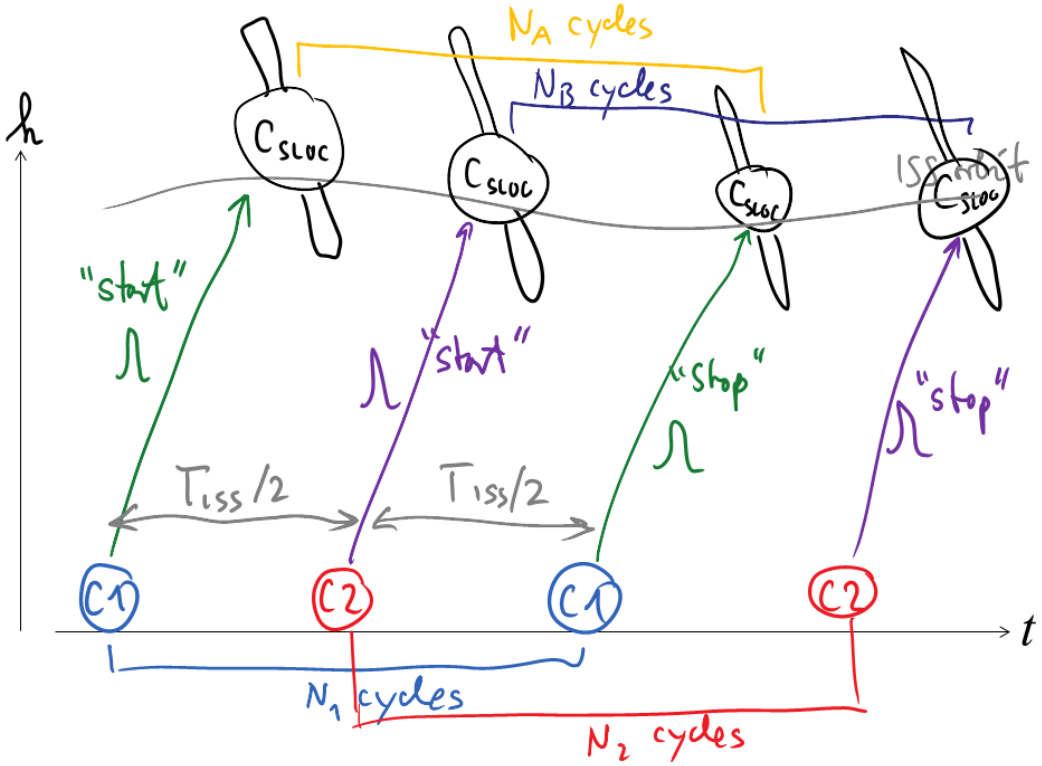

Figure 3-5: Principle of the measurement of the Sun's (null) gravitational time dilation effect. One measurement block is shown, which consists of two interleaved measurements by the I-SOC clock of two time intervals defined by two ground clocks C1, C2. The slant of the arrows indicating the start/stop pulses is for clarity only.

We consider two clocks, C1, C2 which are located approximately on opposite sides of the Earth. The goal of a single measurement "block" is to determine the ratio of local time intervals $T1(N_1)/T2(N_2)$ elapsed during N_1 oscillations of C1 and N_2 oscillations of C2. T_1 and T_2 are chosen to be approximately equal to one ISS period T_{ISS}. Thus the measurement block has a duration of approximately 1.5 T_{ISS}, about 140 min.
The measurement is performed by sending "start" and "stop" pulses to the ISS clock from each clock C1, C2. The ISS clock records the number of own oscillations N_A that occurred between start-stop signals received from clock C1, and the equivalent number N_B during the interval defined by start-stop signals received from clock C2. In terms of the ISS clock's time scale, the corresponding time intervals are T_A and T_B.
From the measured values N_A and N_B, the ratio of ground clock frequencies can be determined.
This measurement block is first performed around a time at which the two clocks are "parallel" to the Earth-Sun line, then, approximately 12 h later, when they are "anti-parallel", see Figure 3-2. Over the course of the mission, a time series of frequency ratios is built up. Of course, the measurement blocks cannot always be done when the clocks are optimally oriented, but only when the ISS orbit passes overhead.
Neglecting again Doppler shifts, and applying Eq. (1), we can set up the relationships:

$$\frac{T_1}{T_A} = \frac{N_1/\nu_{C1}}{N_A/\nu_{SLOC}} = 1 - c^{-2}\left(\frac{1}{T_A}\int_{T_A} U\big(\boldsymbol{r}_{SLOC}(t')\big)dt' - \frac{1}{T_1}\int_{T_1} U\big(\boldsymbol{r}_{C1}(t')\big)dt'\right), \qquad (6)$$

$$\frac{T_2}{T_B} = \frac{N_2/\nu_{C2}}{N_B/\nu_{SLOC}} = 1 - c^{-2}\left(\frac{1}{T_B}\int_{T_B} U\big(\boldsymbol{r}_{SLOC}(t')\big)dt' - \frac{1}{T_2}\int_{T_2} U\big(\boldsymbol{r}_{C2}(t')\big)dt'\right). \quad (7)$$

We divide these two equations by each other and obtain:

$$\frac{\nu_{C2}}{\nu_{C1}} = \left(\frac{N_2/N_1}{N_B/N_A}\right)\left(\frac{1-c^{-2}\left(\frac{1}{T_A}\int_{T_A} U\big(\boldsymbol{r}_{SLOC}(t')\big)dt' - \frac{1}{T_1}\int_{T_1} U\big(\boldsymbol{r}_{C1}(t')\big)dt'\right)}{1-c^{-2}\left(\frac{1}{T_B}\int_{T_B} U\big(\boldsymbol{r}_{SLOC}(t')\big)dt' - \frac{1}{T_2}\int_{T_2} U\big(\boldsymbol{r}_{C2}(t')\big)dt'\right)}\right). \quad (8)$$

This expression states that it is possible to determine the ratio ν_{C2}/ν_{C1} of the two ground clock frequencies after transmitting to ground (by data link) the values of N_A, N_B measured on the ISS and combining them with the values N_1, N_2 measured locally on the ground. The second factor is a correction factor and is further discussed below.
The expression (8) does not depend on the intrinsic space clock frequency ν_{SLOC} any more. Thus, the inaccuracy of the space clock, i.e. the deviation of its frequency from the "ideal" value, does not matter (as long as it is constant). Only the stability of its frequency matters (perfect stability is implicitly assumed in the above derivation, so the instability does not appear explicitly). The fractional instability of SLOC + links will directly impact on the statistical error of the derived ratio and is discussed further below.
In order to compute the ratio ν_{C2}/ν_{C1}, the second factor in the expression must be known. It can be Taylor-expanded, since the integrals containing U/c^2 are small. We then see that the factor depends on the gravitational potential difference at the C1, C2 ground clock locations and on the difference in mean gravitational potential at the ISS location during the orbital segments of duration T_A and T_B,

$$\Delta U_{AB} = \frac{1}{T_A}\int_{T_A} U\big(\boldsymbol{r}_{SLOC}(t')\big)dt' - \frac{1}{T_B}\int_{T_B} U\big(\boldsymbol{r}_{SLOC}(t')\big)dt'$$

It describes the variation of ISS potential between two orbit tracks shifted in time by half an orbital period, i.e. partially overlapping (see Figure 3-5). These two orbit segments are similar, and so the difference is expected to be small.
We now consider the uncertainties affecting the second factor: (I) for the ground clocks and (II) for ISS orbit [#SR-PL-43, #SR-GS-09], stemming from the fact that we need to take the difference between the measurements in two blocks 12 h apart.

(I) The terrestrial contributions $U(r_{C1}(t'))$ and $U(r_{C2}(t'))$ are nearly constant in time, nevertheless, any variation with a 24-h period and constant phase over the duration of the whole measurement campaign will give rise to a systematic error. The ocean tides have a 12-h period and do not contribute directly. As described above, today's modelling of the time-dependent gravitational potential is accurate at the level of 0.1 m^2/s^2 (1 cm, $1{\cdot}10^{-18}$). An improvement by a factor of 2 may be expected by the time of the mission, to a level $5{\cdot}10^{-19}$. This gravitational-potential-modelling limitation leads to the **goal inaccuracy of $5{\cdot}10^{-7}$** for the Sun's gravitational time dilation. However, we need to establish whether this can actually be reached given the performance of I-SOC link and space clock.

(II) Since the measurement is performed via non-common-mode clock comparisons, using the ISS clock as a relay device, we also have to take into account the variation of the gravitational potential of the ISS clock between the times at which the two comparisons with each ground clock are performed. We must consider the error in the variation of the expression ΔU_{AB} over the time scale of 12 h,

$$\varepsilon_{12h} = \sqrt{\langle \Delta U_{AB}(t) - \Delta U_{AB}(t + 12\ h))^2 \rangle}\ .$$

For the Earth GTD, we have argued that a 40 cm uncertainty in the ISS altitude is required (taking into account the cancellation with Doppler effect). That uncertainty refers to a time average of $U(\boldsymbol{r}_{SLOC}(t'))$ itself. This uncertainty may actually be reduced for ΔU_{AB} , it being a difference.

The accuracy goal of Sun GTD of $5{\cdot}10^{-7}$ is equivalent to $1{\cdot}10^{-12} \cdot 5{\cdot}10^{-7} = 5{\cdot}10^{-19}$ clock uncertainty or 0.5 cm altitude uncertainty in ε_{12h} if the 2nd-order Doppler effect is neglected. This translates into approximately 5 cm ISS altitude variation uncertainty if the cancellation with the second-order Doppler effect is taken into account. This is a requirement on the systematic plus statistical error over the whole duration of the measurement campaign. A large number of measurements during the campaign is expected to bring the nominal 40 cm uncertainty for *U* down to the specific uncertainty ε_{12h} = 5 cm.

We now consider the uncertainty reachable in the measurement of the first factor in Eq. (8). It amounts to $\sqrt{2}\sigma_y(T_{ISS})$ (the factor $\sqrt{2}$ stems from having two non-common-view comparisons per block) and the numerical values were given above. The instability of the ground clocks can be neglected in comparison, as stated above.

We assume that one can perform 2 measurements per day, for 500 days, as also shown in the figure. This results in a measurement uncertainty reduced by $\sqrt{1000}$: [12]

MWL: $6{\cdot}10^{-19}$

ELT+: $6{\cdot}10^{-18}$.

Combining measurement uncertainty (values above) and gravitational potential modelling uncertainty (equivalent to $5{\cdot}10^{-19}$), and neglecting the ground clock instability, we find that a total fractional inaccuracy at the level of **$9{\cdot}10^{-7}$ for MWL** can be reached (limited by statistical uncertainty and geopotential modelling), and **$1{\cdot}10^{-5}$ for ELT+** (limited by statistical uncertainty of the link)[13].

[12] FCOL: $3{\cdot}10^{-19}$.

[13] For the science goal Sun GTD, we recognize the advantage of the FCOL compared to the other links: it is the only link that is suited to take advantage (almost) of the low instability of future ground clocks. A GTD measurement uncertainty of

$6{\cdot}10^{-7}$ is possible using FCOL (limited mostly by geopotential modelling uncertainty). Note that this is similar to the level of the Earth field test, #PSO-01.

The best current results for the solar gravitational frequency shift are at the few % level [RD11,RD12]. Thus, I-SOC provides a large improvement in accuracy.
If the clock comparisons are extended to additional ground clocks, the statistical uncertainty as well as geopotential uncertainty will be reduced.
The analysis presented made use of cycle continuity for the ground and space clock on the time scale of *one ISS period*. This is a conservative assumption.
It is likely that the ACES mission will attempt a determination of the Sun's time dilation effect. The improvement of I-SOC compared to the ACES mission is expected to be a factor 10 to 20, due to the better stability/accuracy of ground clocks, better stability of the I-SOC links, and better modelling of the gravitational potential corrections.

#PSO-03: *Measurement of the Moon gravitational time dilation to a fractional uncertainty of $2 \cdot 10^{-4}$*

The I-SOC mission also provides the possibility to measure the gravitational time dilation induced by the Moon. To our knowledge, no such measurement has been performed before.
The measurement protocol is the same as for the Sun time dilation measurement: a frequent comparison of two ground clocks at large distance in East-West direction. A hypothetical violation signal phase is correlated with the Moon's position. The period of the signal sought differs slightly from 24 hours, because the Moon orbits the Earth. In order to differentiate a Moon signal from a Sun signal the measurements must therefore extend at least over several weeks. This requirement is satisfied since measurements will be performed over a substantial fraction of the mission duration in order to maximize statistical accuracy.
The Moon-related effect is reduced compared to the effect of the Sun, by a factor

$$\left(M_{\mathrm{Sun}}/{d_{\mathrm{Sun}}}^2\right)/\left(M_{\mathrm{Moon}}/{d_{\mathrm{Moon}}}^2\right) \approx 175.$$

The square dependence on the distance d between Earth and Moon or Earth and Sun stems from the fact that in a modulation-type measurement, where the distance change of each ground clock to the Moon and the Sun is much smaller than d, a Taylor expansion can be used to estimate the result.
The peak-to-peak Moon effect on the comparison of ground clocks is approximately at the $6 \cdot 10^{-15}$ level for a Europe-Tokyo and a Boulder-Tokyo comparisons.
The statistical and systematic errors are similar to the Sun case, because the signal period is similar.
Thus, we can simply scale the estimate performed for the Sun field time dilation by the above factor and find that the Moon field dilation test can be performed with inaccuracy of **$1.6 \cdot 10^{-4}$ for MWL** and **$2 \cdot 10^{-3}$** when using **ELT+**[14].

[14] **$1 \cdot 10^{-4}$** inaccuracy can be reached with **FCOL**.

There are no previous determinations of the Moon time dilation. However, it is likely that such comparisons will be made during the ACES mission. The improvement of I-SOC compared to the ACES mission is expected to be a factor 10 to 20, due to the better stability/accuracy of ground clocks, better stability of the I-SOC links, and better modelling of the gravitational potential corrections.

#PSO-04: *Contribution to the realization of atomic time scales to fractional frequency inaccuracy lower than $1{\cdot}10^{-18}$ and synchronized to the ps level.*

Thanks to the precise timing capability, I-SOC will allow the worldwide synchronization of the local timescales on the picosecond level compared to the ns uncertainty that is available at present.

The I-SOC mission will offer the possibility to compare primary standards to a frequency uncertainty better than 10^{-18} (see the discussion on #PSO-02 above). Clock-to-clock comparisons will be used to evaluate the accuracy of global time scales. As an example, TAI might exhibit a long-term drift due to some unidentified source common to all commercial cesium standards that dominate TAI. In this case, comparisons of clocks based on different atomic transitions would allow highlighting that drift. Such comparisons, reaching a frequency uncertainty below the 10^{-18} level with I-SOC, will be used to characterize the long-term behavior of atomic time scales and to set bounds on time variations of the fundamental physical constants. This will also accelerate the process leading to a redefinition of the SI second based on clocks operating in the optical domain.

We foresee that the development of ground clocks in the coming years will provide clocks with $3{\cdot}10^{-19}$ *intrinsic* inaccuracy (i.e. without considering the gravitational potential-related inaccuracy). This level is expected to be reachable without requiring a space-based comparison of distant clocks. Instead, comparisons of co-located same-type clocks and intercomparison of distant clocks via transportable clocks will be employed.

The use of I-SOC is then to distribute the time/frequency signals of these clocks world-wide. As shown in Figure 3-3, the ELT provides a frequency transfer uncertainty below $1{\cdot}10^{-18}$ for integration times longer than 10 days.[15] The accuracy of this distribution will be limited not by I-SOC but by gravitational potential modeling for the ground clocks locations and the ISS orbit (in case of non-common view distribution).

One application of this distribution is to monitor the primary optical clocks' drifts with respect to each other. This monitoring can be done and is useful independently of an accurate knowledge of the gravitational potential at the clock's position, provided that the time-dependent potential variations can be modeled. As discussed in #PSO-02, we may expect this to be possible at the $5{\cdot}10^{-19}$ level.

With the establishment of the I-SOC time/frequency distribution capability to a number of primary receiver stations, each of them can be used as a node of a combined space-ground distribution system. The atomic time scale would be distributed from the primary receiver

[15] The FCOL optical link, with its much faster averaging time, reaches the same frequency uncertainty in only 1 day. This faster time is a significant advantage.

to a large number of surrounding users within a radius of several 100 km by means of a fiber-optic network.
I-SOC will thus provide means for establishing, testing, and applying an integrated space-to-ground network concept for time and frequency distribution.
Within Europe, a network based on optical fibers is already under full development in Europe and will be completed by the time of the I-SOC mission.

#PSO-05: *Enable mapping of the geopotential on the land masses of continents with approximately 30 km grid size, with a resolution of 0.15 m²/s² (1.5 cm on the differential geoid height).*

The ISS orbit covers more than 50% of the Earth surface. Thus, comparisons of ground clocks located over a large fraction of land mass can be performed via I-SOC. This unique feature can be taken advantage of so as to implement, in principle, a simultaneous mapping campaign on all continents.
The proposed concept for mapping a given region (part of a continent) is based on using a pair of transportable clocks 1 and 2 that both have $1{\cdot}10^{-18}$ inaccuracy. This is a realistic value at the time of the I-SOC mission, given the strong development activity of such devices. Currently (2016) the lowest inaccuracy reached is $7{\cdot}10^{-17}$ [RD54].
These two clocks will be placed in sequence at neighbouring points $\boldsymbol{r}_i$, $\boldsymbol{r}_{i+1}$, of a large-scale raster (at distance $|\boldsymbol{r}_i - \boldsymbol{r}_{i+1}| \approx 30$ km). In each configuration, the two clocks will be compared in common-view mode via I-SOC. The clock frequency difference of the two clocks yields the gravitational potential difference $U(\boldsymbol{r}_{i+1}) - U(\boldsymbol{r}_i)$. The high spatial and temporal resolution of the geopotential measurements will complement conventional satellite gravimetry surveys which have a much more coarse spatial resolution (few 100 km).
If we consider coherent oscillation of both ground clocks over the duration τ, then

$$\sigma_y(\tau) = 2\sigma_{x,link}(\tau_{contact})/\tau$$

The factor 2 arises because there are two ground-space link connections at the beginning of the time interval and two at the end, and the four uncertainties add quadratically. The uncertainty $\sigma_{x,link}(\tau_{contact})$ has the approximate values: [16]

MWL: 50 fs
ELT+: 1 ps

The $1{\cdot}10^{-18}$ noise level for common-view comparisons is reached after approximately [17]:

MWL: 1.5 days
ELT+: 12 days

[16] FCOL: 40 fs
[17] FCOL: 12 hours.

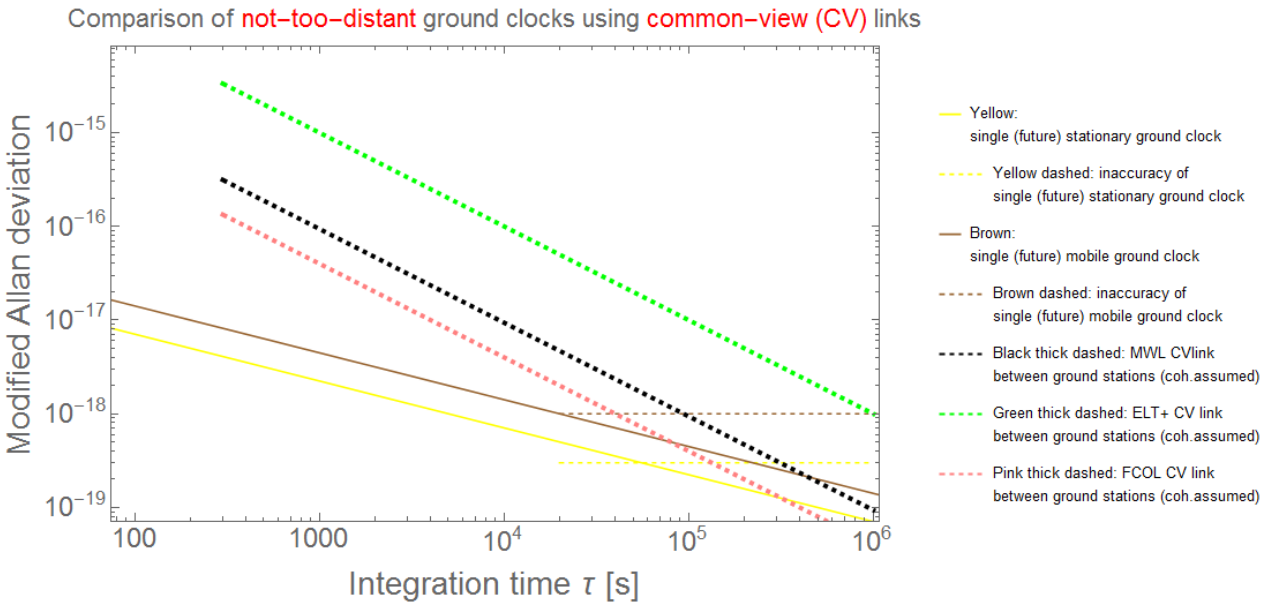

Figure 3-6: Performance of common-view clock comparisons. For the case of measurement of clocks at moderate distance (up to several 100 km) **common-view comparisons** can be performed. This case addresses the science goals: world-wide time scale and relativistic geodesy. The thick dotted lines show the contribution of the three types of links to this measurement, assuming coherence over the duration τ.

It may not be possible to maintain coherence for many days, so the ELT+ is not a good solution for this application [18].

The short measurement duration enabled by the I-SOC links leads to the following scenario:

The pair of mobile clocks (operated in trailers) assigned to a given region will be staffed by a small team of 3-4 persons. The team performs one clock comparison at one new site pair of the grid every 5 days. The 5 days include 1 day for transportation (only 1 clock needs to be transported per 4-day session, over a distance of twice the grid size), 1 day for setting up the measurement, 1 day for verifying systematic effects, 2 days for measurement[19].

Over the ISS mission duration (600 days of link availability), this makes approximately 120 grid points. For a grid size of 30 km, this is an area of 330 km × 330 km.

[18] Considering that FCOL requires clear weather, its theoretical advantage of a factor 4 times shorter integration time will be partially compensated.
Nevertheless, *if* coherence could be maintained over 4 days, and *if* FCOL specification could be extended to that range, the comparison could reach the $1{\cdot}10^{-19}$ instability level. This would allow geoid mapping at the 0.15 cm equivalent height. However, we assume more conservatively that the clocks have $1{\cdot}10^{-18}$ inaccuracy, so the FCOL performance is not fully taken advantage of and MWL is a reasonable choice.

[19] For FCOL: 1 day waiting for clear weather plus 1 day for measurement.

We point out that if this raster approach is used, the error of the potential difference between distant grid points will be significantly higher than for neighbouring grid points, by a factor equal to the square root of the number of in-between grid points.
In an advanced scenario, a large number of teams and clocks could allow mapping of a sizeable part of a continent.
Note that three transportable optical clocks already exist today, and more are under development.

#PSO-06: *Inter- and intracontinental differential geopotential measurements with resolution in the gravitational potential U at the level down to 0.05 m^2/s^2 (0.5 cm on the differential geoid height)*

While the daily modulation of the frequency difference between two ground clocks on different continents is of relevance for determining the Sun or Moon time dilation effect, the time-independent contribution (or mean) provides the difference in the Earth gravitational potential at the clock locations. This quantity is of interest for geophysics applications.
We are here considering next-generation clocks, having inaccuracy at the $3 \cdot 10^{-19}$ level. A small number of them will exist by the time of the mission, probably only in national metrology laboratories. Such clocks can be compared to a frequency uncertainty of $5 \cdot 10^{-19}$, limited by the combined clock and link inaccuracy [#SR-GS-02,#SR-PL-10]. This corresponds to the determination of the difference of local geopotential values to 0.05 m^2/s^2, equivalent to 0.5 cm resolution on the geoid height. The I-SOC mission will be just able to reach this accuracy during the duration of the mission.
Extending on this, a second measurement campaign will consist in placing 2-3 high-performance ($1 \cdot 10^{-18}$ inaccuracy) transportable optical clocks at suitably chosen points on the Earth and operate them there for the duration of the mission.
Together, the above clocks have the scope to (i) to determine the time-variation of the geopotential, (ii) to provide “anchor” data for improving the models generated by satellite gravimetry [RD52].

For intercontinental distances, the link resolution has been discussed in connection with Figure 3-4 (non-common-view). The national metrology laboratory clocks can be compared in non-common-view at the $1 \cdot 10^{-18}$ level (1 cm differential geopotential height) within 200 days using MWL.[20] A significantly lower uncertainty will be difficult to reach.[21] The given integration times assume conservatively that phase continuity is maintained only over 12 h. If this is extended, the integration times reduce correspondingly.

For moderate distances, the common-view link resolution has been discussed in connection with Figure 3-6. The national metrology laboratory clocks can be compared in

[20] within 40 days using FCOL
[21] except for FCOL.

common-view at the $3 \cdot 10^{-19}$ level within 4 days using MWL[22]. This will allow determining the time evolution of the geopotential with a time resolution impossible with satellite gravimetry. This opens up a new dimension in geodesy and can be of significant interest for geophysics models.
National metrology laboratory clocks at moderate distances are also linked by high-performance fiber-optic links. Thus, comparisons of their clocks can be performed with completely independent techniques. *This represents an important performance test of the I-SOC links and will be part of the I-SOC characterization at the beginning of the mission.*

#SSO-01: *Space-to-ground time transfer with inaccuracy lower than 20 ps using ELT+*

The MWL and ELT+ link will also allow the synchronization of ground and space time scales with an absolute accuracy of 50 ps and 20 ps, respectively. This is about a factor 100 better than present state-of-the-art GNSS and similar systems. Space-to-ground synchronization experiments require careful calibration of the differential delays uplink - downlink before launch and their continuous monitoring during flight.

#SSO-02: *Synchronization of clocks on ground to better than 20 ps*

Ground clocks synchronization will also be performed during common-view contacts. Time uncertainty levels below 50 ps and 20 ps are expected to be achieved with the MWL and the ELT+ technology. Although the errors of the two links cumulate, direct calibration of the link delays by means of reference ground terminals will be possible. In addition, as only the double difference of the uplink – downlink delays at the two ground clocks will play a role, it will also be possible to cancel instrumental effects at the space hardware. As an example delay variations induced by temperature fluctuations at the I-SOC spacecraft will be highly correlated bringing to a cancellation of this environmental effect in the double difference[23].

#SSO-03: *Cross-comparisons of different ranging techniques: one-way optical ranging, two-way optical ranging, microwave ranging*

The on-board corner cube reflector will in addition allow ranging of the ISS at the centimeter level providing useful data for the validation and the improvement of the orbit determination of the on-board clock.

The simultaneous operation of the ELT+ optical link and MWL will allow the calibration of MWL for ranging measurements. In addition, space-to-ground clock synchronization experiment performed both using the microwave and the optical link will test one-way

[22] within 1 day using FCOL
[23] In case of FCOL on the ISS, synchronization of clocks on ground could be at a level better than 2 ps.

ranging performances and cross-compare different ranging techniques (1-way vs 2-way, optical vs microwave).

#SSO-04: *Measurement of the differential atmospheric propagation delays in the optical and microwave*

The relative variation of clock de-synchronization measurements (space-to-ground) performed by ELT+ and MWL along the ISS orbit will give access to the difference in the propagation delays both in the optical and microwave domain. This information can be used to improve the modelling of ionosphere and troposphere propagation delays as well as for space weather applications.

3.3.3 *Systematic tests*

A number of systematic tests shall be done during the mission. They will be provide a strong check of overall system performance.

1. The Earth GTD shall be performed from at least three ground stations, with the goal to achieve consistent results for the test of Einstein's prediction.

2. "Three-corner-hat" method for 3 clocks that can be compared in common-view (not necessarily all three simultaneously): from the clock comparisons 1-2, 2-3, 3-1 the respective potential differences U_{12}, U_{23}, and U_{31} are obtained. The sum must be equal to zero because of the properties of the potential:

$$U_{12} + U_{23} + U_{31} = 0$$

3. Three clocks in relative vicinity, e.g. in Europe, are required (available as of today) and also three terminals, for the duration of this test. Two of the terminals would later be sent to Japan/US, as foreseen.

4. "Three-corner-hat" method for 3 clocks that are on different continents, Europe/US/Japan, and that are compared in non-common-view: again, the sum of the potential differences must satisfy: $U_{12}+U_{23}+U_{31} = 0$.

4 I-SOC MISSION SCIENTIFIC REQUIREMENTS

The set of scientific requirements listed in this section allows fulfilling the I-SOC mission objectives described in Section 3. Issues that still need to be resolved will be identified with a TBR (To Be Resolved) and collected in the TBR list in Annex 5.
When needed, explanatory text is provided before the requirement. The applicable requirement is then preceded by the text **Requirement**. After each requirement, we indicate the responsible Party for its implementation and verification, the Party being ESA or the I-SOC Science Team (Resp.: ESA or Science Team).
Requirements applicable to the flight hardware or to operations will be under the direct responsibility of ESA. Those applicable to the ground hardware will be implemented and verified by the I_SOC Science Team, data analysis activities included.

4.1 Mission requirements

#SR-PL-01 ***Accommodation of the I-SOC Payload***
Requirement: The I-SOC payload shall be accommodated external to the ISS, with the microwave antenna and the optical receiver pointing nadir. The axis of the optical lattice laser beam shall be oriented along TBR-03.
Resp.: ESA

#SR-PL-02 ***Performance in the On-flight Environment***
Requirement: All performance requirements of the instruments and subsystems shall be met in the on-flight environment of the ISS.
Resp.: ESA

4.2 Main Instrument requirements

4.2.1 *Space Lattice Optical Clock*

#SR-PL-03 ***SLOC Instability***
Requirement: The fractional frequency instability of the SLOC, expressed in Allan deviation, shall be smaller than $8 \cdot 10^{-16} / \tau^{1/2}$, for integration times τ, expressed in seconds, between 10 s and $2 \cdot 10^{6}$ s.
Resp.: ESA

#SR-PL-04 ***SLOC Inaccuracy***
Requirement: The SLOC fractional frequency inaccuracy shall be $1 \cdot 10^{-17}$.
Resp.: ESA

#SR-PL-05 ***SLOC Operation on Different Zeeman Transitions***
Requirement: The atomic clock shall be able to operate both with the isotope ^{88}Sr and ^{87}Sr. The latter allows higher accuracy while the former is a fall-back option in case of partial laser or vacuum level malfunction. The ^{87}Sr operation will probe opposite spin orientations, i.e. different Zeeman sublevels in the excited state. This is also useful for performing SME tests in the matter sector.
Resp.: ESA

#SR-PL-06 ***Atom Manipulation Sequences***
Requirement: SLOC parameters of the cooling sequence (duration of the cooling period,

intensity and detuning of cooling lasers, etc.) shall be adjustable by TC from ground in near real time (as soon as possible, with the goal of not exceeding 1 hour of delay) or by preloaded command sequences. These sequences will allow characterizing systematics. The sequences will include interleaved stabilization sequences (i.e. two stabilization loops running simultaneously, but based on interleaved atomic interrogation cycles).
Resp.: ESA

#SR-PL-07 ***Magnetic Field Variations with Time***
Requirement: The magnetic field near the magneto-optical trap shall be continuously monitored.
Resp.: ESA

#SR-PL-08 ***Mechanical Vibrations and Spurious Accelerations***
Requirement: The accelerations (three components) shall be continuously monitored both at the reference cavity and at the lattice location.
Resp.: ESA

4.2.2 *Time and Frequency Transfer Link: MWL*

#SR-PL-09 ***Microwave Link Instability***
This requirement specifies the performance of the I-SOC microwave link for ground-to-ground (a) clock and space-to-ground (b) clock comparisons.
For ground-to-ground clock comparisons the specified fractional frequency instability of the I-SOC microwave link σ_{MWLgg} accounts for the following noise terms: white phase noise averaging down to $1.6 \cdot 10^{-14}$ after 10 s of integration time, flicker phase noise with modified Allan deviation of $1.6 \cdot 10^{-13}/\tau$, long-term performance $5.9 \cdot 10^{-17}/\tau^{1/2}$ and flicker floor at the $5.0 \cdot 10^{-19}$ level. The space-to-ground instability is equal to $\sigma_{MWLgg}/\sqrt{2}$.
Requirement (a): The modified Allan deviation of the noise introduced by the STE-QUEST microwave link in the comparison of two clocks on the ground shall be smaller than

$$\sqrt{(5.0 \cdot 10^{-13}/\tau^{3/2})^2 + (1.6 \cdot 10^{-13}/\tau)^2 + (5.9 \cdot 10^{-17}/\tau^{1/2})^2 + (5.0 \cdot 10^{-19})^2}$$

for integration times τ, expressed in seconds, between 10 s and $2 \cdot 10^6$ s.
Resp.: ESA
Requirement (b) The modified Allan deviation of the noise introduced by the STE-QUEST microwave link in the comparison of the on-board clock with clocks on the ground shall be $\sqrt{2}$ smaller than the one given under (a).
Resp.: ESA

#SR-PL-10 ***Time and Frequency Transfer Inaccuracy***
This requirement defines the measurement accuracy and takes into account the end-to-end link including electronics and media contributions.
Requirement: The I-SOC time and frequency transfer MWL link shall be able to compare the space clock and clocks on ground to a fractional frequency inaccuracy smaller than $1 \cdot 10^{-17}$ as well as to compare ground clocks to a fractional frequency inaccuracy smaller than $5 \cdot 10^{-19}$.
Resp.: ESA

#SR-PL-11 ***Phase Comparison Measurements per Second***

Phase measurement (code, carrier or code and carrier) have to be performed inside the transceivers in space and on the ground. Measurements taken at the on-board transceiver shall be transmitted to ground.

Requirement: The I-SOC time and frequency transfer links shall be able to provide at least one phase comparison measurement per second between the space clock and the ground clock with 1 Hz measurement bandwidth.

Resp.: ESA

#SR-PL-12 *Phase Continuity over the Link Dead-time*

This requirement is important for the I-SOC links to reduce the measurement duration of space-to-ground and ground-to-ground comparisons of clocks in the presence of long dead time intervals.

Requirement: The space and ground terminals of the I-SOC time and frequency transfer links shall be able to carry out space-to-ground and ground-to-ground time transfer with the link-induced differential time error between any two observations separated by a dead-time T_d being less than TDEV(T_d), where TDEV represents the time deviation[24] resulting from #SR-PL-09 for the microwave link. This requirement shall be maintained over a minimum measurement interval of 20 days.

Resp.: ESA

#SR-PL-13 *Minimum Number of Independent Channels of the Microwave Link*

This requirement ensures the possibility of performing common-view comparisons with the I-SOC microwave link with a larger number of users, so as to produce more data and enable consistency tests.

Requirement: The I-SOC microwave link shall be able to simultaneously compare the space clock with at least four clocks on ground[25].

Resp.: ESA

#SR-PL-14 *Characterization of Absolute Delays for Space-to-ground Time Transfer Experiments*

Space-to-ground time transfer experiments with I-SOC (#SSO-01) require the calibration of the differential delays between uplink and downlink in MWL. This includes calibration of the differential delays between uplink (transmission from ground to reception in space) and downlink (transmission from space to reception on ground) and of the differential propagation delays in the atmosphere due to the non-reciprocal paths of uplink versus downlink.

---

[24] The time deviation (TDEV) related to the modified Allan deviation (ModADEV) by the following relationship: $\mathrm{TDEV}(\tau) = \mathrm{ModADEV}(\tau)\cdot\tau/\sqrt{3}$, where τ is the integration time.

[25] 4 additional independent channels would be desirable to develop applications in areas other than fundamental physics.

Requirement: The differential delays (uplink - downlink) of the I-SOC MWL used for the dissemination of the I-SOC time scale (space-to-ground) shall be determined to a time uncertainty smaller than 50 ps.
Resp.: ESA

#SR-PL-15 ***Characterization of Differential Delays for Ground Clocks Synchronization***[26]

Clock synchronization experiments (#SSO-02) require the differential calibration of the I-SOC MWL terminals installed at the two ground clocks locations. This includes the calibration of the differential delays (uplink-downlink) for each space-to-ground link.
Requirement: The differential delays (uplink - downlink) of the I-SOC MWL used for the synchronization of two clocks on ground shall be determined to a time uncertainty better than 50 ps.
Resp.: ESA

4.2.3 *Time and Frequency Transfer Link: ELT+*

4.2.3.1 ELT+ End-to-end Requirements

ELT+ operation requires the involvement of ground-based Satellite Laser Ranging (SLR) stations. Participation of these stations to the I-SOC mission requires dedicated agreements between ESA and the scientific institutes responsible for the ground stations operation. Such agreements will also define the responsibilities for the verification of the requirements applicable to the laser ranging stations.
In this section, we define the ELT+ end-to-end performance requirements. These requirements will be later broken down into requirements applicable to the space and to the ground segment hardware. ESA will only be responsible for the requirements applicable to the space segment. Fulfillment of ELT+ ground segment requirements will be under the direct responsibility of the I-SOC Science Team and of the participating SLR stations.

#SR-PL-16 ***Space-to-Ground Clock Comparisons via ELT+***

Requirement: The ELT optical link shall be able to compare the space and ground clock with an induced equivalent noise in time deviation lower than

$$\sigma_x(10\ \mathrm{s} \le \tau < 300\ \mathrm{s})_{ELT+} = 5 \cdot 10^{-12} \cdot \tau^{-1/2}\ \mathrm{s}$$

$$\sigma_x(300\ \mathrm{s} \le \tau \le 10^6\ \mathrm{s})_{ELT+} = 1 \cdot 10^{-12}\ \mathrm{s}$$

where τ is the integration time expressed in s.
Resp.: ESA and Science Team

#SR-PL-17 ***Space-to-Ground Clock Comparisons via ELT+***

[26] Calibration activities might require the availability of transportable ground terminals to characterize the differential delays in the I-SOC links through a common-clock measurement.

The ELT+ fractional frequency inaccuracy when comparing the space clock with clocks on the ground shall be below $1 \cdot 10^{-18}$.
Resp.: ESA and Science Team

#SR-PL-18 ***Calibration of ELT+ Delays for Space-to-ground Time Transfer***

Requirement: The delay in the ELT+ link for the dissemination of the I-SOC time scale shall be calibrated to an uncertainty below 20 ps (15 ps as target). This includes the processes of: laser pulse emission/reception and time stamping in the ground clock time scale, laser pulse reception on-board I-SOC and time stamping in the I-SOC time scale, two-way propagation of the laser pulse in the atmosphere from the reference emission point on ground to the reference reception point in space and back to the reference reception point on ground.
Resp.: ESA and Science Team

#SR-PL-19 ***Calibration of ELT+ Differential Delays for Ground-to-ground Time Transfer***

Requirement: The differential delays of ELT+ links for the synchronization of two ground clocks shall be calibrated to an uncertainty below $\sqrt{2} \cdot 20$ ps ($\sqrt{2} \cdot 15$ ps as target).
Resp.: ESA and Science Team

4.2.3.2 ELT+ End-to-end Space Segment (SS) Requirements

ELT+ space segment requirements are under ESA responsibility.

#SR-PL-20 ***Space-to-ground Clock Comparisons via ELT+: Space Segment Performance Budget Allocation***

Requirement: The following performance budget is allocated to the ELT+ space segment (SS) for the time deviation of the space-to-ground clock comparisons via ELT+:

$$\sigma_X(10\ \text{s} \le \tau < 300\ \text{s})_{\text{ELT+(SS)}} \le 3 \cdot 10^{-12} \cdot \tau^{-1/2}\ \text{s}$$

$$\sigma_X(300\ \text{s} \le \tau \le 10^6\ \text{s})_{\text{ELT+(SS)}} \le 0.5 \cdot 10^{-12}\ \text{s}$$

These figures include, among other noise terms related to ELT+ space segment, on-board detection and time stamping in the local clock time scale, geometric effects related to the offset between reflection at the corner cube and detection equivalent points, atmosphere propagation effects, relativistic effects.
Resp.: ESA

#SR-PL-21 ***Calibration of ELT+ Delays for Space-to-ground Time Transfer: Space Segment Performance Budget Allocation***

Requirement: 3 ps of time error are allocated to the space segment for the calibration of ELT+ differential delays in the space-to-ground time transfer via ELT+. This figure includes, among other terms related to the space segment, laser pulse reception on-board I-SOC and time stamping in the local clock time scale, propagation in the retro-reflector, retro-reflector to ELT+ optics and geometry contribution.
Resp.: ESA

#SR-PL-22 ***On-board Time Tagging***

Requirement: ELT+ laser pulses shall be time stamped when received at the on-board detector in the on-board clock time scale.
Resp.: ESA

#SR-PL-23 ***ELT+ Multi-user Capabilities***

This requirement ensures the possibility of performing common-view comparisons with the I-SOC optical link.

Requirement: ELT+ will be able to perform two simultaneous space-to-ground clock comparisons without significant degradation of the link per-formance (less than 10% in time deviation).

Resp.: ESA

4.2.3.3 ELT+ End-to-end Ground Segment (GS) Requirements

ELT+ ground segment requirements are under the responsibility of the I-SOC science team and of the participating ground-based SLR stations.

#SR-PL-24 ***Space-to-Ground Clock Comparisons via ELT+: Ground Segment Performance Budget Allocation***

Requirement: The following performance budget is allocated to the ground segment (GS) for the time deviation of the space-to-ground clock comparisons via ELT+:

$$\sigma_X(10\ \mathrm{s} \le \tau < 300\ \mathrm{s})_{\mathrm{ELT+(GS)}} \le 4 \cdot 10^{-12} \cdot \tau^{-1/2}\ \mathrm{s}$$

$$\sigma_X(300\ \mathrm{s} \le \tau \le 10^6\ \mathrm{s})_{\mathrm{ELT+(GS)}} \le 1 \cdot 10^{-12}\ \mathrm{s}$$

These figures include, among other noise terms related to the SLR station, on-ground detection and time stamping at the SLR station in the local clock time scale and geometric effects related to local ties.

Resp.: Science Team

#SR-PL-25 ***Calibration of ELT+ Delays for Space-to-Ground Time Transfer: Ground Segment Performance Budget Allocation***

Requirement: 20 ps (15 ps as target performance) of time error are allocated to the ground segment for the calibration of ELT+ differential delays in the space-to-ground time transfer via ELT+. This figure includes, among other terms related to the SLR station, laser pulse emission/reception and time stamping in the local clock time scale, propagation effects due to local ties.

Resp.: Science Team

#SR-PL-26 ***On-ground Time Tagging***

Requirement: ELT+ laser pulses shall be time stamped when emitted and received at the ground laser ranging station in the local clock time scale.

Resp.: Science Team

#SR-PL-27 ***Transportable ELT+ Calibration Device***

Requirement: A transportable ELT+ Calibration Device shall be available for on-site calibration of related signal delays.

Resp.: Science Team

#SR-PL-28 ***Common-View Clock Comparisons with ELT+***

Requirement: The distribution of ELT+ laser ranging stations on ground shall ensure that at least two of them are in common view with respect to the ISS orbit for longer than 100 s.

Resp.: Science Team

#SR-PL-29 ***SLR Station Ranging Performances***

Requirement: ELT+ reflector shall allow ranging to 20 ps one-way time uncertainty per shot (15 ps target) and it shall provide precision in a sense of TDEV not worse than 0.4 ps @ 100 s.
Resp.: ESA and Science Team

4.2.4 *On-board Frequency Generation and Distribution*

#SR-PL-30 ***Clock Laser Instability***
This requirement, driven by the instability of the optical atomic clock #SR-PL-03, defines the performance of the I-SOC optical reference oscillator.
Requirement: The Allan deviation of the optical reference oscillator shall be lower than $3 \cdot 10^{-16}$ between 0.1 s and 100 s of integration time after linear drift removal.
Resp.: ESA

#SR-PL-31 ***Optical Reference Oscillator Frequency Drift***
As a fall-back option, the ground clock comparisons can be performed with the clock laser only. For this purpose, its drift shall be well-controlled. In addition, control of the cavity drift is important to perform Lorentz Invariance tests.
Requirement: The variations of the fractional frequency drift of the optical reference oscillator shall be smaller than $2 \cdot 10^{-16}$ /s in a time interval of 5400 s (ISS orbital period).
Resp.: ESA

#SR-PL-32 ***Space frequency comb (SFC) stability***
Requirement: Given an input optical signal with a frequency instability between $1 \cdot 10^{-13}$ and $5 \cdot 10^{-16}$ $\tau^{-1/2}$ (the upper value considers the worst case that only the reference cavity is available, and exhibits degraded performance), the SFC shall convert it into a microwave signal with instability increased by not more than a factor 1.1, for integration times larger between 20 s and $2 \cdot 10^{6}$ s.
Resp.: ESA

#SR-PL-33 ***SFC inaccuracy***
Requirement: Given a frequency-stable optical frequency input having an instability less than or equal to $1 \cdot 10^{-13}$, the systematic frequency offset of the SFC microwave output signal compared to the exact value corresponding to the downconverted optical frequency shall be no more than $3 \cdot 10^{-18}$ in fractional terms.
Resp.: ESA

#SR-PL-34 ***SFC phase coherence***
Requirement: Given a frequency-stable optical frequency input having an instability less than or equal to $1 \cdot 10^{-13}$, the intervals of time during which the frequency comb output maintains coherence shall be longer than 1 day.
Resp.: ESA

#SR-PL-35 ***Clock Signal Distribution***
Requirement: The Allan deviation of the noise introduced in the distribution of the SLOC signal to the time and frequency transfer links shall be, for integration times larger than 10 s, 3 times smaller than the Allan deviation of the SLOC clock signal itself, as defined in #SR-PL-03.
Resp.: ESA

#SR-PL-36 ***FDP operation***

Requirement: By TC, the signal from SFC can be replaced with the signal of an USO (backup option in case of a malfunction of the SFC).
Resp.: ESA

#SR-PL-37 ***Operational Modes***
Requirement: It shall be possible to operate the links with the optically-derived ultra-pure microwave signal either from the laser stabilized to the atomic transition or stabilized to the reference cavity only or from the USO (fallback option).
Resp.: ESA

4.2.5 *On-board GNSS System Requirements*

#SR-PL-38 ***Orbit determination capabilities***
Requirement: The GNSS system shall allow orbit determination of the I-SOC clock and links to the performance level required for fulfilling the I-SOC science objectives (see #SR-PL-43 to #SR-PL-48).
Resp.: ESA

#SR-PL-39 ***GNSS receiver tracking capabilities***
Requirement: The GNSS system shall be able to receive and track GPS, GALILEO/GIOVE, and GLONASS signals in the L1, L2, and L5/E5a bands.
Resp.: ESA

#SR-PL-40 ***Comparison of clocks via the GNSS network***
Requirement: It shall be possible to lock the internal timing of the GNSS system on the I-SOC clock.
Resp.: ESA

#SR-PL-41 ***Data rate of GNSS science measurements***
Requirement: I-SOC shall support buffering and transmission via telemetry of the generated GNSS scientific data up to a volume of 80 MB/day.
Resp.: ESA

#SR-PL-42 ***GNSS Receiver Driven by the I-SOC Clock Signal***
The GNSS receiver can also be used to monitor GPS, GALILEO, and GLONASS timescales once connected to the I-SOC clock signals.
Requirement: It shall be possible to lock the internal timing of the on-board GNSS system on the space clock signal.
Resp.: ESA

4.3 Orbit and Gravitational Potential Determination in Space

#SR-PL-43 ***Orbit Determination of the Link Reference Points in Space***
Requirement: The uncertainty in the orbit determination (position, velocity, time) of the I-SOC link reference points (e.g. antenna phase center) in space shall introduce a noise in the comparison between the SLOC and ground clocks that, expressed in Allan deviation, shall be 3 times smaller than the links noise (see #SR-PL-09).
Resp.: ESA

#SR-PL-44 ***Orbit Determination of the I-SOC Atomic Clock***
Requirement: The uncertainty in the orbit determination (position, velocity, time) of the clock reference point (i.e. focus of the lattice beam) shall introduce a noise in the evaluation

of the clock relativistic frequency shifts that, expressed in Allan deviation, shall be 3 times smaller than the SLOC clock noise (see #SR-PL-03).
Resp.: ESA

#SR-PL-45 ***Gravitational Potential at the I-SOC Atomic Clock***

In the Earth GTD measurement modality, the gravitational potential at the space clock location shall be known to an inaccuracy lower than equivalent to the SLOC inaccuracy.
In the Sun/Moon GTD measurement modality, the gravitational potential variation over the time scale of 12 h at the space clock location shall be known to an inaccuracy lower than equivalent to the ground clock inaccuracy.
Requirement: (a) The error in the determination of the gravitational potential at the space clock location shall lead to a fractional frequency uncertainty due to Earth GTD smaller than $5 \cdot 10^{-18}$ over the appropriate averaging time for the ground-to-space comparison.
Resp.: ESA
Requirement (b) The error in the determination of the gravitational potential variation at the space clock location shall lead to a fractional frequency uncertainty due to Sun and Moon GTDs smaller than $5 \cdot 10^{-19}$ over the appropriate averaging time for the ground-to-ground comparison.
Resp.: ESA

#SR-PL-46 ***Relative Positioning of MWL Antenna and ELT+ Reference Point***

Requirement: The relative positions of the MWL antenna phase center and the ELT+ reference point both on ground and in space shall be known with 1 mm inaccuracy.
Resp.: ESA

#SR-PL-47 ***ISS Attitude Data for Relative Positioning of MWL Antenna and ELT+ Reference Point On-board I-SOC***

Requirement: Access to ISS attitude data with adequate accuracy is required to define the vector between MWL antenna position and ELT+ reference point on board I-SOC.
Resp.: ESA

#SR-PL-48 ***Orbit Prediction for ELT+ Laser Stations Pointing***

Requirement: Orbit prediction to an uncertainty of 300 m along the link direction is required to point ELT+ laser ranging stations and to ensure night-time operation. A target performance of 15 m is desirable to also allow day-time operation.
Resp.: ESA

4.4 Ground Segment

4.4.1 *Ground Clocks Requirements*

The development, the operation and the maintenance of ground clocks (laboratory instruments or transportable ones) is under the responsibility of the I-SOC science team. This includes provision of all the necessary resources, logistics, and manpower for fulfilling the requirements listed below.

#SR-GS-01 ***Ground Clocks Instability***

Requirement: The fractional frequency instability of the mobile ground clocks participating to the I-SOC mission expressed in Allan deviation shall be smaller than $2 \cdot 10^{-16}/\tau^{1/2}$, for integration times τ, expressed in seconds, between 1 s and 250 000 s. For the stationary clocks, it shall be $1 \cdot 10^{-16}/\tau^{1/2}$.
Resp.: Science Team

#SR-GS-02 *Ground Clock Inaccuracy*

Requirement: The fractional frequency inaccuracy of the mobile ground clocks participating to the mission shall be smaller than $1 \cdot 10^{-18}$, that of the stationary clocks in metrology laboratories, smaller than $3 \cdot 10^{-19}$.
Resp.: Science Team

#SR-GS-03 *Calibration of local UTC by Ground Clocks for Contributing to Atomic Time Scales with I-SOC*

The possibility of participating with I-SOC to the generation of atomic time scales requires that at least two ground clocks be linked to an international atomic time scales (e.g. UTC) with instability better than $1 \cdot 10^{-16}$ after a few days of integration time.
Requirement: A minimum number of two ground clocks with performance as specified in #SR-GS-01 and #SR-GS-02 shall allow to calibrate local UTC to an uncertainty better than 20 ps after 5 day of integration time.
Resp.: Science Team

#SR-GS-04 *Minimum Number of Ground Clocks*

The minimum number of ground clocks required for I-SOC is driven by the need of performing the Sun and Moon GTD measurement with a consistency check. This sets the minimum number to 3 ground clocks, each located on a different continent.
Requirement: A minimum number of 3 ground clocks with performance as specified in #SR-GS-01 and #SR-GS-02 and connected to the I-SOC time and frequency transfer microwave link is required.
Resp.: Science Team

#SR-GS-05 *Minimum Number of Clocks in Common-view for Geodesic Mapping*

Requirement: At least two mobile clocks shall be available with supporting vehicles and personnel.
Resp.: Science Team

#SR-GS-06 *ELT+ Ground Clocks*

Requirement: A minimum number of two ELT+ laser ranging stations shall be operated having time/frequency links to high performance clocks of instability and inaccuracy lower than the SLOC.
Resp.: Science Team

4.4.2 *Additional Ground Segment Requirements*

#SR-GS-07 *Co-location of Microwave and Optical Link Ground Terminals*

This requirement ensures the possibility to cross-compare different ranging techniques (#SSO-03) and conduct studies on atmospheric propagation delays both in the microwave and optical domain (#SSO-04).

Requirement: One I-SOC ground station, as a minimum, shall be equipped with both a microwave and optical ground terminal of the I-SOC links, both referred to the same time scale generated from the local or fiber-linked clock.
Resp.: ESA and Science Team

#SR-GS-08 ***Data Processing and Archiving***
Requirement: The I-SOC science data center shall process the telemetry received from the I-SOC payload and from the participating ground stations (science, housekeeping, and ancillary data) to allow generating the I-SOC science products. The complete set of I-SOC raw data and higher data products shall be archived at the I-SOC science data center.
Resp.: Science Team

4.5 Position and Gravitational Potential Determination at the Ground Stations

#SR-GS-09 ***Position of the Link Reference Points on Ground***
Requirement: The uncertainty in the determination of position, velocity, and time of the SOC links reference points (e.g. antenna phase center) on ground shall introduce a noise in the comparison between the SOC clock and ground clocks that, expressed in Allan deviation, shall be 3 times smaller than the links noise (see #SR-PL-09).
Resp.: ESA and Science Team

#SR-GS-10 ***Ground Clock Position***
The Earth GTD measurement requires the knowledge of the relativistic frequency shifts of the ground clock at the $5{\cdot}10^{-18}$ level (two times lower than the SLOC inaccuracy). In order to perform differential geopotential measurements to 1.5 cm (#PSO-05) or to 0.15 cm (#PSO-06), a the determination of each clock altitude to an uncertainty lower than 1 cm or 0.1 cm is needed ($< 1{\cdot}10^{-18}$ or $< 1{\cdot}10^{-19}$ level).
Requirement: The error in the determination of each ground clock position (mainly elevation) and velocity shall introduce a relative frequency uncertainty in the evaluation of the gravitational red-shift and of the second-order Doppler effect smaller than or equal to $5{\cdot}10^{-19}$ for the mobile clocks and smaller than or equal to $5{\cdot}10^{-20}$ for the ultra-precise metrology laboratory clocks.
Resp.: Science Team

#SR-GS-11 ***Gravitational Potential at the Ground Clocks***
The Earth gravitational potential at the ground clock locations needs to be known at the specified level to perform the GTD measurement in the Earth field.
Requirement: The error in the determination of the gravitational potential at the ground clock location shall lead to a fractional frequency uncertainty due to the Earth GTD effect smaller than $5{\cdot}10^{-18}$ (5 cm).
Resp.: Science Team

#SR-GS-12 ***Daily Variations of the Earth Gravitational Potential at the Ground Clocks***
Daily variations of the Earth gravitational potential need to be quantified at the specified level to perform GTD tests in the Sun and Moon fields. The most stringent requirement stems from the Sun GTD test, since the effect of the Sun is stronger than that of the moon.

Requirement: Variations of the Earth gravitational potential at the ground clock location with 1-day period shall be modeled to a fractional frequency uncertainty smaller than $5 \cdot 10^{-19}$, with the ultimate goal of $2 \cdot 10^{-19}$.
Resp.: Science Team

4.6 Operations

Operations requirements are under ESA responsibility.

#SR-OP-01 ***Mission Duration***
The science goals define the mission duration. This requirement takes into account both the measurement time, as derived in the previous section of this document, and the duration of the initial instruments calibration phase. The characterization of the instruments will be performed after on-orbit commissioning and it will be continuously verified and possibly improved during the mission lifetime.
Requirement: The I-SOC mission shall be operated at nominal levels for a minimum duration of 2 years.
Resp.: ESA

#SR-OP-02 ***Instruments Calibration***
Requirement: A minimum duration of 6 months is allocated for the calibration and on-orbit performance characterization of the I-SOC instruments and main subsystems.
Resp.: ESA

#SR-OP-03 ***Payload Telemetry***
The tuning and the monitoring of the I-SOC instruments and subsystems, in particular during the I-SOC on-orbit calibration and performance characterization, require near-real time availability of the payload science telemetry. This requirement defines the typical time availability of payload telemetry.
Requirement: The parameters defining the performance of I-SOC instruments and subsystems shall be included in the I-SOC telemetry to be downloaded and made available at the I-SOC ground segment in near-real time, e.g. with a delay only depending on link availability and low-level data processing needed to generate the product.
Resp.: ESA

#SR-OP-04 ***Telecommanding (TC) Capabilities***
The tuning and the monitoring of I-SOC instruments and subsystems, in particular during the I-SOC on-orbit calibration and performance characterization, require near-real time telecommanding capabilities. This requirement defines the typical time interval between telecommand generation at the I-SOC ground segment and its execution on board the spacecraft.
Requirement: The parameters defining the performance of I-SOC instruments and subsystems shall be adjustable by telecommand from ground in near real time, e.g. with a delay only depending on link availability and low-level data processing needed to execute the telecommand.
Resp.: ESA

#SR-OP-05 ***Availability of Space-to-ground Comparison Data***
Requirement: The results of the space-to-ground clock comparisons, both via MWL and ELT+, shall be made available at the ground segment in near real time, e.g. with a delay

only depending on link availability and low-level data processing needed to generate the results.
Resp.: ESA

#SR-OP-06 ***Availability of Orbit Information Data***
Requirement: Quick-look orbitography data with sufficient accuracy to evaluate space-to-ground comparisons of clocks at the 10^{-15} level shall be made available in near-real time, e.g. with a delay only depending on link availability and low-level data processing needed to generate the product. The final orbitography for clock comparisons at full performance level shall be available with latency not exceeding 15 days.
Resp.: ESA

#SR-OP-07 ***Mission Operations, Monitoring and Control***
Requirement: The I-SOC USOC shall be responsible for mission operations, monitoring and control, as well as for the archiving of all the ACES data and data products.
Resp.: ESA

Annex 1 I-SOC CLOCK AND LINKS

In this annex, the working principle of the Sr lattice clock, its main subsystems, functions and basic interfaces are detailed. **This section is intended to provide a set of recommendation/guidelines for the instrument design.** The main figures that need to be fulfilled in order to achieve the required clock performance with respect to accuracy and stability are summarized here.

A1.1 The Strontium Lattice Clock

A1.1.1 WORKING PRINCIPLE

The clock uses a narrow line in strontium as reference. In general, two strontium isotopes can be employed with different advantages and disadvantages. The bosonic isotope ^{88}Sr has zero nuclear spin, which makes it less sensitive to magnetic fields; furthermore, its isotopic abundance (82.6%) is much higher than that of the fermionic isotope ^{87}Sr (7.0%), and thus cooling and trapping of ^{88}Sr is easier to achieve. On the other hand, in ^{87}Sr, s-wave scattering (a particular type of atom-atom collision) is suppressed, while for ^{88}Sr the atoms have to be confined properly (i.e. using a 3D lattice) to remove the effect of collisions. At present, all high performance Sr lattice clocks employ the fermionic isotope, as for ^{88}Sr the shifts from the clock laser ac Stark effect and from the quadratic Zeeman effect are too difficult to correct to a level below 10^{-17} as required in I-SOC. Thus in the following we only consider the isotope ^{87}Sr.
Note that isotopically enriched Sr with >90% ^{87}Sr is available commercially, albeit at high cost. This could be a favourable choice for improving the efficiency for loading the lattice with that isotope or for reducing required laser powers.

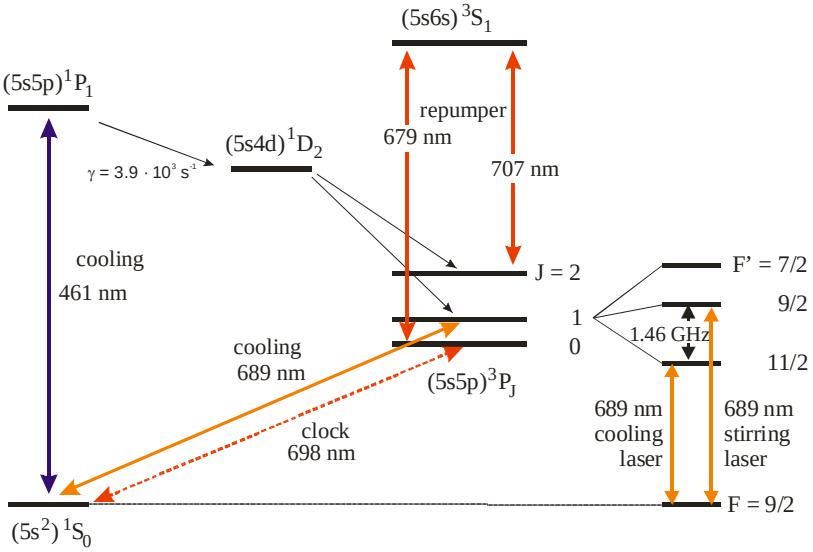

Figure A-1: Partial energy diagram of neutral strontium with relevant optical transitions and spontaneous decay rates. The coloured lines indicate transitions that are excited by lasers in a strontium lattice clock. The hyperfine structure of ^{87}Sr, which is relevant to the second cooling stage (689 nm), is indicated on the right.

A typical strontium lattice clock is based on the repeated interrogation of an ultra-narrow optical transition at $\lambda = 698$ nm ($\nu = 429$ THz) in a small sample (approximately a few thousand atoms) of neutral strontium atoms. After each interrogation the atoms are lost and a new sample has to be loaded. To allow for long, Doppler-free interrogation, the atoms are trapped in an optical lattice – hence the name lattice optical clock. Its wavelength is chosen such that the light shift for both levels of the clock transition ($^1S_0$ and $^3P_0$) are exactly the same, so the clock transition frequency is not shifted by the trapping field. For strontium, this magic wavelength is at $\lambda_L = 813$ nm.
The strong dipole allowed $^1S_0$-$^1P_1$ transition at 461 nm, with a linewidth of 32 MHz, is used to slow down the atoms in a thermal atomic beam produced by an oven, and to trap them into a magneto-optical trap (MOT). Since the temperature of the atoms in this first-stage MOT (2-3 mK) is not low enough for high precision spectroscopy, a second-stage MOT is necessary, operating on the $^1S_0$-$^3P_1$ transition (wavelength 689 nm): after this stage the temperature of the atoms is at 1 μK level. In contrast to ^{88}Sr, for an efficient cooling of ^{87}Sr in the second-stage MOT, a second ("stirring") laser emitting at a frequency shifted by a few GHz with respect of the cooling laser is required.
After cooling down the atoms to such μK temperature, at which the atoms' velocity is still on the order of a few cm/s, they must be trapped in an optical lattice. Then, the sub-μm spatial confinement of the atoms in one spatial direction allows spectroscopy with ultra-narrow resonance lines, free of 1st-order Doppler shifts.
To allow for a high signal-to-noise ratio and efficient use of the trapped atoms, state preparation by spin-polarization has to be performed for 87Sr. Otherwise, the population is equally distributed over all Zeeman sublevels, which leads to reduction of the signal by a factor of ten. Additional preparation steps may be necessary to enable high clock accuracy like additional filtering of motional or internal states.
The sequence of steps performed in operating the clock is:

- atoms are evaporated from a thermal source,
- formed into a directed atomic beam,
- Slowed and cooled by lasers,
- trapped in an optical lattice,
- state preparation,
- excited on the clock transition.
- the excitation probability determined
- the clock laser frequency corrected accordingly

This sequence is repeated and typically lasts 1 s. The sequence is shown in Figure A-2. About 350 ms are needed for cooling, trapping and atomic state preparation, then the atoms are interrogated for about 600 ms with the clock laser and finally the excitation probability is detected within 80 ms. The interrogation time is usually limited by the coherence time of the clock laser; the corresponding Fourier limited FWHM linewidth with 600 ms pulses is about 1 Hz (for Rabi interrogation, the FWHM is 1.2 Hz and for Ramsey interrogation 0.83 Hz). Concerning the frequency stability achievable with the clock, the discontinuous interrogation of the atoms leads to aliasing of the laser noise (Dick effect). With thermal-noise-limited laser instability of $\sigma_y \approx 7\times10^{-16}$, a clock instability of $\sigma_y \approx 1.2\times10^{-15}\ \tau^{-1/2}$ was observed in a stationary lattice clock [RD75]. The precise estimate of the clock performance (I-SOC requires $\sigma_y(\tau) < 5\times10^{-16}\ \tau^{-1/2}$) due to the Dick effect, but also due to quantum projection noise and other technical fluctuations of the atomics package, needs to

be established through calculations and simulations taking into account estimated spectra of frequency fluctuation of the laser.

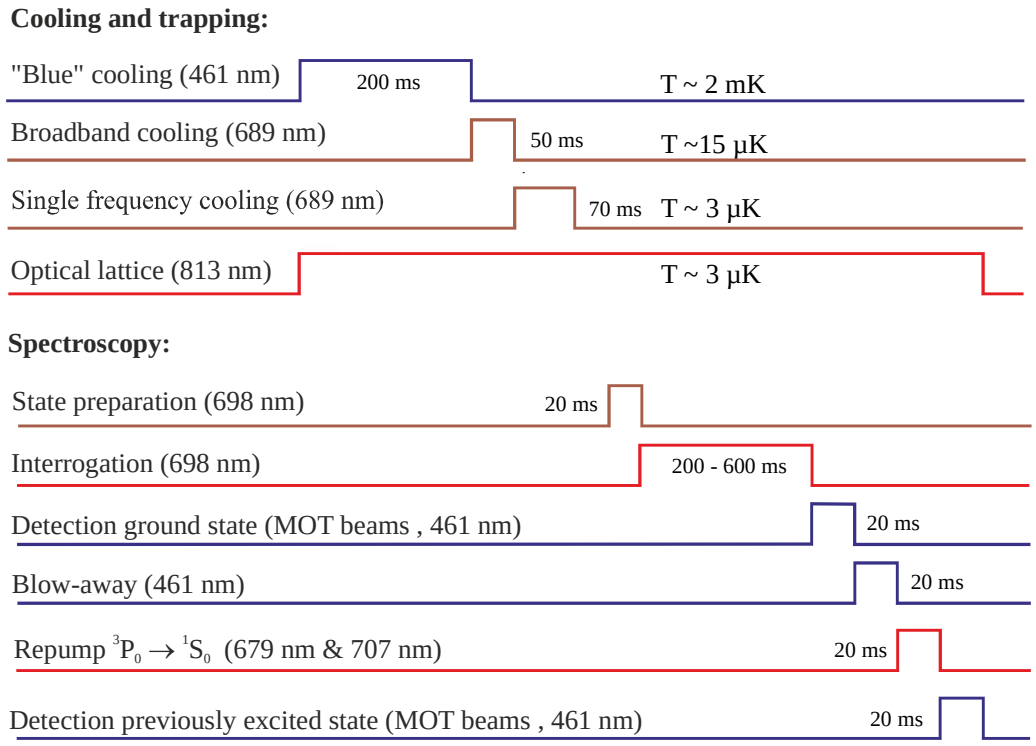

Figure A-2: Typical time sequence of a ^{87}Sr optical lattice clock.

A1.1.2 MAIN SUBSYSTEMS

The schematic setup of the full instrument is shown in Figure A-3. Besides the optical clock it consists of:

- A femtosecond frequency comb to convert the 698 nm clock frequency to a radio-frequency signal and to a pulse sequence of suitable wavelength (e.g. 1550 nm) for the optical link,
- A microwave time & frequency link to Ground,
- A femtosecond-laser-based optical link to Ground (optional).

The main constituents of the optical clock are:

- the atomics package where atoms are laser cooled, trapped and interrogated
- four laser breadboards for cooling, trapping, and detection
- the ultrastable clock system with laser breadboard and reference resonator laser for interrogating atoms
- a computer control unit to generate the time sequence, evaluate the interrogation, implement the correction algorithm to keep the clock laser locked to the centre of the atomic transition
- the diagnostics unit to stabilize the wavelength of all involved lasers

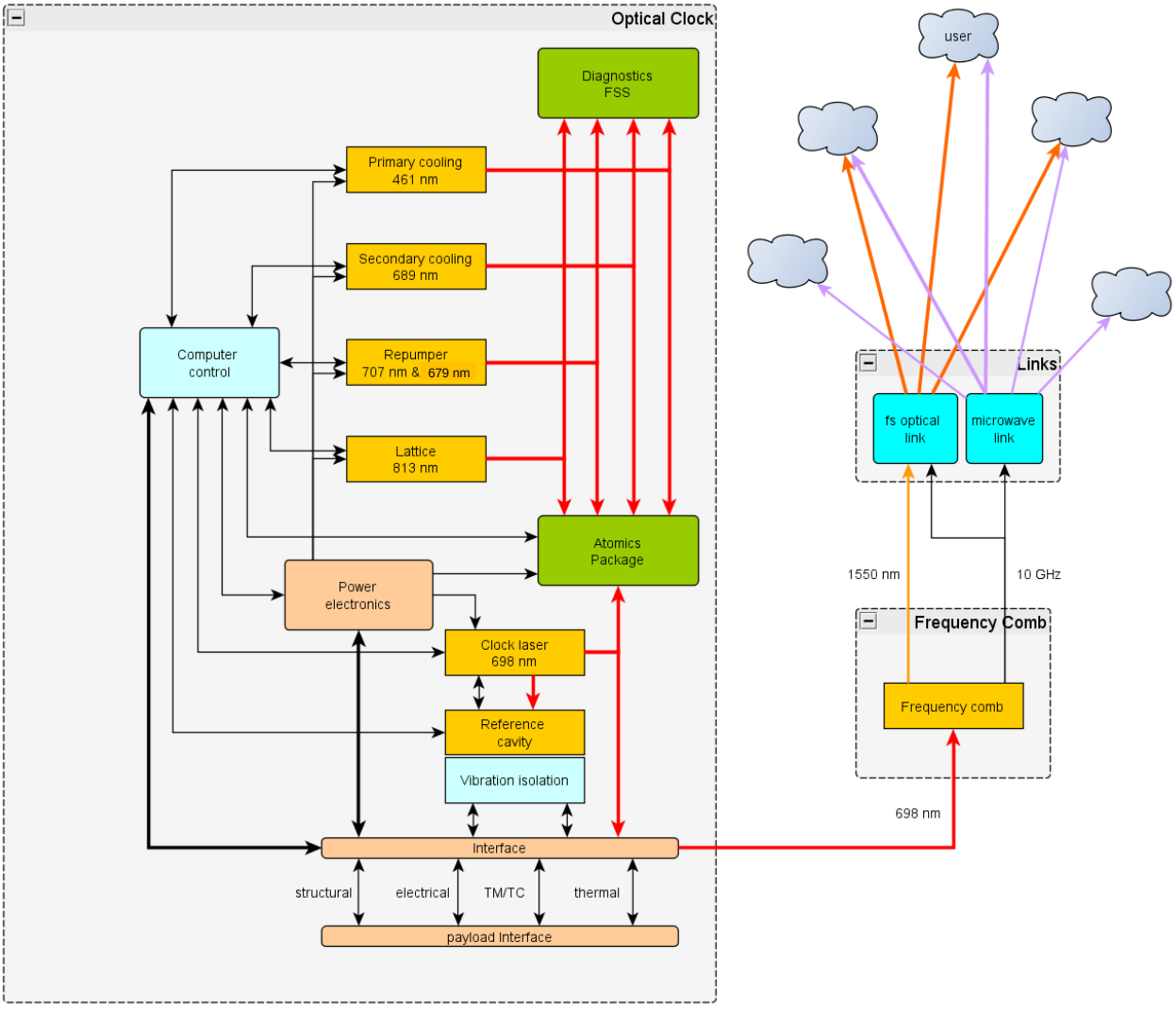

Figure A-3: Instrument breakdown with detailed optical lattice clock substructure.

The mass and volume of the full instrument is restricted by the conditions on the ISS. Indicative masses and sizes for the clock only are shown in Table A-1. In the following details of the individual subcomponents are given.

Table A-1: Subsystems with indicative mass and sizes.

Subsystem	**Electronics included**	**Mass [kg]**	**Volume [l]**	**Power [W]**
atomics package: vacuum system with optics interface to MOT	Y	23	250	20
Blue cooling laser (461 nm) including distribution module	Y, except for AOM drivers	13	15	10
Red cooling and stirring laser (689 nm)	Y, except for AOM drivers	7	15	5
Repumpers (707 and 679 nm)	Y	6	15	5
Lattice laser (813 nm)	Y, except for AOM drivers	10	15	5
Frequency stabilization system	Y	10	6	5
Power electronics: AOM drivers, magnetic coil driver, oven	Y	8	20	30
Subtotal atomics unit (with electronics)	**Y**	**77**	**336**	**80**
Clock laser cavity:	Y	9	5	2
Clock laser vibration isolation unit	Y	6	10	5
Clock laser breadboard	Y, except for AOM drivers	6	15	5
Total clock (with electronics)	**Y**	**98**	**366**	**92**

A1.1.3 ATOMICS PACKAGE

In the ultrahigh vacuum chamber of the atomics package, atoms are emitted by an oven, decelerated, cooled and trapped in a lattice, interrogated and finally the excitation is detected. Its main constituents are:

- ultrahigh-vacuum chamber
- atomic source & Zeeman slower
- magneto-optical trap
- optical access for laser slowing and trapping
- access for the optical lattice, possibly with enhancement cavity
- optical coupling by fibres for the cooling, trapping and detection lasers
- access for detection of the excitation on the clock transitions
- laser power diagnostics
- temperature diagnostics
- magnetic & electric field diagnostics

The I-SOC clock will be an evolved version of the SOC2 setup breadboard, whose atomics subsystem is shown in Figure A-4 [RD78]. .

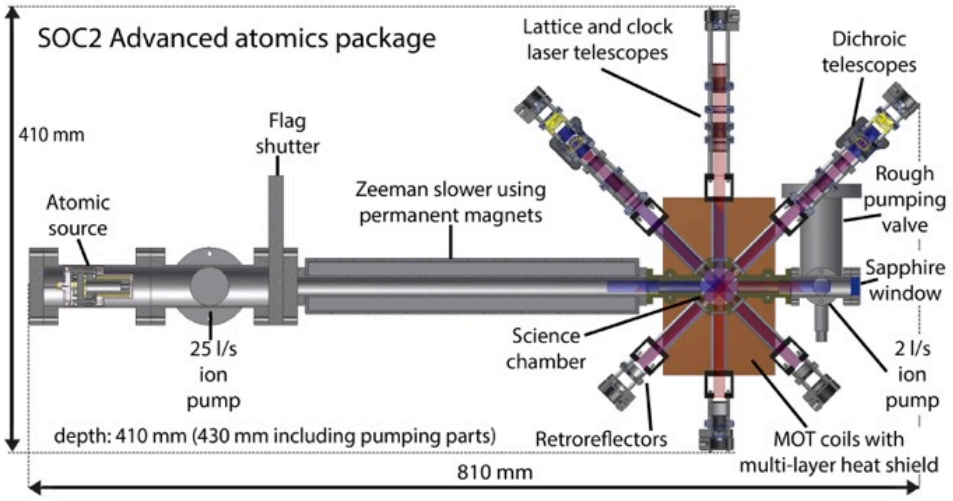

Figure A-4: Overview of the advanced atomics package of the SOC clock.

As the environment around the atoms largely determines the achievable accuracy, several requirements have to be fulfilled by the atomics package as detailed in Table A-2.

Table A-2: Potential shifts related to the design of the atomics package expressed as frequency shift coefficient ζ and fractional frequency shift coefficient η. A lattice depth of $U = 150\ E_{rec}$ is assumed.

Quantity	Effect	Requirement	specific measure
Vacuum	collision induced losses, collision induced shifts	lifetime > 5 s and shifts $\delta\nu/\nu < 10^{-17}$	pressure $p < 10^{-9}$ mbar
Temperature	blackbody-radiation shifts $-2.4\ \text{Hz}\cdot(T/300\ \text{K})^4$ $= -5.6\times10^{-15}\cdot(T/300\ \text{K})^4$ i.e. $\zeta = -32$ mHz/K or $\eta = -7.5\times10^{-17}$ /K at $T = 300$ K (same for ^{87}Sr and ^{88}Sr)	shifts $\delta\nu/\nu < 10^{-17}$	temperature variations over atomic field-of-view (assuming a rectangular probability distribution of width ΔT): $\Delta T < 0.35$ K Absolute temperature T needs to be known to better than 0.1 K
Electric Fields	Stark effect $\eta = 7.2\times10^{-15}/(\text{kV/m})^2$	shifts $\delta\nu/\nu < 10^{-17}$	$\lvert E\rvert < 40$ V/m
Neighbouring lines	frequency pulling	shifts $\delta\nu/\nu < 10^{-17}$	- reduce neighbouring lines by optical pumping - increase separation by magnetic bias field - reduce neighbouring lines (σ transitions) by purity of clock laser polarization - reduce radial sidebands by parallel alignment of clock laser and lattice laser
Magnetic Fields	^{87}Sr: linear Zeeman effect $m \cdot 1.08$ Hz/μT $\eta = m \cdot 2.5\times10^{-15}$ /μT	Stability during interrogation	for $m = \pm 9/2$: magnetic field variations $\Delta B < 1$ nT over times < 10 s or periodic with interrogation
	2nd order Zeeman effect: ^{87}Sr: -25 μHz/μT² or $\eta = 5.8\times10^{-20}$ / μT² ^{88}Sr: $\eta = -23.3$ μHz/μT² [RD86]	correctable to $\delta\nu/\nu < 10^{-17}$	^{87}Sr: bias field of typically 25 μT needs to be known and stable to < 3.4 μT. ^{88}Sr: bias field of typically 1 mT leads to shift of 4×10^{-14}, so field needs to be known (via Zeeman shift measurement) and stable to 0.25 μT for goal of 1×10^{-17}. Translates into ≈ 1 A coil current to be stable within δI=0.25 μA. Shift can be measured as function of coil current so that coil current accuracy can be significantly less stringent than δI.
Collisions with hot Sr atoms	collision induced losses, collision induced shifts		atomic beam shutter, or deflection of atoms by radiation pressure, see also 'Temperature'.
Lattice	Hyperpolarizability 0.45 μHz/E_{rec}^2 [RD74]		Requires variation of lattice depth over wide range
	E2/M1 shifts: $\Delta\nu/\nu = \eta(n + 1/2)\sqrt{U}$ with $\eta = (0 \pm 7\times10^{-19})/\sqrt{E_{rec}}$ [RD83]		trap depth $U < 150\ E_{rec}$ average vibrational number $\langle n\rangle = 0.5$
	Tunnelling		on Ground, gravity prevents tunnelling; in Space, a deeper lattice might be required.

	lattice detuning: $\eta = 3.6\times10^{-20}\ /E_{rec}$ / MHz		
	Lattice vector shift: elliptic polarization can modify the total effective magnetic field, which leads to quadratic shift depending on trap depth much larger than by hyperpolarizability [RD81]		ensure linear lattice polarization, e.g. use lattice build-up resonator with polarization dependent elements.
	lattice tensor shift: $\eta = -6.3\times10^{-20}\ /E_{rec}\times\beta$ [RD81]		keep angle between lattice polarization and B-field constant $\beta = (3|\vec{e}\cdot\vec{e}_z|^2-1)[3m^2-F(F+1)]$
Probe laser	ac Stark shift ^{88}Sr: $\zeta = -15$ mHz / (mW/cm^2) $\eta = -3.5\times10^{-17}$ (mW/cm^2) ([RD86] gives -18 mHz / (mW/cm^2))		only important for ^{88}Sr
cold collisions	^{88}Sr: $\zeta = 7.2\times10^{-11}$ Hz cm^3; $\frac{\Delta\nu}{\nu} = \zeta\times n$; ^{87}Sr: $\frac{\Delta\nu}{\nu} < 10^{-16}$ for density $n = 10^{11}$/cm^3		operate at low atom number larger trap diameter (i.e larger beam diameter) and spreading atoms over a larger length to work at densities n <10^9/cm^3

The **blackbody radiation shift** is a large contribution, especially taken the fact that magnetic coils are required to provide the quadrupole field of the MOT with gradient dB/dz ≈ mT/cm during the cooling phase, which needs to be switched to a homogeneous field of B ≈ μT during interrogation.

Keeping this heat source away from the atomic environment under the conditions of space will pose quite some challenge.

Overall, for an uncertainty below 10^{-17}, temperature gradient over the environment seen by the trapped atoms needs to be 0.35 K, while the absolute average temperature needs to be measured with uncertainty below 0.1 K. While reduction by a cryogenically cooled environment is possible, the additional complications to achieve space compatability do not seem to justify the effort at this time.

Electric dc stray fields can easily lead to significant fractional frequency shifts of more than 10^{-14} [RD75]. In Space, in addition to patch charges, charging by ionising radiation has to be considered. Thus all surfaces (also window surfaces) should have a good conductivity and be well grounded. In addition, discharging by UV radiation can be employed. It should be possible to monitor and compensate potential electric stray fields by applying additional electric fields through dedicated electrodes. Any additional static field would show up as asymmetry of the dc-Stark shift versus externally applied electric field [RD75].

Static and slowly varying **magnetic fields**: In ^{87}Sr both extreme Zeeman sublevels $m_F = \pm 9/2$ are interrogated sequentially. If the field is sufficiently stable during the interrogation, the average frequency is the atomic transition without first order Zeeman effect (and also without vectorial lattice ac-Stark shift). The method is however sensitive to variations with a period of e.g. twice the cycle time, which will lead to considerable frequency shifts. The

difference is proportional to the magnetic field B and can be used to correct the quadratic Zeeman effect using measured or known coefficients.
In addition, rotation of magnetic field can have an influence on the magic wavelength and thus also lead to shifts. Thus, additional fields have to be small and stable on that level compared to the bias field.

Lattice light shifts depend linearly, quadratically and like square-root on the lattice depth. The depth is usually expressed in multiples of the atomic recoil energy $E_{\mathrm{rec}} = (\hbar k)^2/2m$ = 0.17 µK due to one lattice photon with the lattice wavevector k and the atomic mass m. Tunnelling between adjacent lattice sites also leads to frequency shifts. To be able to evaluate these effects in Space, the lattice depth needs to be varied over a large range in a well-defined way. This might be considered in the design of a build-up cavity for the lattice light.

A1.1.4 STABILITY

The frequency stability of optical clocks is determined by the signal-to-noise ratio in the detection of the excitation probability in combination with the slope of this frequency discriminating signal and by the Dick effect, which stems from the incomplete frequency information that is obtained from the atomic signal in comparison to the true average frequency emitted by the laser during the full experimental cycle.
Detection noise:

- Electronic noise in fluorescence detection
- Fluctuations in the repumping efficiency and the fluorescence rate from power and frequency fluctuation of the corresponding lasers
- Quantum projection noise (QPN) from the limited number N_{at} of atoms
- Photon shot noise of the detected fluorescence photons

The expected instability from quantum projection noise and technical fluctuations σ_N of the detected number of atoms is given by [RD79]:

$$\sigma_y(\tau) = \frac{\kappa \cdot \Delta\nu}{\nu}\sqrt{\frac{T_C}{\tau}\left(\frac{1}{N_{\mathrm{at}}} + \frac{2{\sigma_N}^2}{{N_{\mathrm{at}}}^2}\right)}$$

with a numerical factor $\kappa \approx 1/\pi$ for Ramsey interrogation and a FWHM of the line of $\Delta\nu$. In typical setups, with $N_{\mathrm{at}} \approx 1000$ the QPN dominates. With $T_c \approx 1$ s and $\Delta\nu \approx 1$ Hz, the instability is $\sigma_y(\tau) = 7 \cdot 10^{-17}\,\tau^{-1/2}$.
The Dick effect for pure flicker noise (e.g. from a cavity limited by Brownian thermal noise) can be roughly estimated by the first term in the Dick effect formula:

$${\sigma_y}^2(\tau) = \frac{1}{\tau}\frac{1}{|g_0|^2}\sum_{k=1}^{\infty}|g_k|^2 \cdot S_y(k/T_0)$$

With the above data, assuming a duty cycle of 60 % and a laser instability $\sigma_y^{(\mathrm{las})} = 5{\cdot}10^{-16}$ it contributes to the instability by $\sigma_y^{(\mathrm{Dick})} \approx 5{\cdot}10^{-16}\,\tau^{-1/2}$.

A1.1.5 DESIGN GUIDELINES

The current setup uses a low-power atomic beam oven [RD80] with a permanent magnet Zeeman slower. This setup provides slow Sr atoms with velocity of a few 10 m/s that can be further slowed by a 461 nm MOT followed by a second cooling stage at the 689 nm intercombination transition. An additional "stirring" laser offset-locked at 1.4 GHz is used with the fermionic isotope ^{87}Sr. The 461 nm and the 689 nm laser light is brought in by three fibres for each of the two wavelengths, and the outputs are overlapped in specially designed dichroic beam expanders, that provide collimated beams ($1/e^2$ diameter ≈ 4 mm). Polarization-maintaining fibre splitters can be efficiently used to combine the different wavelengths and split them into 3 outputs for MOT operation.

A1.1.5.1 *Laser packages*

The light is brought to the atomics package and the diagnostics package by polarization-maintaining single mode fibres. Currently, we believe that a modular design, where the various required wavelengths are produced in separate modules, is a suitable choice. The approach followed in SOC is based on extended cavity diode lasers (ECDLs) that are integrated on small boxed breadboards. In those, free-space optics are used to split the beams, send them through mechanical shutters and acousto-optic modulators (AOMs) for fast switching and frequency shifting and finally for coupling the light to the output fibres.
As guideline, the laser breadboards used in SOC with their specifications are presented in Table A-3. Compared to the current SOC setup, the size and weight was reduced by a factor of two as a realistic estimate for an optimized design.

Table A-3: Overview of the laser breadboards with indicative size and weight, based on a further optimized SOC setup. The masses agree with Table A-1.

Laser Breadboard	**Wave-length**	**Frequency Stability**	**Indicative breadboard size and mass**	**Power at fiber output**
Cooling #1 Laser and distribution	461 nm ECDL+SHG	1 MHz	30×45×10 cm^3 13 kg	50 mW MOT, 30 mW Slower, 1 mW Detection, 1 mW (IR) FSS
Cooling #2 incl. stirring and spin pol. frequencies	689 nm ECDL+TA	< 1 kHz in 1 h, linewidth two frequencies offset by 1.4 GHz	30×45×10 cm^3 7 kg	10 mW MOT , 1 mW FSS 10 mW MOT (stirring) 2×1 mW Spin polarization
Repumpers	707 nm, 679 nm ECDL	FM +/- 3 GHz with a few kHz modulation frequency; center: 100 MHz	30×45×10 cm^3 6 kg	2 mW each wavelength to MOT, 1 mW to FSS
Lattice	813 nm ECDL	< 1 MHz in 10 h	30×45×10 cm^3 10 kg	>200 mW to atomics 1 mW to FSS
Clock laser	698 nm ECDL	<1 Hz $\sigma_y < 2\times10^{-16}$ for 0.1 s < τ < 20 s	30×45×12 cm^3 6 kg	2 mW to atomics, 2 mW to comb, 0.5 mW to cavity, 1 mW to FSS

Clock cavity	698 nm	thermal noise $2x10^{-16}$ for τ = 0.1 s to 20 s	55×55×55 cm^3 9 kg	input: 0.5 mW
Frequency stabilization system (FSS)	All, excl. 698 nm	To levels indicated above	30×20×10 cm^3 10 kg	Fiber input for the above fiber outputs

In the SOC project, so far compact laser breadboards have been used, where commercial components and miniature mirror mounts were connected to a custom-made aluminum base plate (Figure A-6). Inventor drawings for most of these breadboards can be made available during the study.
The required fractional power stability at the fiber outputs of the atomics package is approximately a few percent both on the timescale of a fraction of a second and on the long-term over the lifetime of the clock. Depending on the design, passive or active means will be required to fulfil these specifications.

A1.1.5.1.1 Lattice laser

Critical issues of lattice laser as expressed in ESA ITT AO8382 (Development of a high power, high spectral purity red-detuned lattice laser at 813nm for neutral strontium).
Spectral purity of 813 nm lattice laser can hamper magic wavelength conditions. Even with careful spectral filtering, this issue so far has prevented the use of high-power MOPA diode-laser based system for the most accurate clocks. In several instances, fluctuating fractional frequency shifts of the order of 10^{-15} have been observed [RD74]. So far, no procedure is available that would give a reliable way to calculate the shift from measured spectral properties. At least the effect of a spectral background can be mitigated by the use of a build-up cavity for the lattice. However, in this case parametric atomic heating from fluctuations of the intracavity power due to laser frequency noise can appear. Thus this approach requires a tight (high- bandwidth) locking of the lattice laser to the build-up cavity.
With a typical cavity (finesse 200, waist 60 μm) and a reasonable mode-matching between the laser and the cavity (70 %), the trapping depth is 1000 E_{rec} for 100 mW. This depth is sufficient both to capture the atoms from a second-stage MOT (689 nm) and quantify the systematics related to the trapping potential. For the spectroscopy phase, the depth is reduced to typically 100 or 200 E_{rec}.
In the current ESA ITT on a lattice laser the following requirements were set:

Lattice Laser System Requirements	
Wavelength	813.428 nm (ν_{mag} = 368 554 725 MHz).
Power(1)	> 100 mW at the primary fibre output;
	~ 1 mW at the secondary fibre output,
Linewidth(2)	100 kHz.
Frequency tunability	± 500 MHz around ν_{mag}.
Frequency drift	< 3 MHz/day.
Power stability(3)	Power stability below 1% of the average laser power in a 1 kHz bandwidth.
Intensity noise(4)	- 120 dBc/Hz between 100 kHz and 600 kHz; - 50 dBc/Hz between 100 Hz and 600 Hz.
Amplified Spontaneous Emission(5)	- 70 dBc below the carrier when integrated in an interval of 10 nm around the carrier; - 80 dBc below the carrier when integrated over all wavelengths between 10 and 100 nm away from the carrier.

Laser output IFs	Two optical outputs with FC/APC polarization maintaining fiber; at least 8 m of fibre length shall be provided.
Electronics input IFs	- Fast modulation input with bandwidth dc to 10 MHz (e.g. bias tee); - Modulation input with bandwidth dc to 100 kHz (e.g. at the laser driver); - The frequency tuning port at the driver of the acousto-optic modulator shall be accessible. In case diode lasers in extended cavity configuration are used: - The electronics driving the piezoelectric actuator shall provide a modulation input with a few kHz bandwidth on the voltage driving the actuator; - The connector of the piezoelectric actuator shall be accessible; a piezo driver is not mandatory at this stage.
Mass (guideline)(6)	10 kg
Volume (guideline) (6)	15 l
Lifetime (guideline)	> 3 years

(1) Total power at the laser output interfaces.
(2) After stabilization on the mock-up cavity (15 cm long cavity, finesse around 200).
(3) After laser power stabilization, e.g. via an acousto-optic modulator, with bandwidth of a few tens of kHz.
(4) E.g. by FFT of the mock-up cavity transmission
(5) E.g. by optical spectrum analyser measurement. If needed, the SOC team can provide guidance.
(6) Laser system and optical isolator, excluding electronics, mock-up cavity, etc. devices are available at the required wavelengths.

A1.1.5.1.2 First-stage cooling Laser

Critical issues are the high power required. So far, in the SOC2 breadboard, the radiation is generated by a frequency doubled ECDL, which is amplified by a tapered optical semiconductor amplifier (TA). Direct generation of the 461 nm radiation by blue laser diodes could be another option. As the laser is used for the detection of the atomic excitation, excessive frequency noise can degrade the signal and increase the detection noise. Thus, a frequency stability of 1 MHz is required.
In the recent ESA ITT O8322 (Development of high reliability lasers at 461 nm and 689 nm (Sr lattice) and 422 nm (single trapped Sr ion)) the following specifications are required:

Laser System Requirements		
Property	**Sr first stage cooling**	**Sr second stage cooling**
Wavelength	461 nm	689 nm
Atomic transition	^{87}Sr: $^1S_0 \rightarrow {}^1P_1$	^{87}Sr: $^1S_0 \rightarrow {}^3P_1$
Power[1]	> 150 mW	> 20 mW
Linewidth[2]	< 1 MHz	< 1 kHz
Frequency deviation[3]	< 1 MHz in 24 h	< 1 kHz in 24 h
Frequency tuning[4]	> 400 MHz in 10 s	> 400 MHz in 10 s
Frequency modulation	NA	30-50 kHz 2 MHz amplitude
Power stability[5]	Fluctuations < 3% in a bandwidth 1 Hz to 10 kHz. Absolute level within 5 % during 24 h.	
Laser output I/Fs	Max 4 fiber coupling units(6), 2 delivering more than 50 mW	1 fiber coupling unit(6) FC/APC connector.

	each; FC/APC connectors.	
Mass (guideline)	13 kg	7 kg
Volume (guideline)	11 liter	5 liter
Lifetime (guideline)	> 3 years	

[1] Total power at the laser output interface(s). Should the specified laser power output of the 461 nm laser system require the implementation of more than one laser head, appropriate locking of the different laser outputs shall be demonstrated.
[2] After stabilization on FSS/CCU or dedicated reference cavity. 95% of the power shall be within a spectral bandwidth equal to the linewidth specified above. The spectral power density in the sidebands shall be -65 dBc/1 Hz in a bandwidth of 1 kHz – 100 kHz.
[3] Maximum frequency deviation after absolute stabilization of the laser on FSS/CCU or dedicated reference cavity over 24 h.
[4] Possibility to tune the laser frequency (e.g. using a phase modulator, see [RD7]) within 10 s while locked to FSS/CCU or to the reference cavity.
[5] If needed, the required power stability can be achieved by an active control loop (e.g. via an acousto-optic modulator).
[6] Polarization maintaining single mode optical fiber.

A1.1.5.1.3 Frequency distribution subsystem

The 1st stage cooling laser output needs to be distributed to several outputs with different frequencies and adjustable power levels that typically require the use of AOMs for frequency shifting. A first-generation distribution board for the 461 nm radiation has been developed during the SOC2 project [RD71]. A more compact version would be part of the first-stage cooling laser system, as specified in Table A-3.

A1.1.5.1.4 Second-stage cooling laser

For the second cooling stage, because of the narrow atomic transition linewidth also a relatively high frequency stability and sub-kHz linewidth of the 689 nm cooling laser is required. The FSS provides the corresponding correction signal to achieve these requirements. To accommodate the initially hot atoms, during the first cooling phase the laser frequency needs to be frequency modulated in a well-defined 1 MHz wide frequency range and with modulation frequency 30 – 50 kHz. For the cooling of ^{87}Sr also an additional optical field, detuned by +1.42 GHz from the cooling light is required from the stirring laser. The 689 nm laser system can be simplified to replace the offset lock by modulation techniques and obtain a single beam containing both frequencies.

A1.1.5.1.5 Repumpers

Atoms need to be repumped from the upper clock level $^3P_0$ both during the first stage laser cooling where atoms get trapped by a spontaneous decay from the $^1P_1$ level and for state-selective detection of the excitation fraction after the interrogation of the clock transition. In ^{87}Sr, these repumpers have to cover the hyperfine structure of the involved levels, thus the linewidth has to be actively increased to several GHz with modulation frequency of a few kHz, while the centre frequencies only need to be stable to 100 MHz.
Here ECDLs are available, but the requirements could be easily fulfilled by simpler and more power efficient VCSELS or DBR laser diodes. However, so far no such devices are available at the required wavelengths.

A1.1.5.1.6 Clock Laser

The clock laser system is typically based on a 698 nm ECDL, as the fast free-running linewidth should be well below 1 MHz to enable electronic locking the frequency to sub-Hz linewidth and sufficient stability well below 10^{-15} to enable the clock to reach a total frequency instability of $\sigma_y(\tau) = 5\times10^{-16}\ \tau^{-1/2}$ (Figure A-6). Besides AOMs, the breadboard also needs to contain optical elements for the active fibre-length stabilization to the reference cavity, to the atomics package and to the frequency comb, in order to avoid degradation of the frequency stability by vibration-induced length fluctuations of the connecting fibres [RD82].
A current ESA ITT AO8657 (Development of an acceleration insensitive, thermal noise mitigated, Optical Stabilising Reference Cavity (OSRC) Engineering Model) requires fractional frequency instability of 3×10^{-16} for an integration time 0.1 s < τ < 100 s after subtraction of the linear drift with the following parameters:

OSRC System Guidelines	
Parameter	**Value**
Mass	<10 kg (incl. optics arm, ion pump)
Volume	<10 liter
Cooling requirement	<15 Watt
Vacuum pump	<6 Watt
Footprint area	< 25 cm × 30 cm
Temperature Limits Non operational	non-operational -20°C to 50°C
Temperature Limits Operational	TBD by mission scenario

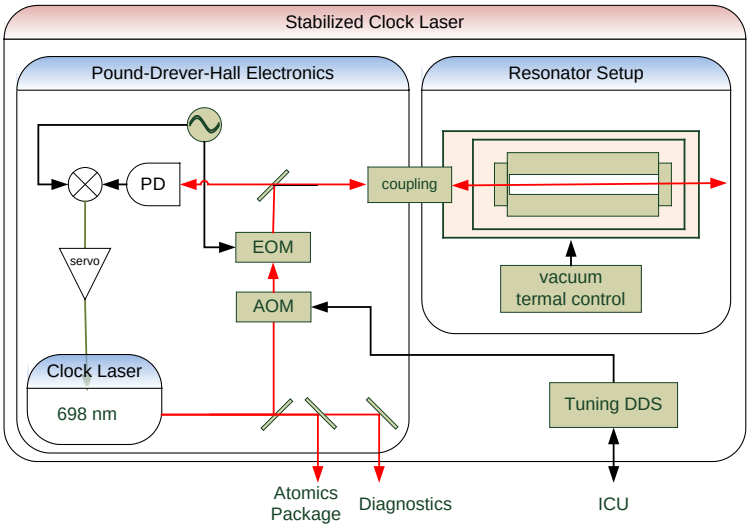

Figure A-5: Block diagram of the clock laser system

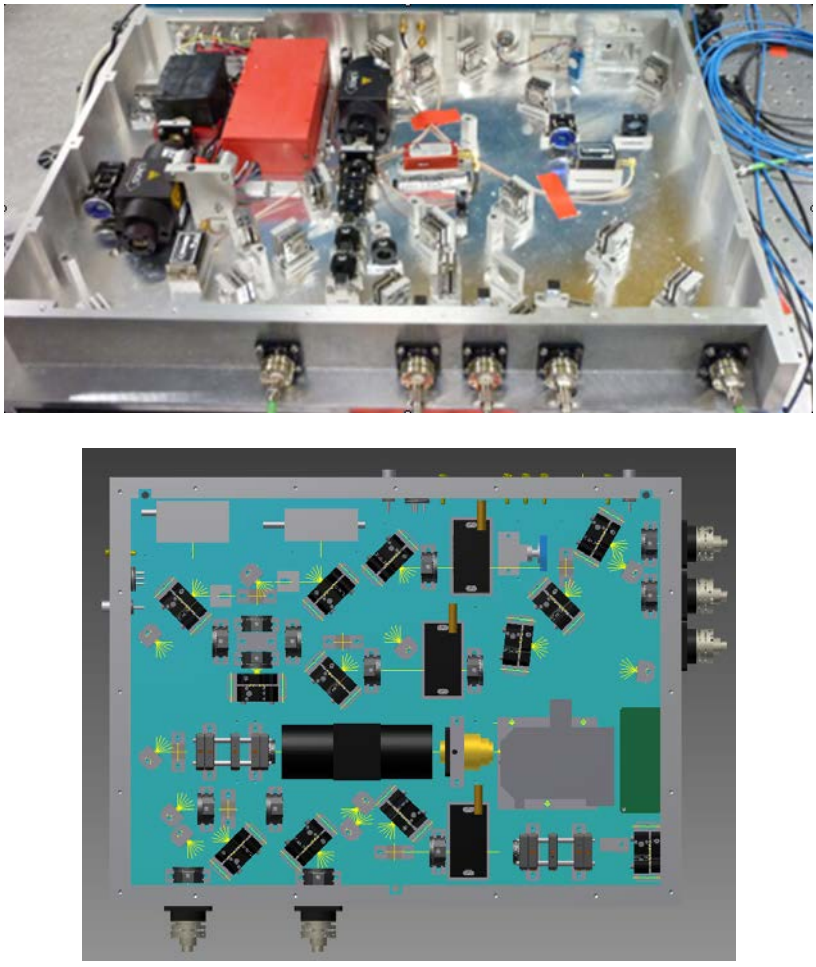

Figure A-6: The compact laser breadboard for the 698 nm clock laser system from SOC, containing a master and an injection-locked slave laser system with AOMs, fiber distribution, in a box 450 mm × 600 mm × 120 mm (top) and the next-generation design using a half sized breadboard of 300 mm × 450 mm × 120 mm (bottom).

A1.1.5.1.7 Clock cavity

The frequency stability of the clock interrogation laser and the clock instability due to the Dick effect is mostly determined by the instability of the reference cavity of the clock laser. The main issues are a sufficiently low thermal noise, due to Brownian motion of the constituents, mostly of the mirrors and length fluctuations of the mirror separation induced by vibrations. For averaging times above a few seconds also temperature fluctuations acting on the spacer can degrade the stability.

Current dielectric mirrors on fused silica substrates set the thermal noise level for a typical 10-cm long cavity to $\sigma_y = 5\times10^{-16}$. Lower values can be achieved by increasing the length, using especially large mode diameters or switching to novel crystalline coating with reduced thermal noise [RD72]. Ultrahigh reflective crystalline mirrors are now available that permit to achieve a finesse above 100 000. However, the material is not suitable for the 698 nm wavelength of the clock transition, thus either the subharmonic at 1396 nm

would be needed to be stabilized to such a cavity or the fs-comb would be required also to transfer the stability from the near IR to the 698 nm clock laser [RD77].
The sensitivity of the cavity length on vibrations can be minimized by optimizing the shape and the mounting of the cavity, using FEM simulations. Typical values for the sensitivity are around 4×10^{-11}/g (with the gravitational acceleration g = 9.8 m/s^2) [RD70].
A particular issue concerning reaching a high frequency stability of the reference cavity on the ISS is related to the relatively high acceleration noise present there. There are three approaches that appear suitable for reaching the I-SOC specification of $\sigma_y = 3\times10^{-16}$:

(1) cavity design with reduced acceleration sensitivity and feed forward correction of frequency based on real-time measurement of the acceleration component for which the cavity exhibits the largest sensitivity. This has led to sensitivities smaller or equal 2×10^{-12}/g [RD85]
(2) active vibrational isolation stage, e.g. hexapod or similar
(3) a combination of (1) and (2).

It is suggested that a 3-axis accelerometer is placed near the reference cavity, monitoring vibrational noise levels and transmitting this data to the on-board computer for diagnostics and control.

A1.1.5.1.8 Fibre noise cancellation

In the fibres that connect the optical clock laser package with the atomics package, the reference cavity, and with the femtosecond comb, any temperature fluctuations or mechanical stress will introduce unwanted phase fluctuations that will degrade the performance of the optical clock. Thus, a phase noise cancellation [RD84] for these fibres needs to be implemented, where part of the light is returned through the same fibre. Additional complexity appears in the link to the atomics package. There, the noise cancellation is only active during the time when the atoms are interrogated. Here more sophisticated fibre-noise cancellations methods need to be applied as e.g. detailed in [RD73]. In contrast to [RD73], the noise cancellation has to recover the laser phase from pulse to pulse modulo 2π to allow for Ramsey spectroscopy.

A1.1.5.1.9 Diagnostics package

The lasers need to provide different levels of frequency stability as expressed in Table A-3. This frequency stability is ensured by a diagnostics package that:

- provides correction signals to the lasers to keep their frequency within the required range.
- provides information for the initial tuning of all lasers to the correct wavelengths.

The corresponding ESA ITT AO8334 (Development of clock control unit (CCU)) describes the requirements as follows:

Quantity	Requirement
Absolute Stability	The CCU shall be capable of robust absolute frequency stabilization of the Sr lasers at 462 nm (first stage cooling), 689 nm (second stage cooling), 813 nm (optical lattice) with an absolute deviation of less than 1 MHz, 1 kHz, and 100 kHz respectively over 1 h. Repumpers at 707 nm and 679 nm shall also be frequency stabilized by using the CCU.
Long-term drift	Any long term drift has to be taken into account to allow for reaching the specified optical frequencies for a duration of at least 3 years.
Error signals	The CCU shall provide an error signal with sufficient bandwidth and SNR to frequency lock lasers to the following linewidth: • 1 MHz for 461 nm, • 100 kHz for 813 nm, • 1 kHz for 689 nm. Note: 95% of the power shall be within a spectral bandwidth equal to the linewidth specified above.
Spectral power density	For the 689 nm laser the spectral power density in a frequency range of 1 kHz –100 kHz away from the carrier shall be -65 dBc/Hz.
Tuning	It shall be possible to tune the frequency of the lasers to ±10 MHz within 2 s.
Modulation	The CCU shall allow for frequency modulation of the 689 nm laser at a modulation frequency of 30 – 50 kHz with a modulation amplitude of 2 MHz peak-to-peak relative to the given center frequency. It shall be possible to switch on and off the frequency modulation via a TTL input. Modulation frequency and amplitude shall be adjustable. It shall be possible to connect different center frequencies by TTL control for switching the modulation.

As an example, the SOC2 Frequency Stabilization System (FSS) [RD76] fulfills the first task by using a set of 3 optical cavities in a common ULE block.

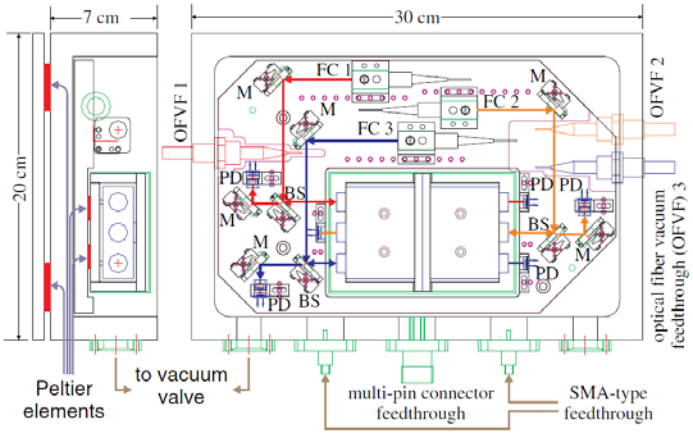

Figure A-7: Setup of the SOC frequency stabilization system (from [RD76])

The second task could be achieved by a wavelength meter, e.g. similar to commercially available system (e.g. HighFinesse WS8) based on static Fizeau interferometers. These systems would also allow stabilizing the repumper frequencies on the long term. Very robust units (that have passed shake tests) have been demonstrated by companies.

A1.1.6 INTERFACES

A1.1.6.1 *Optical*

All the modules will be connected by polarization maintaining fibres. To avoid optical feedback, angled connectors need to be used, e.g. FC-APC style.

A1.1.6.2 *Electrical*

Needs to be decided: Here similarities with ACES can be exploited.
The acousto-optical modulators are expected to be driven by amplifiers that are all located in the power module, so as to concentrate the most strongly heat-dissipating elements into one unit.
The time sequence for controlling the switches, AOMs, electric and magnetic fields are produced as TTL signals by the clock control computer.

A1.1.6.3 *Mechanical/Structural*

The atomics package needs to be rigidly mounted to the container, while the optical breadboards and the optical diagnostics module are expected to be mounted in a stress-free way, e.g. as in ACES.

A1.1.6.4 *Thermal*

The dissipated power of the laser modules and of the atomics package needs to be removed and transported to the baseplate of the payload.
The required temperature stability of the breadboards is expected to be 1 K and of the atomic environment to better than 0.1 K over the full course of the mission.
The power electronics, where most of the heat is dissipated is expected to need much less demanding requirements.

A1.1.6.5 *TM/TC*

Standard connection/serial bus between the components

A1.1.7 OTHER

A1.1.7.1 *Exchange file formats*

We propose to use the XML based GraphML file format for the graphs that describe the interaction between the various parts inside the clock and with the environment (spacecraft, frequency comb).
This format can be easily read by various programs (e.g. PyGraphML for Python) to perform simulations etc.

Simulations: Program code (Python, C++, ...) in ASCII format.

Technical Drawings: TBD

A1.2 The links of I-SOC

A1.2.1 MICROWAVE LINK (MWL)

A1.2.1.1 *Design*

The MWL design is an evolution of the science link presently under development for the ACES mission. The end-to-end system is composed of a flight segment unit and a distributed network of ground terminals, respectively connected to the clocks on-board the STE-QUEST spacecraft and on the ground. The input clock signal is up-converted and used to coherently generate the microwave signals that are transmitted through the atmosphere and received by the remote terminal at the other end of the link. The space segment provides 4 independent receiving channels capable of performing up to 4 simultaneous comparisons of the space clock with clocks on ground.
The comparison of two ground clocks in common-view can be obtained by evaluating the difference of the two simultaneous space-to-ground comparisons. As the noise of the space clock is in common-mode, common-view comparison can be carried out without the need for a high performance on-board clock. A commercial ultra-stable oscillator (USO) is indeed sufficient for this purpose.
The comparison of a ground clock with the space clock by means of MWL consists in measuring the desynchronization between the space clock and clocks on the ground, or equivalently the difference between the space clock proper time τ^s and the ground clock proper time τ^g at a given coordinate time t.
While propagating from space to ground and vice-versa, the phase of the signal is perturbed by several effects that need to be evaluated and corrected for. They are:

- The range between the ground station and the spacecraft, responsible for propagation delays on the order of 400 km/c $\approx$ 1 ms.
- The propagation delays induced by the troposphere, typically ranging between 10 ns and 100 ns, depending on the local atmospheric conditions and satellite elevation.
- Ionosphere propagation delays, varying between 0.1 ns and a few ns and depending on the frequency.
- Multipath effects: The detection of the direct signal can be disturbed by reflections (multipath signal) generated at surfaces in the immediate vicinities of both the space segment and ground terminal antennae. The multipath signal combines with the direct signal introducing a delay depending on relative phase and amplitude.
- Internal delays due to the ground terminal and flight segment electronics: Such delays need to be carefully calibrated before launch and continuously monitored during the mission.

MWL is an asynchronous three-frequency link based on a two-way geometry, which operates continuously with an up-link in the Ka-band and two down-links in the Ka and X-band (Figure A-8).

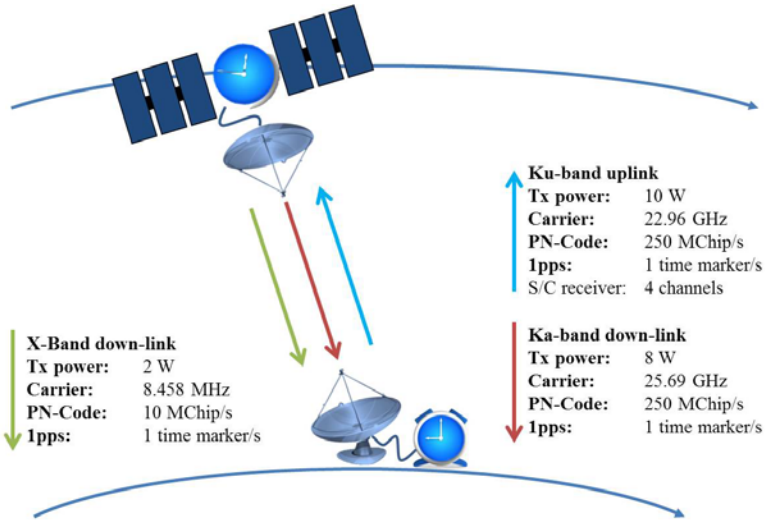

Figure A-8: MWL architecture

The two-way configuration is important to correct for the range-induced delays, which cancel to first order when the desynchronization between the space and the ground clock is calculated. Residual corrections due to link asymmetries depend on the knowledge of antennae phase centre positions as well as on the two-way geometry of the link. The two-way configuration is also important for removing the non-dispersive delays introduced by the propagation through the troposphere. Frequency dependent tropospheric delays, if not corrected, can still degrade the performance of the MWL link. A semi-empirical correction model, similar to the one developed in [RD55] for the ACES mission can be used to estimate this effect and remove it to the required level. Ionospheric delays are frequency-dependent and they influence with opposite sign both group and phase velocity of the microwave signal. To this purpose, the link measures the differential delay on the Ku-band and X-band downlink signals to calculate the total electron content (TEC) of the ionosphere and correct for the ionospheric time delay [RD56].

The two ends of the link transmit a carrier that is phase-modulated by a pseudo-noise code (PN-code) at a rate of 250 MChip/s. Carrier and code are both coherently generated from the local clocks. The code and the carrier phase of the received signal are compared to their local replicas at the space and ground terminals. While the noise on code phase measurements defines the long-term stability of the link, the ultimate performance can only be reached with carrier phase measurements. To this purpose, the code signal is also used to remove phase cycle ambiguities, allowing for continuous phase comparison measurements on the carrier signal. The PN-sequence is also modulated with a PPS (Pulse Per Second) that defines the on-board time scale.

As shown in Figure A-9, acquisition and tracking is achieved by correlating the incoming signal, down-converted to the intermediate frequency IF, with an early and late replica of the locally generated PN-code sequence [RD57]. The use of narrow early-late correlators is important to control multipath effects [RD58]. The 1st IF is mixed with a replica of the carrier frequency shifted according to the experienced Doppler effect. After the early-late correlator, the signal is cleaned in a surface acoustic wave (SAW) filter and digitised in a fast A/D converter. A/D conversion as well as signal correlation can be digitally implemented in a field programmable gate array (FPGA). Using fast electronics, internal

delays can be precisely controlled with respect to standard analogue beat techniques. Local code and carrier frequencies are generated by direct digital synthesizers (DDS), which are phase-locked to the local clock and controlled by the tracking loops.
Following the ACES heritage, the space antenna is designed for circular polarisation in order to optimally reject multipath and suppress Faraday rotations in the Earth magnetic

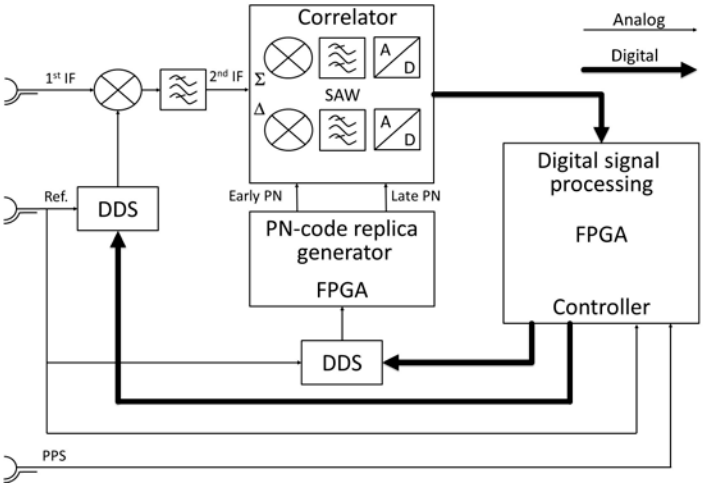

Figure A-9: Schematic of code signal tracking in MWL.

field. The beam angle shall allow coverage of the Earth in the main lobe at all orbit conditions. Choke rings are used to improve directivity and reduce the effects of signal reflections.
The MWL ground terminal design follows the ACES technology after re-adaptation of the systems to the Ka-band and X-band frequencies. It is a microwave station interfacing the local clock on ground to the ISS payload (Figure A-10). To reduce phase instabilities due to the tracking motion, the electronics unit is rigidly attached to the antenna unit. The antenna is a 60 cm offset reflector with a dual-band feed system automatically pointed in azimuth and elevation by a steering mechanism. A computer controls the steering unit based on the STE-QUEST orbit prediction files, collects telemetry and science data both from the local clock and the MWL GT electronics, and interfaces directly with the Mission Operations Center (MOC). The system is housed below a protective radome cover, which also allows stabilizing the temperature by an air conditioning system.

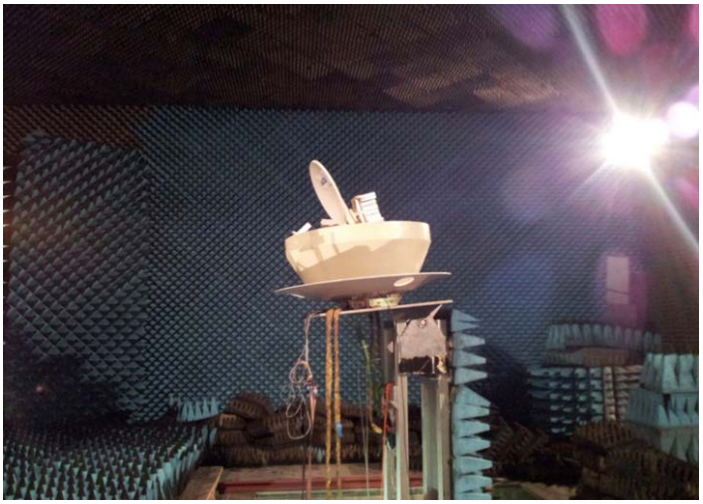

Figure A-10: ACES MWL ground terminal under test in compensated compact range facility. The I-SOC ground terminals will be based on the ACES technology.

Due to the early-late correlator properties, only multipath signals which result to be time-shifted by less than 1 chip for the carrier and 1.5 chip for the code introduce errors on the phase comparison measurements [RD59]. Therefore, reflections from surfaces at more than 2 m are strongly attenuated by the PN-code autocorrelation properties. The effect of reflections from shorter distances will have to be minimized through a careful antenna design and its positioning on-board the spacecraft.
The link stability requirement reported in#SR-PL-09 translates into a time error with a flicker phase noise as low as 92 fs [RD60]. Reaching the ultimate link performance requires a control on the delays affecting code and carrier phase measurements at a few tens of femtoseconds. This translates into an optimized thermal design of the end-to-end link. To that purpose, a two-stage temperature control system is foreseen both for the flight segment and ground terminal electronics. In addition, early digitization of the science signal, use of short cables and signal paths, symmetric designs for amplifiers and other critical components become important to meet the scientific requirements. Finally, the calibration of the terminal delays against temperature variation will be performed both in space and on the ground and continuously updated during the mission lifetime thanks to built-in test loop transponders.
The key link parameters have been identified, the link budget at apogee has been calculated for different elevation angles and atmospheric conditions (clear sky or rain), together with the S/N and the expected jitter (white phase noise) of the code and phase comparison measurements. From the design, a link availability better than 99% can be predicted.

A1.2.1.2 *Interfaces and resource requirements*

The interfaces at the MWL ground terminal and at the flight segment unit with the signals generated by the local clock (USO or atomic clock) include:

- 8.8 GHz reference input signal coherently generated from the local atomic clock;
- 1 PPS input for synchronization, calibration and test purposes;
- 1 PPS output for synchronization, calibration and test purposes.

On the ground, the connection between the local clock and the MWL input connector shall not degrade the performance of the clock signal itself. This connection is under the responsibility of the institutes operating the ground clocks. Distances of several hundreds of kilometres can today be covered by fibre links introducing negligible noise on the distributed clock signal. The PPS output port is also the reference point for performing time transfer experiments. This connector provides a timing signal synchronously generated from the local atomic clock.
MWL phase comparison measurements are time tagged both in space and on the ground in the local clock timescales. In addition, absolute internal delays at reception and transmission need to be calibrated to 1 ns. This includes the calibration of the MWL flight segment and ground terminal channel delays from reception at the antenna reference point to time stamping in the local time scale and from time stamping in the local time scale to emission at the antenna reference point. Control of internal delays at reception and emission is important to correctly apply the two-way formula and achieve optimal rejection of phase variations due to the Doppler effect. Finally, phase comparison measurements shall be linked to UTC with an uncertainty better than 1 μs to correctly retrieve velocity and position of the clocks and the antennae reference points from the orbitography files (see Sec. 3.3.2).
MWL is also used to perform time transfer experiments. To this purpose, the MWL ground terminals need to be calibrated against a transportable unit that will be kept as a reference. Calibration campaigns will take place as a minimum at the beginning and at the end of the mission.
Standard data links are used by the terminals to transfer telemetry, housekeeping, and science data as well as to receive telecommands, orbitography files, etc. Communication between the ground terminals and the MOC takes place through the internet.
The MWL flight segment unit has a mass of 33 kg and a power consumption of 110 W. Both figures include 20% of margin at unit level.

A1.2.1.3 *Operation requirements*

MWL space-to-ground contacts are scheduled on the basis of the visibility windows available at each ground station. As discussed before, weather conditions do not pose any restriction to MWL operation.
MWL uses Code Division Multiple Access (CDMA) to simultaneously connect up to 4 ground terminals to the 4 receiving channels of the flight segment unit. At signal acquisition, frequency and delay of the code oscillator need to be steered on the basis of the predicted range and Doppler shift. Range and Doppler steering files are prepared by MOC and uploaded before the start of each pass to support signal acquisition routines. The MWL ground terminal is automatically pointed in azimuth and elevation by a steering mechanism controlled by a computer on the basis of the orbit prediction files generated by MOC. Signal acquisition is expected to start slightly above the horizon, with the system entering the full tracking mode before reaching 5 deg of elevation.
Both the flight segment unit and the ground terminals are remotely controlled by MOC.

A1.2.1.4 *Heritage*

The development of the I-SOC MWL will take advantage of the ACES heritage and STE-QUEST mission study. Many of the techniques and procedures discussed before have already been established and tested in the frame of the ACES mission. The ACES MWL engineering model has been completed and tested. The flicker floor of the carrier phase measurements has been measured to 70 fs, compatible with the I-SOC needs. The instrument is now undergoing signal simulator tests to characterize the performance under realistic signal dynamics.
The issues identified to upgrade MWL from ACES to I-SOC are the following:

- Frequency plan to be re-adapted to Ka-band and X-band;
- Antennae design and power amplification stages to be dimensioned to the I-SOC link budget;
- High speed electronics, now available, to be implemented to increase the chip rate to 250 MChip/s (compared to the 100 MChip/s of the ACES MWL) and to perform an early digitization of the regenerated code and carrier signals.

An upgrade of the ACES MWL to a space mission with a high Earth orbit (STE-QUEST) has been considered. An ESA study has addressed the above issues relative to that orbit and showed compatibility with the STE-QUEST scientific requirements. A second study has recently been initiated to verify the performance through a breadboarding activity of the critical system elements.

A1.2.2 ELT+ LASER TIME TRANSFER

A1.2.2.1 *Design*

ELT+ is a pulsed laser time transfer technique. It is based on an existing and mature technique of satellite laser ranging (SLR). The ultra-short laser pulses fired at 1 kHz towards the satellite by a ground laser ranging station are time tagged with respect to the ground time scale**.** They are detected in space and also time-tagged in the local time scale. At the same time the optical retroreflector is re-directing a part of the laser pulse back towards the ground station. Detecting the reflected optical pulse on a ground is providing accurate two-way propagation time and hence it is providing the information about the ground-to-space signal propagation delay.

A1.2.2.2 *Application to I-SOC science goals*

Pulses received by the ISS at the beginning and end of a time interval T (as defined by a ground clock) can be correlated with timing pulses generated by the space clock. Thus, the time interval T can be measured in terms of the time scale defined by the space clock. If T is for example defined as the interval corresponding to M cycles of the ground clock oscillation, I-SOC will be able to determine the number of cycles M' of the space clock hat correspond to M. The ratio M'/M corresponds to the frequency ratio ν'/ν and contains information about the GTD.

By receiving on the ISS pulses arriving from different ground stations with respective clocks, it will be possible to compare the frequencies/time intervals of ground clocks.

The detection, on ground, of the retroreflected pulses serves to determine the ground-to-space propagation delay and to correct for it in the clock comparison measurements.

Note that this measurement procedure requires the cycle counting to be gapless, both on ground and in space. Loss of single or few cycles give rise to additional measurement errors.

In absence of such additional uncertainty, the fractional accuracy of measuring a time interval (or determining a frequency ratio) is given by $\Delta t(T)/T$, where $\Delta t(T)$ is the timing error (TDEV) arising in the pulse reception over the time interval T. This holds for common-view comparisons. For non-common-view comparisons, one has to add the time error arising from the on-board clock as it accrues during flight of the ISS from one ground station to the other (for a general discussion of extrapolation errors, see RD69).

The application of this concept to the Sun/Moon GTD, where a putative signal would give a frequency ratio varying periodically (period close to 24 h), has been discussed in connection with #PSO-02 above.

A first estimate of the expected timing performance of the ELT+ laser time transfer for the I-SOC mission is presented here. The data are based on the best results obtained in experiments of individual parts of the ELT laser time transfer chain within the last years. Considering the physical nature of all the individual contributors, no significant improvement is expected to appear in laser time transfer technique of ELT type in the future.

A1.2.2.3 *Space segment*

The key parts of the ELT+ space segment are a photon counting detector, an epoch timing system and a passive optical retroreflector. Recently, a number of improvements of technology components of the laser time transfer signal chain occurred. The timing performance of photon counting detectors and epoch timing systems has improved several times [RD66,RD67].

The performance of the detector, the timing system, test laser pulses ~ 40 ps long, and an electro-optical switch was tested in indoor experiments (at CTU in Prague). The precision in a sense of TDEV is 0.4 ps @ 100 s. Improvement of this value down to 100 fs @ 100 s is expected. A long-term stability better than 0.4 ps from 100 s to 100 000 s was verified experimentally and repeatedly. Timing stability better than 0.5 ps over $1{\cdot}10^6$ s is expected as a qualified estimate. These values are valid for a laser repetition rate of 1 kHz. Realistic margin exists, thanks to laser pulse lengths expected to be < 10 ps in future SLR operation.

A1.2.2.4 *Ground segment*

The ground SLR systems participating in I-SOC are expected to operate at 1-2 kHz rate, using laser pulse lengths of ~ 10 ps. The precision of determining one-way ground-to-space delay will be better than 0.4 ps for averaging time 100 s. This value is expected to be obtained when ranging to a spherical laser retroreflector – a Luneburg sphere [RD68]. The long-term stability of a good SLR system will be below 1 ps (0.5 ps as a goal) over hours up to one month. This estimate is based on a performance of the world's most stable SLR system (Graz, Austria). No significant improvement is expected in the future.

A1.2.2.5 *Overall laser time transfer performance*

Combining the ground and space segments, one can conclude that the precision obtainable within one pass of I-SOC / ISS could be below 0.5 ps @ 100 s. The value of overall timing stability ≈ 1 ps is expected for time intervals of up to 10^6 s. Thus, the maximum fractional accuracy possible with this method will be 1 ps/10^6 s = $1 \cdot 10^{-18}$.
Considering the nature of all the individual contributors to noise and systematic errors, no significant improvement of these values is expected.

A1.2.2.6 *Interfaces and resource requirements*

Data flow
Uplink: – very limited data volumes – control commands only. Total data volume expected is well below 100 bits / orbit.
Downlink: The operational ELT+ will generate measurement data at a rate ~ 200 kbits / s. This data flux must be accepted by the control computer. To reduce the total data volume stored on-board and downlinked to ground, the data blocks corresponding to (possible) laser time transfer activity can be stored and downlinked only. This approach might reduce the data volume for on-board storage and downlink more than 30-fold. To enable efficient operation of ELT+ link, the data must be downlinked to the ground data center at least once per ISS orbit.

Resources
Power: – the total power requirements of the ELT+ hardware is ~ 13 W. The power supplies voltages in a range of +/-5V are needed only. The highest voltage operated in a detector is below 30 V.
Timing signals: – the clock signal of 100 MHz is needed for the epoch timing device. In addition the "1PPS" epoch reference. These clock frequency and epoch reference will define the local time scale. In addition the UTC timing signal (1 PPS or similar) will be needed for gate generation for the ELT+ detector.

A1.2.2.7 *Operation requirements of space segment*

The laser retroreflector will operate in free space, nadir looking, no additional requirements.
The optical detector will operate with the input aperture opened into free space, nadir looking. The operational temperature of the detector itself can be within a range of -40 up to +30 deg. C. The temperature change over one orbit should be within 6 K (analogy to ACES/ELT).
The epoch timing device will operate inside the Columbus module. The operational temperature of the timing device itself can be within a range of -40 up to +30 deg. C. The temperature change over one orbit should be within 2 K.
To provide maximum system stability, all the electronics is expected to be powered all the time.

A1.2.2.8 *Heritage*

ELT+ has heritage from ACES (where it is named ELT) and several previous missions of laser time transfer. Within the last two decades 5 operational space missions were

performing time transfer using laser light. The experiment prepared by CNES is operational on board of Jason-2 mission (launched by NASA, June 2008). The device called T2L2 is operating at an altitude ~ 1500 km above the Earth surface. It provides the precision in a sense of time deviation ~ 10 ps at 200 s integration time. The overall timing performance is limited by the quality of on-board clock – a quartz oscillator. The main limitation of systematic errors is the multiphoton concept of laser time transfer. The systematic errors of the system are on a level of 100 ps.
The photon counting concept was used for the first time on board of Compass satellites both on GNSS orbits (2 satellites) and on inclined geostationary orbits (2 satellites). The laser time transfer system was operational during the years 2007 to 2012. The precision was typically 30 ps @ 500 s integration time. It was limited by data volume available for downlink communication and hence by the experiment repetition rate of 1 to 10 Hz only.
For the ACES mission, the laser time transfer link ELT was prepared. It is based on a photon counting approach to minimize the systematic errors. The nominal repetition rate is 100 Hz. The extensive ground tests verified the performance better than 3 ps at 100 s integration time and the stability of ~ 1 ps over long time intervals exceeding 1×10^6 s.
For all the listed space missions the optical receivers for both space and ground segments were developed at CTU in Prague. In all listed missions the planned laser time transfer performance was achieved.
The laser time transfer ELT+ will be based on a heritage of the ELT optical detector and on the newly developed New Pico Event Timer (NPET) developed at CTU in Prague. This event timing system is currently used as an epoch timing device for calibration purposes of a ground segment participating in ELT mission.
A laser retroreflector of a special concept (Luneburg sphere) has to be used to reach sub-ps precision. The retroreflectors of this type and origin have a space heritage (Meteor 3, Blits,..).

A1.2.2.9 *Budget of the space segment*

Photon counting detector (Qualified estimate based on ELT/ACES mission experience)
- mass 0.5 kg
- power < 0.6 W
- dimensions 110 x 110 x 170 mm

Epoch timing device (estimate based on laboratory sample of device)
- mass 1 kg
- power 12 W
- dimensions 160 x 250 x 42 mm

Signal cabling (Qualified estimate based on ELT/ACES mission experience)
- mass < 0.5 kg
- dimensions -

Laser retroreflector + holder (space heritage)
- mass 1 kg
- dimensions 100 x 100 x 100 mm^3

Comments

The detector and laser retroreflector have to be installed on the external part of Columbus module,

The shape of the detector and epoch timer may be modified, once necessary
Their total mass and power consumption cannot be reduced significantly,
The space-qualified laser retroreflector should be commercially available (Russian origin).

A1.2.3 FREQUENCY-COMB OPTICAL LINK (FCOL)

In this section, a brief overview of the femtosecond time/frequency transfer technique is given. This technique would be a benefit for I-SOC but is not yet available in Europe and thus not yet ready for consideration.

Time transfer via an optical link based on frequency comb is a new technique that was recently developed at the National Institute of Standards and Technology by the group of Nathan Newbury. It relies on the two-way transmission in free space of trains of ultra-short laser pulses generated by Optical Frequency Combs (OFC), whose repetition rate is frequency-locked to local time scale references.

In a first test, timing inaccuracy of 1 fs over 10 000 s for a 4 km stationary air path parallel to ground at an altitude of 2 km (Boulder, Colorado) was demonstrated, corresponding to $1 \cdot 10^{-19}$ time interval/frequency comparison inaccuracy within 3 hours integration time, and to $< 1 \cdot 10^{-17}$ in 100 s. Remarkably, this technique is robust to link interruption and link length variations, for example caused by turbulence. The 4 km horizontal air path used in Boulder is roughly equivalent to the thickness of atmosphere that will have to be traversed by a laser beam going from ground to the ISS when the station is close to the zenith, because the density of the atmosphere has a 1/e length scale of 9 km and turbulence strongly decreases with height above ground.

A second test with a link spanning up to 11 km of free space also demonstrated similar performances.

In the following paragraph the working principle of the femtosecond laser link is presented together with the architecture of the transmitting laser stations. In the paper Newbury's group reports the scheme of Figure A-11 used to verify the optical link performances [RD87].

The experimental set up is housed in a rooftop laboratory at the NIST building in Boulder (Colorado). A folded free-space link is used for measurements so that the frequency/time between the two end sites can also be directly compared, allowing to test the "truth" of the data.

A more detailed description of the system is shown in Figure A-12.

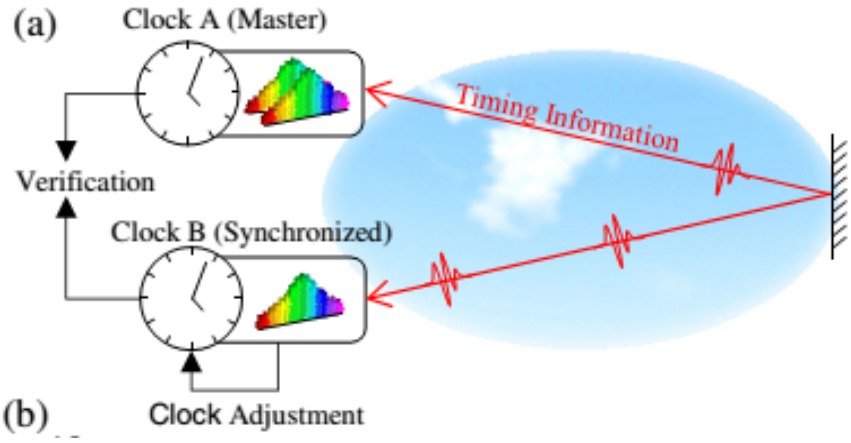

Figure A-11 Principle of the test set-up for demonstration of time transfer via femtosecond pulses. Clock B is synchronized to clock A. For this purpose, femtosecond pulses must be transferred from A to B and from B to A.

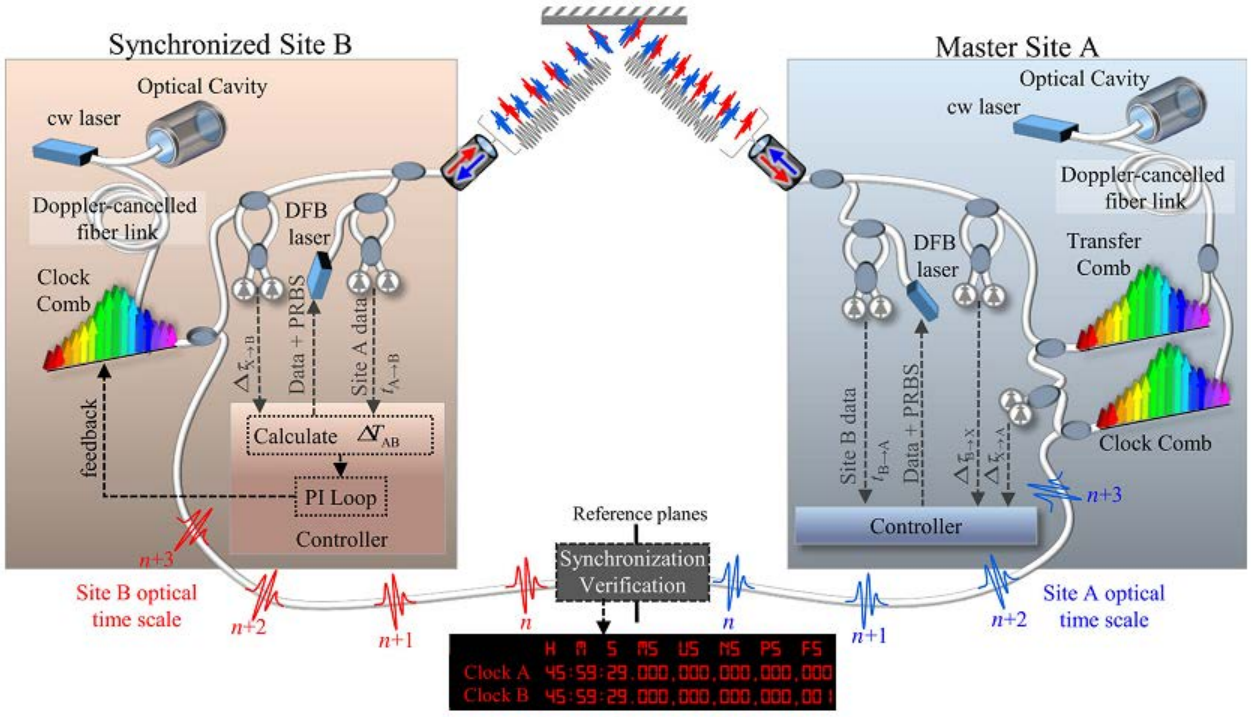

Figure A-12 Complete layout of a femtosecond optical link, which includes a verification subsystem.

Sites A and B are connected via a free-space single-spatial-mode optical link covering up to 4 km. This link is folded by use of plane mirrors so that sites A and B are physically adjacent, enabling synchronization verification via an out-of-loop measurement of the time offset ΔT, independent of the "in-loop" calculated time offset ΔT_{AB}.
The optical time scale at each site is based on a cavity stabilized laser, which acts as an optical oscillator (that can in principle be steered to any atomic clock).

To generate a time scale, at each site a self-referenced “clock” frequency comb is used, which is phase-locked to the cavity-stabilized laser. Each comb produces a pulse train leaving from its site to the other site: a two-way link is thereby implemented.
It is necessary to coarse-tune the optical link, which is done by a DFB laser whose beam carries a Pseudo Random Modulation Code. Its beam is superimposed with the comb beam. This is similar to what is done in a microwave link. Each site A and B uses such a laser. This coarse adjustment allows reaching an synchronization uncertainty of 50 ps.
Once the system is coarse-tuned, the real time optical communication between the two “clocks” can start. The pulses detected at each clock are used to clock a field programmable gate array (FPGA) controller that counts and labels each pulse with its arrival time at the selected reference plane, based on a given start time and known pulse repetition period.
The optical time scale from each site is defined by the arrival of pulses from the clock comb at a specified reference plane. For example, the *n*-th pulse from each site arrives at the reference plane at the time shown in the lower display, while the (*n* + 1)-st pulse arrives at a time $1/f_r$ later (being f_r the comb repetition rate). In the setup here, the two co-located clocks have a common reference plane to allow for out-of-loop synchronization verification. The timing and data exchange between the two sites occurs only over the free-space path shown in the upper part of the figure, and mimics a point-to-point link.

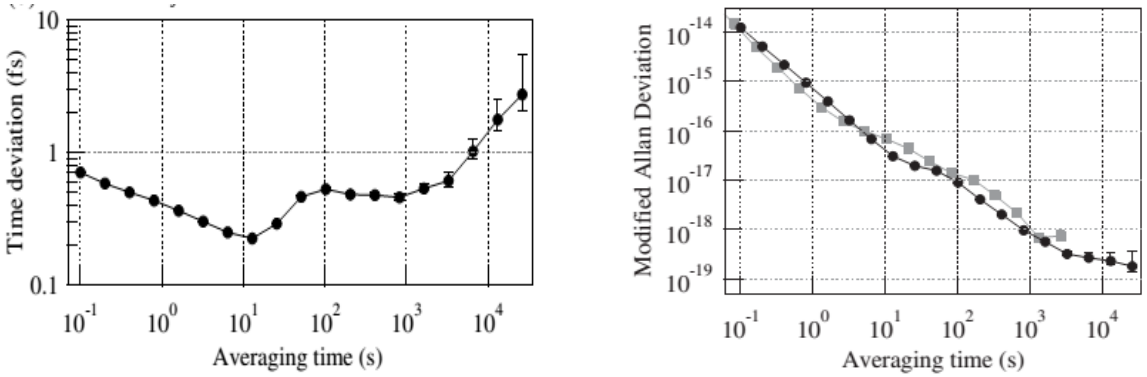

Figure A-13 Performance of the 4-km free-space link.

The stability results of the comb synchronization are expressed both in terms of Time Deviation and Modified Allan Deviation, which is more familiar in the frequency domain analysis. Figure A-13 shows the performance of the 4-km link.
The performance of the optical link has the potential to satisfy the most demanding ground-to-space and ground-to-ground-via-space clock comparisons, even if the optical clock exhibits an inaccuracy and instability in the low 10^{-18} range.
This technology, once properly developed, will be useful not only for I-SOC mission but also for all possible future synchronization and T&F comparison needs in space to space and ground to space applications.
A general overview of the laboratory realized to perform the experiment at NIST is reported in the following picture.

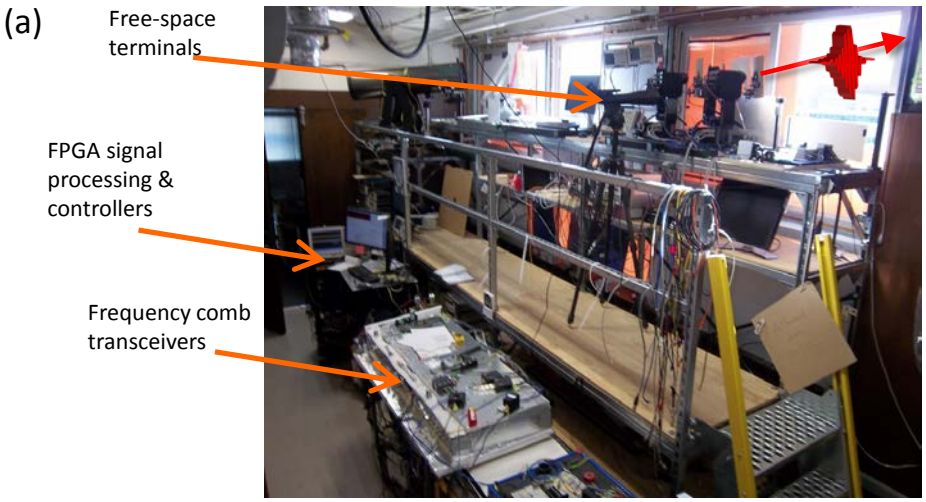

The comb-based timing measurements (i.e. cross-correlation) are accomplished via heterodyne detection between the local comb light and the incoming comb light. This heterodyne signal is digitized and processed within a field programmable gate array (FPGA). For this proposal the "Signal processing unit" is designate as the combination of the optical subsystem for the heterodyne detection and the FPGA processor; together they measure the relative timing between the two combs. The heterodyne detection system is comprised of standard telecommunication components.
Another key elements of the free space optical link are the two transmitting and receiving stations. A picture of the NIST prototype station is shown in Figure A-14.

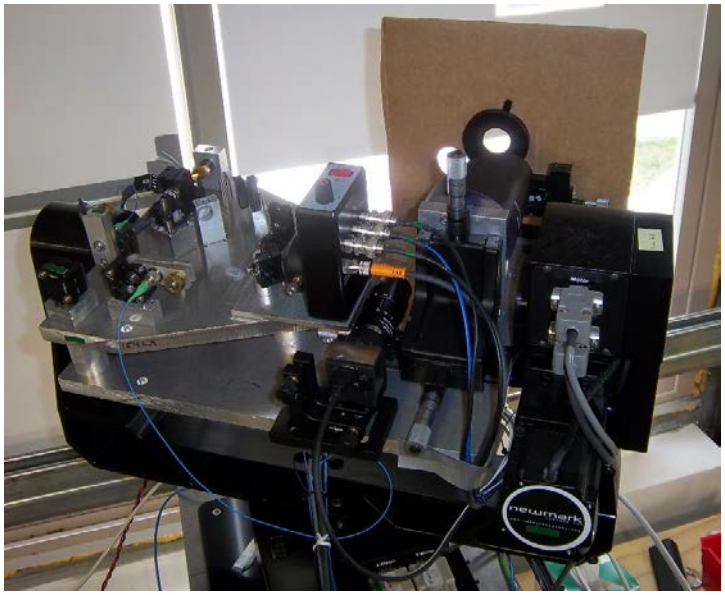

Figure A-14 A prototype optics transmission/receiving terminal. Visible are the detection electronics and the large optical system used to shape the transmitted beam as well as to collect the incoming light arriving from the remote station. The terminal also uses a beacon laser and tip-tilt mirrors to correct for turbulence-induced beam pointing.

For application to a mission such as I-SOC one may consider two options: a single optical terminal on the ISS or two. In the first case, only synchronization between one ground clock and the space clock is possible. A frequency comb on the ISS is required, just as with the MWL. The same comb can be used, of course.
With two terminals, a synchronization of two ground clocks in common-view is possible. Within the common-view duration, an inaccuracy at the level of $1 \cdot 10^{-17}$ could be expected.
Even if only such ground clock synchronization is desired, a space comb is still required, stabilized to a reference cavity. This unit serves as a “transfer clock”.
The major difference between the ground tests and application to space is the fast movement of the ISS. Thus, both the ground and the space terminals require active target tracking.

Annex 2 ORBIT MODELING AND ERRORS

In this section we discuss the model used to derive the errors of the gravitational potential at the space clock location.

Access to data and existing models is needed to complete the estimation of obit modeling and errors.

Annex 3 COMPOSITION OF THE I-SOC STUDY SCIENCE TEAM

The I-SOC Study Science Team is composed of:

S. Schiller (*Coordinator*), Heinrich-Heine-Universität Düsseldorf (UDUS), DE
U. Sterr, Physikalisch-Technische Bundesanstalt (PTB), Braunschweig, DE
C. Lisdat, Physikalisch-Technische Bundesanstalt (PTB), Braunschweig, DE
N. Poli, European Laboratory for Non-Linear Spectroscopy (LENS), Firenze, IT
G. Tino, European Laboratory for Non-Linear Spectroscopy (LENS), Firenze, IT
I. Prochazka, Czech Technical University of Prague (CTU), CZ
R. Le Targat, Observatoire de Paris (OBSPARIS), FR
J. Lodewyck, Observatoire de Paris (OBSPARIS), FR
C. Salomon, Laboratoire Kastler Brossel (ENS), Paris, FR
Y. Singh, University of Birmingham (UOB), UK
K. Bongs, University of Birmingham (UOB), UK
F. Levi, Istituto Nazional Ricerche Metrologiche (INRIM), Torino, IT

ESA Project Scientist
L. Cacciapuoti, ESA/ESTEC, SCI-S

Annex 4 SCIENCE TEAM SIGNATURE PAGES

ESA UNCLASSIFIED - For Official Use

APPROVAL

Title I-SOC Scientific Requirements	
Issue Number 1	**Revision Number** 0
Author Luigi Cacciapuoti (SCI-S) and Stephan Schiller (HHU Düsseldorf)	**Date** 10/03/2017
Approved By	**Date of Approval**
I-SOC Science Team: S. Schiller (UDUS) Stephan Schiller U. Sterr (PTB) C. Lisdat (PTB) N. Poli (LENS) G. Tino (LENS) I. Prochazka (CTU) R. Le Targat (OBSPARIS) J. Lodewyck (OBSPARIS) C. Salomon (ENS) Y. Singh (UOB) K. Bongs (UOB) F. Levi (INRIM)	6.4.2017
ESA Project Scientist: L. Cacciapuoti (SCI-S)	
UIB Board: L. De Parolis (acting HRE-UP)	
UIB Board: L. De Parolis (HRE-PI)	
UIB Board: A. Schoen (HRE-PI)	

ESA UNCLASSIFIED - For Official Use

APPROVAL

Title I-SOC Scientific Requirements	
Issue Number 1	**Revision Number** 0
Author Luigi Cacciapuoti (SCI-S) and Stephan Schiller (HHU Düsseldorf)	**Date** 10/03/2017
Approved By	**Date of Approval**
I-SOC Science Team:	
S. Schiller (UDUS)	
U. Sterr (PTB)	2017-04-03
C. Lisdat (PTB)	
N. Poli (LENS)	
G. Tino (LENS)	
I. Prochazka (CTU)	
R. Le Targat (OBSPARIS)	
J. Lodewyck (OBSPARIS)	
C. Salomon (ENS)	
Y. Singh (UOB)	
K. Bongs (UOB)	
F. Levi (INRIM)	
ESA Project Scientist:	
L. Cacciapuoti (SCI-S)	
UIB Board:	
L. De Parolis (acting HRE-UP)	
UIB Board:	
L. De Parolis (HRE-PI)	
UIB Board:	
A. Schoen (HRE-PI)	

ESA UNCLASSIFIED - For Official Use

APPROVAL

Title I-SOC Scientific Requirements	
Issue Number 1	**Revision Number** 0
Author Luigi Cacciapuoti (SCI-S) and Stephan Schiller (HHU Düsseldorf)	**Date** 10/03/2017
Approved By	**Date of Approval**
I-SOC Science Team: S. Schiller (UDUS) U. Sterr (PTB) C. Lisdat (PTB) N. Poli (LENS) G. Tino (LENS) I. Prochazka (CTU) R. Le Targat (OBSPARIS) J. Lodewyck (OBSPARIS) C. Salomon (ENS) Y. Singh (UOB) K. Bongs (UOB) F. Levi (INRIM)	C. Lisdat 03.04.2017
ESA Project Scientist: L. Cacciapuoti (SCI-S)	
UIB Board: L. De Parolis (acting HRE-UP)	
UIB Board: L. De Parolis (HRE-PI)	
UIB Board: A. Schoen (HRE-PI)	

ESA UNCLASSIFIED - For Official Use

APPROVAL

Title I-SOC Scientific Requirements	
Issue Number 1	**Revision Number** 0
Author Luigi Cacciapuoti (SCI-S) and Stephan Schiller (HHU Düsseldorf)	**Date** 10/03/2017
Approved By	**Date of Approval**
I-SOC Science Team: S. Schiller (UDUS) U. Sterr (PTB) C. Lisdat (PTB) N. Poli (LENS) G. Tino (LENS) I. Prochazka (CTU) R. Le Targat (OBSPARIS) J. Lodewyck (OBSPARIS) C. Salomon (ENS) Y. Singh (UOB) K. Bongs (UOB) F. Levi (INRIM)	3/4/2017 4/4/2017
ESA Project Scientist: L. Cacciapuoti (SCI-S)	
UIB Board: L. De Parolis (acting HRE-UP)	
UIB Board: L. De Parolis (HRE-PI)	
UIB Board: A. Schoen (HRE-PI)	

ESA UNCLASSIFIED - For Official Use

APPROVAL

Title I-SOC Scientific Requirements	
Issue Number 1	**Revision Number** 0
Author Luigi Cacciapuoti (SCI-S) and Stephan Schiller (HHU Düsseldorf)	**Date** 10/03/2017
Approved By	**Date of Approval**
I-SOC Science Team:	
S. Schiller (UDUS)	
U. Sterr (PTB)	
C. Lisdat (PTB)	
N. Poli (LENS)	
G. Tino (LENS)	
I. Prochazka (CTU)	28.3.2017
R. Le Targat (OBSPARIS)	
J. Lodewyck (OBSPARIS)	
C. Salomon (ENS)	
Y. Singh (UOB)	
K. Bongs (UOB)	
F. Levi (INRIM)	
ESA Project Scientist:	
L. Cacciapuoti (SCI-S)	
UIB Board:	
L. De Parolis (acting HRE-UP)	
UIB Board:	
L. De Parolis (HRE-PI)	
UIB Board:	
A. Schoen (HRE-PI)	

ESA UNCLASSIFIED - For Official Use

APPROVAL

Title I-SOC Scientific Requirements	
Issue Number 1	**Revision Number** 0
Author Luigi Cacciapuoti (SCI-S) and Stephan Schiller (HHU Düsseldorf)	**Date** 10/03/2017
Approved By	**Date of Approval**
I-SOC Science Team: S. Schiller (UDUS) U. Sterr (PTB) C. Lisdat (PTB) N. Poli (LENS) G. Tino (LENS) I. Prochazka (CTU) R. Le Targat (OBSPARIS) J. Lodewyck (OBSPARIS) C. Salomon (ENS) Y. Singh (UOB) K. Bongs (UOB) F. Levi (INRIM)	April 3 2017 2017/04/03
ESA Project Scientist: L. Cacciapuoti (SCI-S)	
UIB Board: L. De Parolis (acting HRE-UP)	
UIB Board: L. De Parolis (HRE-PI)	
UIB Board: A. Schoen (HRE-PI)	

ESA UNCLASSIFIED - For Official Use

APPROVAL

Title I-SOC Scientific Requirements	
Issue Number 1	**Revision Number** 0
Author Luigi Cacciapuoti (SCI-S) and Stephan Schiller (HHU Düsseldorf)	**Date** 10/03/2017
Approved By	**Date of Approval**
I-SOC Science Team: S. Schiller (UDUS) U. Sterr (PTB) C. Lisdat (PTB) N. Poli (LENS) G. Tino (LENS) I. Prochazka (CTU) R. Le Targat (OBSPARIS) J. Lodewyck (OBSPARIS) C. Salomon (ENS) Y. Singh (UOB) K. Bongs (UOB) F. Levi (INRIM)	05/04/2017
ESA Project Scientist: L. Cacciapuoti (SCI-S)	
UIB Board: L. De Parolis (acting HRE-UP)	
UIB Board: L. De Parolis (HRE-PI)	
UIB Board: A. Schoen (HRE-PI)	

ESA UNCLASSIFIED - For Official Use

APPROVAL

Title I-SOC Scientific Requirements	
Issue Number 1	**Revision Number** 0
Author Luigi Cacciapuoti (SCI-S) and Stephan Schiller (HHU Düsseldorf)	**Date** 10/03/2017
Approved By	**Date of Approval**
I-SOC Science Team: S. Schiller (UDUS) U. Sterr (PTB) C. Lisdat (PTB) N. Poli (LENS) G. Tino (LENS) I. Prochazka (CTU) R. Le Targat (OBSPARIS) J. Lodewyck (OBSPARIS) C. Salomon (ENS) Y. Singh (UOB) यशपाल सिंह K. Bongs (UOB) F. Levi (INRIM)	March 28, 2017 March 28, 2017
ESA Project Scientist: L. Cacciapuoti (SCI-S)	
UIB Board: L. De Parolis (acting HRE-UP)	
UIB Board: L. De Parolis (HRE-PI)	
UIB Board: A. Schoen (HRE-PI)	

ESA UNCLASSIFIED - For Official Use

APPROVAL

Title I-SOC Scientific Requirements	
Issue Number 1	**Revision Number** 0
Author Luigi Cacciapuoti (SCI-S) and Stephan Schiller (HHU Düsseldorf)	**Date** 10/03/2017

Approved By	Date of Approval
I-SOC Science Team:	
S. Schiller (UDUS)	
U. Sterr (PTB)	
C. Lisdat (PTB)	
N. Poli (LENS)	
G. Tino (LENS)	
I. Procházka (CTU)	
R. Le Targat (OBSPARIS)	
J. Lodewyck (OBSPARIS)	
C. Salomon (ENS)	
Y. Singh (UOB)	
K. Bongs (UOB)	
F. Levi (INRIM)	Filippo Levi
ESA Project Scientist:	
L. Cacciapuoti (SCI-S)	
UIB Board:	
L. De Parolis (acting HRE-UP)	
UIB Board:	
L. De Parolis (HRE-PI)	
UIB Board:	
A. Schoen (HRE-PI)	

Annex 5 TBR LIST

List of issues related to the I-SOC Scientific Requirements to be resolved.

	Description	Input needed	Date
TBR-01 : USOC Location	Location of the I-SOC User Support and Operation Center (USOC) to be identified.		
TBR-02: DAC location and functions	Location and specific functions of the I-SOC data analysis center to be detailed.		
TBR-03: Lattice orientation	Orientation of optical lattice axis to be defined.		
TBR-04: Definition of O/B time scale	I-SOC O/B time scale to be defined		
TBR-05: I-SOC orbitography errors	Orbitography errors (position, velocity) to be refined		